RECONSTRUCTION OF CARDIOMYOCYTE ENERGY METABOLISM AND INVESTIGATION OF THE HEALTHY AND DISEASE CASES BY METABOLIC ENGINEERING TECHNIQUES

by

Çiğdem Filiz

B.S., Chemical Engineering, Boğaziçi University, 2006

Submitted to the Institute for Graduate Studies in
Science and Engineering in partial fulfillment of
the requirements for the degree of
Master of Science

Graduate Program in Chemical Engineering

Boğaziçi University

2009

ACKNOWLEDGEMENTS

I would like to express my sincere and utmost gratitude and thanks to my thesis advisor, Prof. Kutlu Ülgen, for her everlasting support, encouragement, guidance and patience throughout my studies. I also thank the other members of my thesis committee, Prof. Zeynep İlsen Önsan and Assist. Prof. Nevra Özer for their paticipitation and time.

I am very grateful and indebted to Asst. Prof. Yalçın Arğa and Betül Kavun Özbayraktar for all the answers and experience they provided me during my studies. I could not have survived without them.

I thank all my former colleagues and friends from Yeditepe University. I am especially grateful to Özlem Ateş and Deniz Rende, both for being caring friends and guiding mentors for my academic and personal life.

I also want to thank my friends Ela Bilginoğlu, Çiğdem Karaca and Özgenur Süzmetaş, who were always ready to listen whenever I needed and supported me with their friendship.

Finally, I want to thank Seda Aktaş and Ilgaz Soykal for their encouragement and help in difficult times, and for their "supply of optimism" which I seem to lack a lot. I am deeply grateful to them for turning my graduate life into a fun and memorable experience.

ABSTRACT

RECONSTRUCTION OF CARDIOMYOCYTE ENERGY METABOLISM AND INVESTIGATION OF THE HEALTHY AND DISEASE CASES BY METABOLIC ENGINEERING TECHNIQUES

In the present study, a reaction network of the cardiomyocyte energy metabolism is reconstructed by extensive literature survey and using the information obtained from the online databases of Kyoto Encyclopedia of Genes and Genomes (KEGG) and Reactome. The reconstructed network includes the metabolisms of carbohydrates, fatty acids and ketone bodies used for energy maintenance and it is employed for the investigation of the behaviour of the cell under different physiological conditions. Flux Balance Analysis is applied to the reconstructed network to obtain the flux distributions that maximize the ATP consumption of the cell at healthy normoxic conditions, under physiological stress conditions of fasting and ischemia, and in case of enzyme deficiencies of Primary Carnitine, Mitochondrial NADH-CoQ reductase (complex I) and HMG-CoA Synthase. Flux Variability Analysis is used to obtain the flux ranges of the energy metabolism of the healthy cardiomyocyte. The clustering method of Self-Organizing Maps is applied to obtain the reaction sets that exhibit similar behaviour under different conditions such as healthy and disease cases. As the conclusion of the present study, the flux ranges and the substrate preference of the model cell were found to be in good agreement with the experimental reports given in literature. So the reconstructed reaction network is deduced to be a good candidate for future studies on cardiomyocyte energy metabolism.

ÖZET

KALP HÜCRELERİNDE ENERJİ METABOLİZMASININ OLUŞTURULMASI VE SAĞLIKLI VE HASTALIK KOŞULLARININ METABOLİZMA MÜHENDİSLİĞİ TEKNİKLERİ İLE İNCELENMESİ

Bu araştırmada, bir kalp hücresinin enerji metabolizmasına ait reaksiyon ağı literatür taraması yapılarak ve KEGG ansiklopedisi, Reactome gibi çevrimiçi veritabanları kullanılarak oluşturulmuştur. Karbonhidrat, yağ asitleri ve keton metabolizmaları gibi enerji üretiminde kullanılan metabolizmaları kapsayan bu reaksiyon ağı ile farklı fizyolojik koşullar altındaki hücre davranışları incelenmiştir. Normal koşullar yanında enzim bozuklukları (Primer Karnitin Yetmezliği, Mitokondriyal NADH-CoQ Reduktaz Yetmezliği, HMG-CoA Sentaz Yetmezliği gibi), açlık ve iskemik koşullar altında hücrenin ATP harcamasını maksimize eden akı dağılımları Akı Denklik Analizi kullanılarak hesaplanmıştır. Kalp hücresinin sağlıklı enerji metabolizmasındaki akı aralıklarını elde etmek için ise Akı Değişkenlik Analizi, oluşturulan bu reaksiyon ağına uygulanmıştır. Sağlıklı ve farklı hastalık koşulları altında benzer davranış gösteren reaksiyon kümeleri Özdüzenleyici Haritalar yöntemi kullanılarak elde edilmiştir. Araştırma sonucunda modelin akı aralıklarının ve hücrenin sübstrat tercihlerinin literatürdeki deneysel sonuçlarla benzer özellikler gösterdiği bulunmuştur. Böylece, oluşturulan reaksiyon ağının, gelecek çalışmalarda örnek model olarak kullanılabilir olduğu sonucuna varılmıştır.

TABLE OF CONTENTS

LIST OF FIGURES

LIST OF TABLES

LIST OF SYMBOLS / ABBREVATIONS

$d(N_1, N_2)$	Distance function
f	The objective function vector
$f_i(N)$	The position of node N at iteration *i* is denoted
i	Index number
j	Index number
M	Number of reactions
N	Node
N	Number of metabolites
R_{max}	Upper limits of all flux ratios
R_{min}	Lower limits of all flux ratios
S	Stoichiometric matrix of reactions
v	Flux vector
v_{max}	The vector containing the maximum capacities of the fluxes
Z_{obj}	The value of the objective function
τ	The learning rate
CPT	Carnitine palmitoyltransferase
FBA	Flux balance analysis
FCF	Flux Coupling Finder
GAPDH	Glyceraldehyde 3-phosphate dehydrogenase
GLUT	Glucose transporter
GP	Glycogen phosphorylase
GS	Glycogen synthase
HK	Hexokinase
LDH	Lactate dehydrogenase
LP	Linear Programming
MCT	Monocarboxylate transporter
OP	Oxidative phosphorylation
PDH	Pyruvate dehydrogenase

PFK-1	Phosphofructokinase-1
s.s.	Steady state
SOM	Self-organizing maps
TCA	Tricarboxylic acid cycle

1. INTRODUCTION

Heart is the most important part of the body and its failure has crucial effects. Cardiomyocytes are contractile muscle cells, which constitute approximately 75% of the myocardium. The major function of the cardiomyocytes is the contraction of the heart, which plays a crucial role in the regulation of the circulation of blood.

A model that will represent the function of the heart overally must contain systems for uptake and metabolism of substrates for energy production (glucose, fatty acids including acetate, and oxygen); the cell's central system for energy supply, including mitochondrial oxidative phosphorylation; ionic currents, leaks and pumps, and their role in governing the membrane potential; energy usage for contraction, biochemical reactions, and ion pumping; excitation-contraction coupling, calcium balance and the contractile process; and balances of reducing equivalents and pH (Bassingthwaighte and Vinnakota, 2004).

The cardiac energy metabolism is very crucial for the function of the heart. Fatty acids and glucose are the main substrates for cardiac energy production under normal circumstances. Ketone bodies and lactate are used in times of starvation or excessive exercise, respectively. However, amino acids and ethanol never play a major role in the cardiac energy production (Kodde *et al*., 2007). The cardiac energy substrate metabolism and the relationships between these metabolisms are explained in Chapter 2 in detail.

For the normal cardiac function, the myocyte requires continuous production of ATP, which depends on adequate delivery of oxygen and oxidizable substrates. This process is achieved through different metabolic pathways, including glycolysis, β-oxidation, ketone body oxidation, Krebs cycle, and oxidative phosphorylation (Carjaval and Moreno-Sanchez, 2002). To construct the reaction network of the cardiomyocyte, these metabolisms are considered as the base and their corresponding reactions are added to the network one by one in the light of intense literature survey and with the information obtained from the online databases of Kyoto Encyclopedia of Genes and Genomes

(KEGG) and Reactome. Chapter 3 includes detailed information about the reconstruction of the network and its pathways and metabolisms.

Cardiomyopathies are diseases of the myocardium and most of them are genetic. There are about 8.2 million individuals suffering from heart disease in the world. The prevalence rate of cardiomyopathy is about 0.02% in USA and 0.06% in Turkey. The deficiencies of the enzymes in the cardiomyocytes are reported to lead to the malfunctioning of myocardium, i.e. cardiomyopathies.

In order to test the potential of the reconstructed network in the analysis of diseases, some enzyme deficiencies such as, Primary Carnitine Deficiency, Mitochondrial NADH-CoQ Reductase (Complex I) Deficiency, Tangier Disease and Fabry Disease that are known to manifest cardiac symptoms are selected and studied for their applicability in the present study. Chapter 4 includes detailed information about these diseases and their symptoms.

Ischemia is a condition in which blood flow (and thus oxygen) is restricted to a part of the body. Heart is one of the important organs that are most sensitive to insufficient blood supply. Chapter 5 gives more insight to ischemia. Ischemia leading to an undersupply of oxygen and consequently undersupply of energy for cardiomyocytes is a good physiological stress condition to be studied by a model of cardiomyocyte energy metabolism.

Flux balance analysis (FBA) is a mathematical tool to calculate the flux distribution within the metabolism. By choosing the right objective function, a metabolic system can be investigated for various perturbations like an enzyme deficiency or nutrient limitation in a cell. In the present study, Flux variability analysis, self-organizing maps (SOM) and flux coupling analysis are also used to obtain reaction sets that exhibit similar behaviour under similar conditions. Chapter 6 includes detailed information about the methods used in the present study.

In Chapter 7, the results of the FBA methods and SOM are presented and a detailed discussion of the results are also given. Chapter 8 summarizes the key points of the study with a conclusion.

2. LITERATURE SURVEY

2.1. Cardiac Energy Substrate Metabolism

Fatty acids and glucose are the main substrates for cardiac energy production under normal circumstances. Ketone bodies and lactate are used in times of starvation or excessive exercise, respectively. However, amino acids and ethanol never play a major role in the cardiac energy production (Kodde *et al*., 2007). In the well-perfused heart, 60-90 % of the total energy production comes from β-oxidation of fatty acids and 10-40 % comes from the oxidation of pyruvate that is derived approximately in equal amounts from glycolysis and lactate oxidation (Stanley *et al*., 2005).

Table 2.1. Substrate Preference (Kodde *et al*., 2007)

Energy Substrate	**Contribution to total production (%)**
Fatty acids	60-90
Glucose	10-40
Lactate	< 1-40
Amino acids	< 1-5
Ketone bodies	< 1-40
Ethanol	< 1-5

Hence the cardiac energy substrate metabolism can be divided into three main categories:

- Carbohydrate Metabolism
- Fatty Acid Metabolism
- Ketone Body Metabolism

2.1.1. Carbohydrate Metabolism

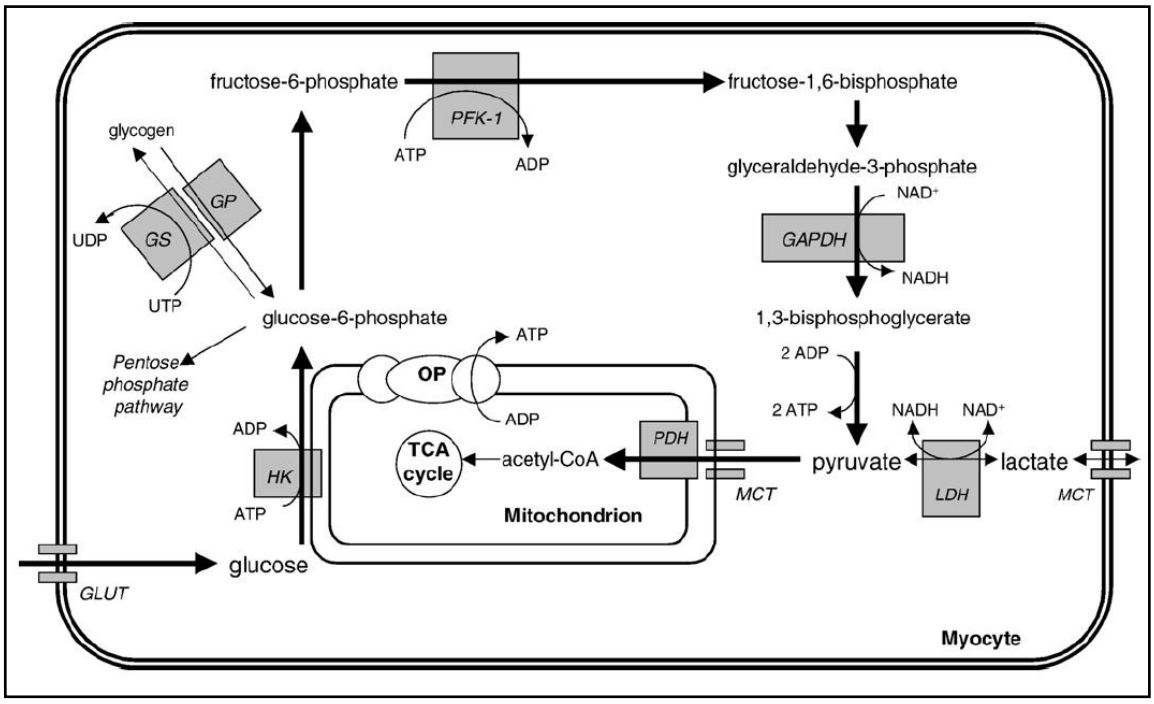

Figure 2.1. Cardiac carbohydrate pathways (Kodde *et al*., 2007)

2.1.1.1. Glucose: Glucose for the heart is provided from exogenous glucose derived from bloodstream or from intracellular glycogen stores (Depre *et al*., 1999, Stanley *et al*., 2005). The primary source is from the plasma and glucose is transported passively (Quinn and Pagano, 2004). Glucose transport is facilitated by glucose transporters GLUT-4 and GLUT-1; GLUT-4 being the dominant one during normal oxigenated flow (Kodde *et al*., 2007).

Glucose transport is slower than its phosphorylation and limits the overall rate of glucose uptake (Depre *et al*., 1998). Intracellular glucose is rapidly phosphorylated thus a steep, constant gradient for glucose uptake is maintained (Depre *et al*., 1998, King and Opie, 1998).

Glucose is then metabolized to glycogen by glycogen synthesis, or becomes a substrate for glycolytic pathway and ribose synthesis depending on oxygen availibility (Depre *et al*., 1999, Quinn and Pagano, 2004). The glycolytic pathway converts glucose to pyruvate and also generates ATP and pyruvate becomes a substrate for further metabolic pathways (Stanley *et al*., 2005). Glycolysis occurs in the cytoplasm and the ATP generated

is directed preferentially toward ion homeostasis and glycogenesis (rather than contraction) (Quinn and Pagano, 2004). Glycolysis ('lysis of glucose') is the biochemical process that transforms glucose into pyruvate and, eventually, into lactate and CO_2. The carbon atoms come either from exogenous glucose or from glycogen. Therefore, a correct metabolic balance of glycolysis should take into account glucose uptake, glycogen breakdown, lactate release and glucose oxidation (Depre *et al*., 1998).

2.1.1.2. Glycogen: The glycogen pool in the heart is relatively small compared to skeletal muscle (~30 μmol/g wet wt, ~150 μmol/g wet wt) and has a relatively rapid turnover rate despite stable tissue concentrations (Stanley *et al*., 2005). The amount of accumulated glycogen depends on the availibility of other substrates and hormone stimulation.

There are two distinct pathways for glycogen synthesis and breakdown (glycogenesis and glycogenolysis) (King and Opie, 1998).

After phosphorylation by hexokinase, a variable amount of imported glucose is temporarily stored as glycogen, which serves as a small energy reserve for the myocytes (Kodde *et al*., 2007). Unlike liver and skeletal muscle, heart muscle increases its glycogen content with fasting. During fasting enhanced fatty acid oxidation inhibits glycolysis more than glucose uptake, hence rerouting glucose toward glycogen synthesis (Depre *et al*., 1999, King and Opie, 1998). Glycogen synthesis is also stimulated by insulin and when lactate is the predominant fuel for the heart (Depre *et al*., 1999).

Glycogen provides glucose derivatives for glycolysis which are preferentially metabolized by oxidative rather than anaerobic pathways (Quinn and Pagano, 2004). Glycogenolysis is stimulated during increased heart work (e.g. exercise), during oxygen deprivation or by adrenaline (Depre *et al*., 1998, Kodde *et al*., 2007). During no-flow ischemia, when glucose uptake is negligible, increased glycogen breakdown produces about 1-2 μmol glucose equivalent/min g wet mass (Depre *et al*., 1998).

2.1.1.3. Lactate: Lactate is a significant source of oxidative fuel for the heart being a net consumer of lactate produced by muscle and erythrocytes (Kodde *et al*., 2007). The healthy heart is a net consumer of lactate even under conditions of near-maximal cardiac power. The myocardium becomes a lactate producer only under conditions of accelerated glycolysis or poorly controlled diabetes (Stanley *et al*., 2005).

2.1.1.4. Pyruvate: Although pyruvate is an end product of glycolysis and it is not an extracted substrate for carbohydrate metabolism, it is located at a metabolic crossroad thus it is an important key metabolite.

- Pyruvate has three main fates depending on the energy status of the cell:
- Conversion to lactate
- Decarboxylation to Acetyl-CoA
- Carboxylation to oxaloacetate and malonate (Quinn and Pagano, 2004, Stanley *et al*., 2005, King and Opie, 1998).

If glucose transport and glycolysis exceeds glucose oxidation, glycolysis is maintained by the metabolism of pyruvate to lactic acid. This anaerobic process occurs in cytoplasm and regenerates the essential glucolytic co-enzymes NAD+ and NADH (Quinn and Pagano, 2004). Under aerobic conditions or with extreme exercise, the TCA cycle is inhibited by accumulated NADH from inhibition of oxidative phosphorylation. The reduction of pyruvate to lactate allows regeneration of NAD+ and continuation of glycolysis (King and Opie, 1998). Lactate is then either exported from the cell with a H+ ion with monocarboxylate transporters to the blood stream. These transporters not only remove lactate but also maintain the intracellular pH by removing the protons produced by glycolysis (Kodde *et al*., 2007). Lactic acid may also be converted to pyruvate after sufficient oxygen is reintroduced into the cell (Quinn and Pagano, 2004, King and Opie, 1998).

Under aerobic conditions and reduced free fatty acid levels, pyruvate is transported to mitochondria for decarboxylation to acetyl-CoA and carbon dioxide by pyruvate dehydrogenase (Quinn and Pagano, 2004). This enzyme is a complex of three enzymes and regulated by the ratios of NAD+/NADH, acetyl-CoA/CoA and ATP/AMP, as well as phosphorylation and dephosphorylation (Kodde *et al*., 2007). Acetyl-CoA is committed to

the tricarboxylic acid cycle and subsequent complete oxidation of glucose, and can proceed only if there is sufficient oxygen for the electron transport chain.

Pyruvate is a major anaplerotic substrate supplying intermediates of the TCA cycle (King and Opie, 1998). Pyruvate carboxylase and malic enzyme convert pyruvate to oxaloacetate and malate. A third intermediate α-ketoglutarate is also produced by transamination of pyruvate with glutamate and a side product alanine (Kodde *et al*., 2007).

2.1.2. Fatty Acid Metabolism

Under normal conditions 60-80% of the total ATP produced is generated from the β-oxidation of fatty acids (FA) (van der Vusse *et al*., 2000, Quinn and Pagano, 2004). Since like most organs cardiac muscle is not capable of de novo fatty acid synthesis and has a small storage capacity, it relies on exogenous FA (van der Vusse *et al*., 2002).

Fatty acids in blood are in esterified (mono-, di- and triacylglycerol, phospholipids and cholesterol esters) and unesterfied forms. However, the main sources for the heart are the free FA bound to albumin and triacylglycerol core of circulating chylomicrons and very low density lipoproteins (Kodde et al., 2007, van der Vusse *et al*., 2002). Albumin bound FA provides the majority of FA used by the heart, while the triacylglycerol component only accounts for ≤20-25% of the cardiac consumption (Kodde *et al*., 2007).

After dissociation of the albumin-fatty acid complex or hydrolysis of the triacylglycerols, fatty acids are transferred from the capilary lumen through the capillary endothelium and interstitial compartment to the cardiac muscle cell (van der Vusse *et al*., 2000).

Once fatty acids are transported into cytoplasm, they are transformed to long-chain acyl-CoA, which can be either esterified to triglyceride or to long chain fatty acyl carnitine to be transported into mitochondria for β-oxidation. The acyl-CoA flux to the mitochondrial matrix is ~100-150 nmol min^{-1} g cardiac $tissue^{-1}$ at rest and may increase to 200 nmol min^{-1} g^{-1} during exercise (Kodde *et al.,* 2007). Studies show that 70-90% of the oleate or palmitate that is taken by the heart is immediately released into venous effluent as

CO_2 or H_2O, suggesting that 70-90% of that fatty acids entering the cell are converted to acylcarnitine and immediately oxidized and the rest enter the intracardiac triglyceride pool (Stanley *et al*., 2004).

Myocardial triacylglycerol contains about 4mmol fatty acyl moieties per gram of tissue and under steady state conditions no major alterations take place, thus at normal conditions cardiomyocyte heavily depends on adequate supply of blood-borne fatty acids (van der Vusse *et al*., 2000). Triglyceride turnover can be accelerated by adregenic stimulation and is increased in uncontrolled diabetes and during reperfusion of ischemic hearts (Stanley *et al*., 2004).

At physiological workloads the amount of fatty acids oxidized is about 50-100 nmol/min per gram wet weight. Thus at steady state conditions a similar amount of fatty acid moieties must be transferred from the microvascular compartment to the cardiomyocytes (van der Vusse *et al*., 2000).

The rate of fatty acid uptake by the heart is primarily determined by the concentration of nonesterified acids in the plasma. Under conditions of metabolic stress, such as ischemia, diabetes or starvation plasma free FA concentrations can increase to higher levels (Stanley *et al*., 2005).

2.1.3. Ketone Body Metabolism

The heart extracts and oxidizes ketone bodies (acetoacetate, 3-hydroxybutyrate and acetone) in a concentration dependent manner. Plasma ketone bodies are formed from fatty acids in the liver and diffuse into the blood (Stanley *et al*., 2005).

Arterial plasma concentrations are very low thus, they are normally a minor substrate for the myocardium (Stanley *et al*., 2005). However, ketone body levels can increase in times of starvation, in poorly controlled diabetes, in chronic heart failure and during consumption of a high-fat diet (Kodde *et al*., 2007).

Oxidation of ketone bodies inhibits myocardial fatty acid oxidation. Diabetic myocardium has a high rate of 3-hydroxybutyrate uptake and relatively low rates of fatty acid uptake suggesting that in diabetic patients elevated plasma level concentrations can act to inhibit fatty acid uptake and oxidation (Stanley *et al*., 2005).

A ketone body pathway does not exist because ketone bodies enter both the cardiomyocyte and the mitochondria through the monocarboxylate transporter (MCT). The rate of substrates entering the TCA cycle depends on their amounts in this cycle (Kodde *et al*., 2007).

2.2. Relationships between Energy Metabolisms

Metabolism of glucose and fatty acids compete for the delivery of acetyl CoA to the tricarboxylic acid cycle. The products of β-oxidation inhibit the transport and metabolism of glucose at a number of sites in glycolysis/glucose oxidation. High concentrations of NADH and acetyl CoA generated from β-oxidation inhibit the oxidation of glucose. High concentrations of citrate (an intermediary in the tricarboxylic acid cycle) inhibit phosphofructokinase. These inhibitors suppress complete glucose oxidation via pyruvate relative to glycolysis to lactate, so reducing the competition between β- and glucose oxidation for the electron transport chain and increasing production of lactic acid. Conversely, acetyl CoA derived from pyruvate metabolism can be converted to malonyl CoA, a process stimulated by insulin. Glucose, lactate and malonyl CoA in turn diminish the availability of fatty acids for subsequent β-oxidation by inhibiting the transport of fatty acids to the mitochondrion (Quinn and Pagano, 2004).

Under normoxic conditions, glucose provides the tricarboxylic acid cycle not only with acetyl-CoA but also with oxaloacetate (anaplerosis). This anaplerotic mechanism is particularly important during prolonged oxidation of fatty acids or ketone bodies, which can deplete the tricarboxylic acid cycle intermediates (Depre *et al.*,1998). The need for anaplerosis may explain why glucose uptake is never completely inhibited in hearts perfused with fatty acids (Depre *et al.*, 1999).

The higher carbon content of fatty acids generate more ATP per mole during β-oxidation (e.g. palmitate produces 129 molecules of ATP) than is generated per mole during aerobic (38 molecules of ATP) and anaerobic (2 molecules of ATP) glucose metabolism (Quinn and Pagano, 2004).

β-oxidation requires more oxygen/ATP to be generated than complete glucose oxidation, making glucose metabolism about 10–15% more oxygen efficient. In conditions of ischemia, fatty acids and their metabolites exert a toxic effect, as well as consuming available oxygen rapidly. Thus the relative concentrations of fatty acids and glucose are of major importance in determining the tolerance of a heart to ischemia (King and Opie, 1998).

3. NETWORK RECONSTRUCTION

For the normal cardiac function, the myocyte requires continous production of ATP, which depends on adequate delivery of oxygen and oxidizable substrates. This process is achieved through different metabolic pathways, including glycolysis, β-oxidation, ketone body oxidation, Krebs cycle, and oxidative phosphorylation (Carjaval and Moreno-Sanchez, 2002).

3.1. Glycolysis

The glycolysis pathway is presented in Figure 3.1 and the reaction are given in Table 3.1. After glucose is transported into the cell by GLUT transporters (TRANS 01), it is phosphorylated by hexokinase with the hydrolysis of ATP consuming an additional ATP (GLY 01). The product glucose-6-phosphate (g6p) then undergoes a reversible change to fructose-6-phosphate (GLY 02) (King and Opie, 1998).

Phosphofructokinase-1 (PFK) catalyzes the irreversible step (GLY 05) of fructose-6-phosphate towards fructose-1,6-bisphosphate and is considered to be the key-regulating enzyme in this pathway (Kodde *et al*., 2007). Since PFK utilizes ATP to produce fructose 1,6-bisphosphate it accelerates flux through glycolysis when the phosphorylation potential falls (Stanley *et al*., 2005).

Glucose utilisation has thus consumed two ATP at this stage, but if glycolysis goes through pyruvate 4 ATP will then be produced, resulting with a net production of 2 ATP (King and Opie, 1998).

Next, two 3-carbon (3-C) molecules glyceraldehyde 3-phosphate (g3p), and dihydroxyacetone phosphate (dhap) are formed (GLY 06). Dhap is converted to g3p (GLY 07) by triose phosphate isomerase (King and Opie, 1998).

Glyceraldehyde-3-phosphate dehydrogenase (GAPDH) catalyzes the conversion of g3p to 1,3-diphosphoglycerate (GLY 08) and produces the NADH molecules that originate from glycolysis (Stanley *et al*., 2005).

One phosphate group on each 3-C molecule is subsequently cleaved off to form ATP, when 1,3-bisphosphoglycerate is converted to 3-phosphoglycerate (3pg) by phosphoglycerate kinase (GLY 09). 3pg undergoes a conformational change to 2-phosphoglycerate (GLY 10), which is dehydrated with the formation of an enol group, to phosphoenolpyruvate (pep) (King and Opie, 1998).

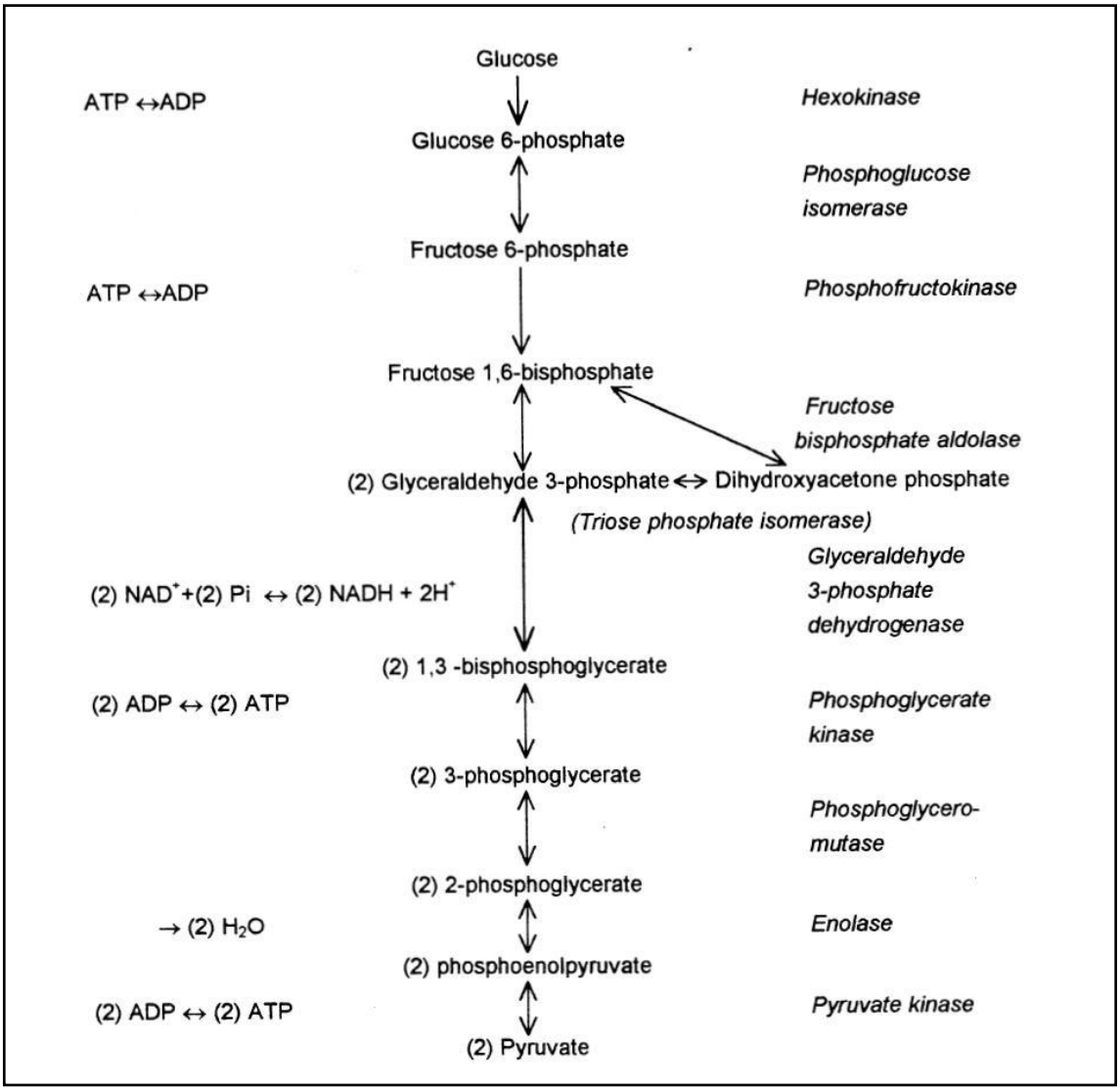

Figure 3.1. Glycolytic pathway (King and Opie, 1998)

The high phosphoryl-transfer potential of PEP allows the transfer of the remaining high energy phosphate group to ADP+ and H+, with the end products of pyruvate and ATP. This reaction catalysed by pyruvate kinase (PK) (GLY 12), is virtually irreversible (King and Opie, 1998).

The final product of glycolysis is pyruvate, which can then follow a number of pathways, which determines the total amount of ATP derived from a glucose molecule. Anaerobic glycolysis implies that pyruvate is converted to lactate (King and Opie, 1998).

Table 3.1. Glycolysis reactions

Reaction Name	**Enzyme**	**Reaction**	**E.C. #**
TRANS 01		glc-D[e] -> glc-D[c]	
GLY 01	hexokinase 1	[c]: atp + glc-D -> adp + g6p	2.7.1.1
GLY 02	glucose phosphate isomerase	[c]: g6p <=> f6p	5.3.1.9
GLY 03	6-phosphofructo-2-kinase	[c]: atp + f6p -> adp + f26bp	2.7.1.105
GLY 04	Fructose-2,6-bisphosphatase	[c]: f26bp + h2o -> fbp + pi	2.7.1.105
GLY 05	phosphofructokinase tetramer	[c]: atp + f6p -> adp + fbp	
GLY 06	aldolase A, fructose-bisphosphate	[c]: fbp <=> dhap + g3p	4.1.2.13
GLY 07	triosephosphate isomerase	[c]: dhap <=> g3p	5.3.1.1
GLY 08	glyceraldehyde-3-phosphate dehydrogenase	[c]: g3p + nad + pi <=> 13dpg + h + nadh	1.2.1.12
GLY 09	phosphoglycerate kinase 1	[c]: 13dpg + adp <=> 3pg + atp	2.7.2.3
GLY 10	phosphoglycerate mutase 2 (muscle)	[c]: 3pg <=> 2pg	5.4.2.1
GLY 11	enolase 3 (beta, muscle)	[c]: 2pg <=> pep + h2o	4.2.1.11
GLY 12	pyruvate kinase, muscle	[c]: adp + pep -> atp + pyr	2.7.1.40

3.2. Pentose Phosphate Pathway

G6p is a junction for the formation and breakdown of glycogen, as well as the pentose shunt. In the pentose shunt, g6p is converted to D-glucono-1,5-lactone-6-phosphate by glucose 6-phosphate dehydrogenase (PPP 01, given in Table 3.2), which uses NADP. This compound is hydrolysed to 6-phosphogluconate (PPP 02), which is converted to D-ribose 5-phosphate (PPP 03), with an additional NADP utilised. 2 molecules of NADPH are thus regenerated. NADPH is converted back to NAD by glutathione complex with the consumption of hydrogen peroxide (H_2O_2) (OTHERS in Table A.1). D-ribose 5-phosphate can then be converted to f6p or g3p (PPP 08), re-entering the glycolytic pathway. The proportions which flow along the pathways are dependent on the requirement of the cell for D-ribose 5-phosphate, NADPH, or continued glycolysis (King and Opie, 1998).

Table 3.2. Pentose Phosphate Pathway Reactions

Reaction Name	**Enzyme**	**Reaction**	**E.C. #**
PPP 01	glucose-6-phosphate dehydrogenase	[c]: g6p + nadp -> 6pgl + nadph + h	1.1.1.49
PPP 02	6-phosphogluconolactonase	[c]: 6pgl + h2o -> 6pgc	3.1.1.31
PPP 03	phosphogluconate dehydrogenase	[c]: 6pgc + nadp -> ru5p + co2 + nadph + h	1.1.1.44
PPP 04	ribulose-5-phosphate-3-epimerase	[c]: ru5p <=> x5p	5.1.3.1
PPP 05	ribose 5-phosphate isomerase A	[c]: ru5p <=> r5p	5.3.1.6
PPP 06	transaldolase 1	[c]: g3p + s7p <=> e4p + f6p	2.2.1.2
PPP 07	transketolase	[c]: r5p + x5p <=> s7p + g3p	2.2.1.1
PPP 08	transketolase	[c]: x5p + e4p <=> g3p + f6p	2.2.1.1

3.3. Glycogen Synthesis and Degradation

3.3.1. Glycogen synthesis (Glycogenesis)

Glycogen is synthesized from uridine diphosphate glucose (udp-glucose), an activated form of glucose derived from glucose 1-phosphate (g1p) and uridine triphosphate (utp) (GLCGN 02, given in Table 3.3). Pyrophosphate (ppi) is formed, and then hydrolysed to 2 orthophosphate (pi), an essentially irreversible reaction which drives glycogen synthesis. The udp is then cleaved from the glucose by glycogen synthase (GLCGN 03) and the glucose moiety is attached to the non-reducing end of a glycogen branch (King and Opie, 1998).

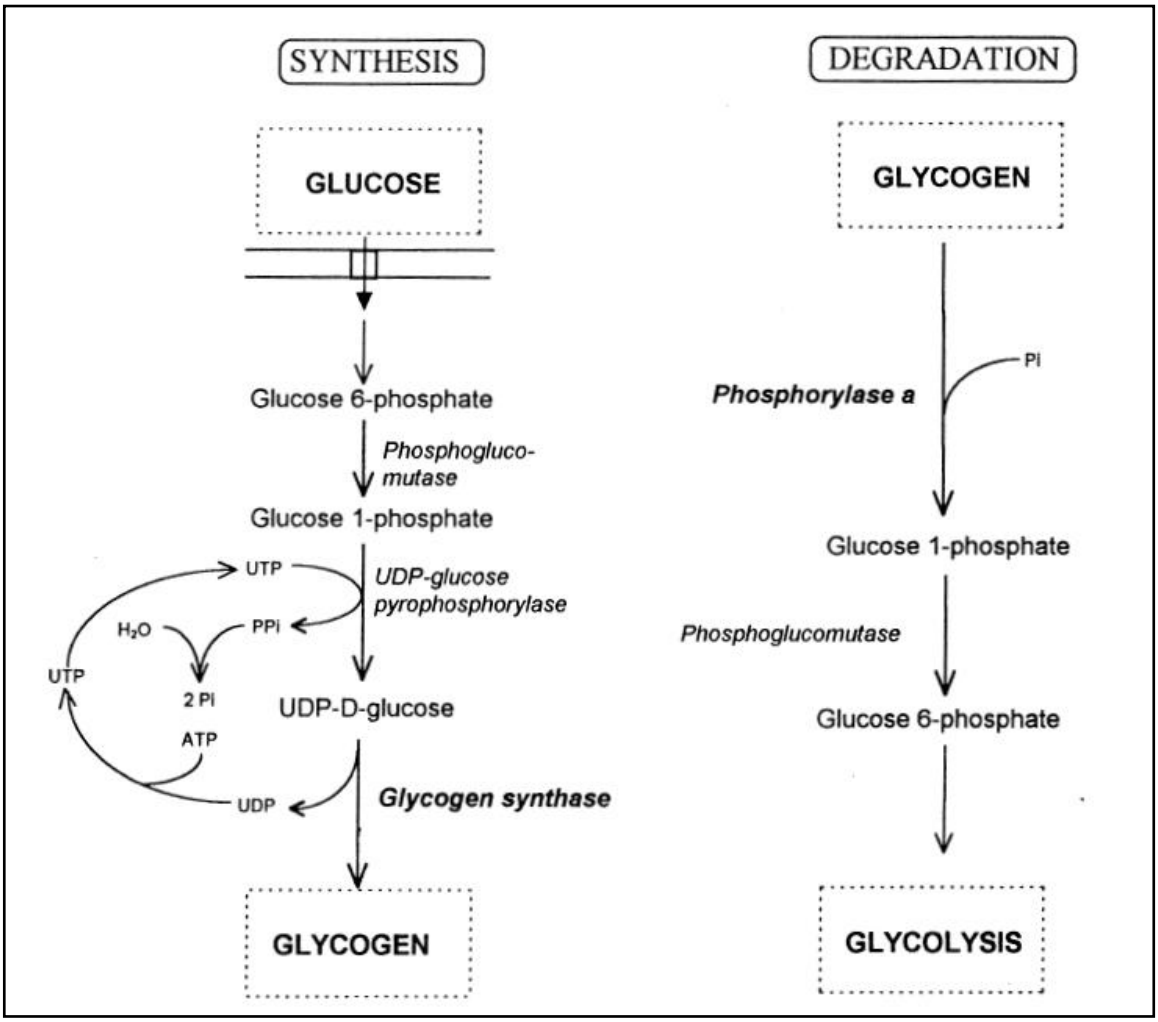

Figure 3.2. Glycogen synthesis and degradation (King and Opie, 1998)

3.3.2. Glycogen degradation (Glycogenolysis)

Glycogen breakdown follows a simple pathway as presented in Figure 3.2. A glucose moiety bound by an a-1,4 (straight) bond is cleaved from the large macromolecule and phosphorylated by phosphorylase a with pi (GLCGN 04). This occurs without the expenditure of an ATP molecule, and prevents diffusion out of the cell. G1p is converted to g6p by phosphoglucomutase (GLCGN 01), an enzyme which favours the formation of g6p, unless g6p is in high concentrations. G6p then enters the glycolytic pathway. The equilibrium favours glycogen breakdown, thus the force yield is very efficient (King and Opie, 1998).

Table 3.3. Reactions of glycogen metabolism

Reaction Name	Enzyme	Reaction	Pathway/Metabolism	E.C. #
GLCGN 01	phosphoglucomutase 1	[c]: g6p <=> g1p	Glycogen Metabolism	5.4.2.2
GLCGN 02	UDP-glucose pyrophosphorylase 2	[c]: g1p + utp -> ppi + udpg	Glycogen Metabolism	2.7.7.9
GLCGN 03	glycogen synthase 1 (muscle)	[c]: udpg -> glycogen + udp	Glycogen Metabolism	2.4.1.11
NUCLEO 01		[c]: udp + atp <=> utp + adp	Nucleotide	
GLCGN 04	phosphorylase, glycogen, muscle	[c]: glycogen + pi + atp -> g1p + adp	Glycogen Metabolism	2.4.1.1
TRANS 02		glycogen[c] <=> glycogen[e]	Glycogen Transport	

3.4. Pyruvate Metabolism

3.4.1. Lactate

Lactate transport across the plasma membrane (TRANS 03, given in Table 3.4) is facilitated by monocarboxylate transporters (Stanley *et al*., 2005, Kodde *et al*., 2007). Intracellular lactate reacts with NAD+ in a reversible reaction (PYR 01) catalyzed by lactate dehydrogenase (LDH) and pyruvate, NADH and H+ is formed. Under conditions of adequate oxygenation and a high lactate uptake, the equation TRANS 03 proceeds toward pyruvate (Kodde *et al*., 2007). Under anaerobic conditions, pyruvate is converted to lactate to allow regeneration of NAD+, and continuation of glycolysis (King and Opie, 1998).

3.4.2. Pyruvate Decarboxylation

Pyruvate decarboxylation is the key irreversible step in carbohydrate oxidation and is catalyzed by pyruvate dehydrogenase (PDH), a multienzyme complex located in the mitochondrial matrix (Stanley *et al*., 2005). PDH is a complex of three enzymes which require a number of cofactors. The pyruvate dehydrogenase complex on the inner mitochondrial membrane transports pyruvate across the membrane and catalyzes the irreversible transformation into acetyl-CoA (PYR 03). This complex comprises three enzymes and five coenzymes clustered on the innermitochondrial membrane. The enzymes decarboxylate, acetylate and dehydrogenate pyruvate during its passage into the mitochondrial matrix. The net reaction PYR 03 is considered to be the key irreversible step in carbohydrate oxidation (Kodde *et al*., 2007).

3.4.3. Anaplerosis

In addition to lactate formation and oxidation, pyruvate enters the citric acid (TCA) cycle via carboxylation to either malate or oxaloacetate. Pyruvate can be converted to oxaloacetate by pyruvate carboxylase (PYR 05), and then or directly to malate (PYR 04). These are important anaplerotic mechanisms, and are involved in the malate-aspartate shuttle (King and Opie, 1998).

Table 3.4. Reactions of pyruvate metabolism

Reaction Name	**Enzyme**	**Reaction**	**E.C. #**
TRANS 03		lac-L[e] + h[e] <=> lac-L[c] + h[c]	
PYR 01	lactate dehydrogenase	[c]: lac-L + nad <=> pyr + nadh + h	1.1.1.27
PYR 02	mitochondrial pyruvate carrier	pyr[c] + h[c] -> pyr[m] + h[m]	
PYR 03	pyruvate dehydrogenase, mitochondrial	[m]: coa + nad + pyr -> accoa + co2 + nadh	1.2.1.51
PYR 04	malic enzyme 2, NAD(+)-dependent	[m]: mal-L + nad <=> pyr + nadh + co2 + h	1.1.1.38
PYR 05	pyruvate carboxylase	[c]: pyr + co2 + atp -> adp + pi + oaa	6.4.1.1
PYR 06	malic enzyme 1, NADP(+)-dependent, cytosolic	[c]: mal-L + nadp <=> pyr + co2 + nadph + h	1.1.1.40
PYR 07	malic enzyme 3, NADP(+)-dependent, mitochondrial	[m]: mal-L + nadp <=> pyr + co2 + nadph + h	1.1.1.40

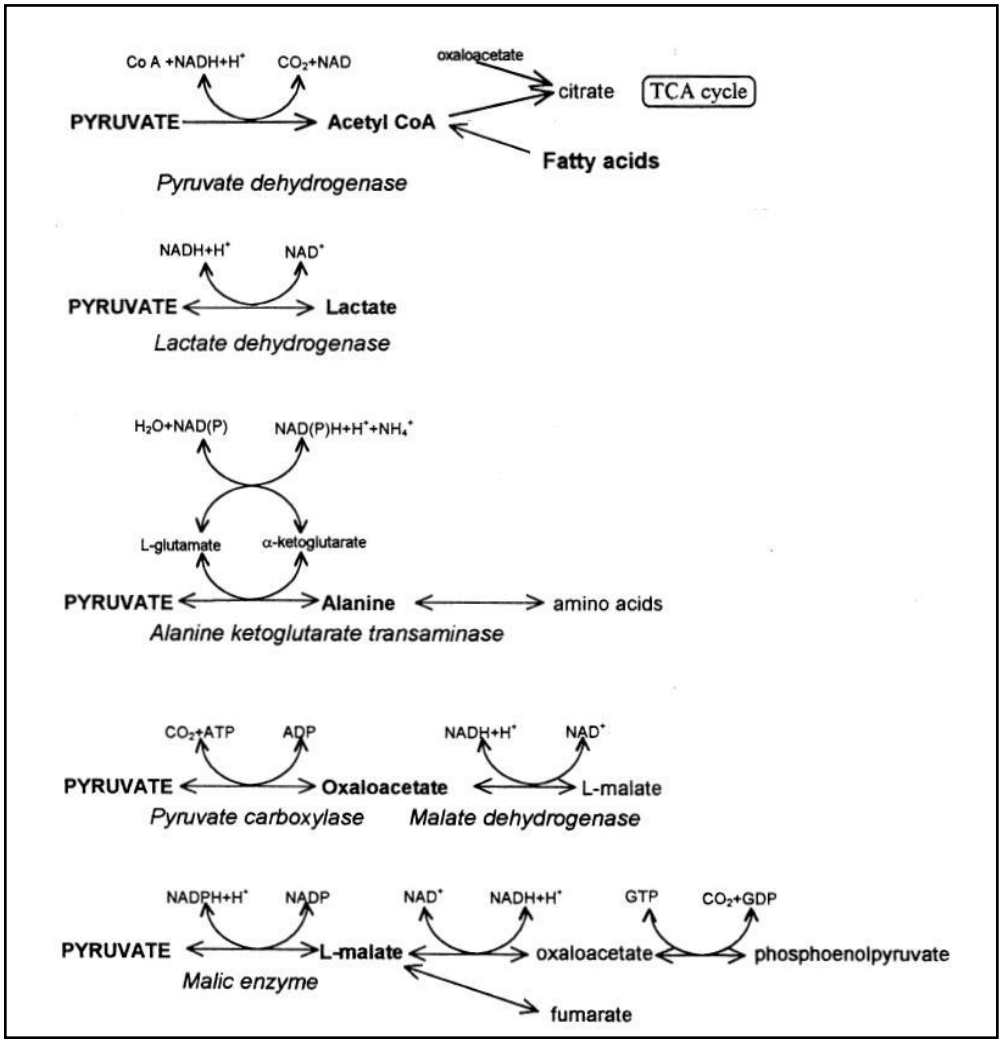

Figure 3.3. Fates of pyruvate (King and Opie, 1998)

Pyruvate can also contribute to anaplerosis by transamination with glutamate to form alanine and the CAC intermediate α-ketoglutarate as shown in Figure 3.3. The rate of alanine output by the myocardium is relatively low in dogs, pigs, and humans and is unaffected by acute ischemia or when glycolysis is accelerated with hyperinsulinemia and hyperglycemia (Stanley *et al*., 2005).

3.5. Fatty Acid Metabolism

3.5.1. Transport

Three mechanisms are thought to play an important role in FA transcardiomyocyte membrane transport:

- Passive diffusion
- Albumin receptor mediated diffusion
- Protein mediated FA-transport system (Kodde *et al*., 2007)

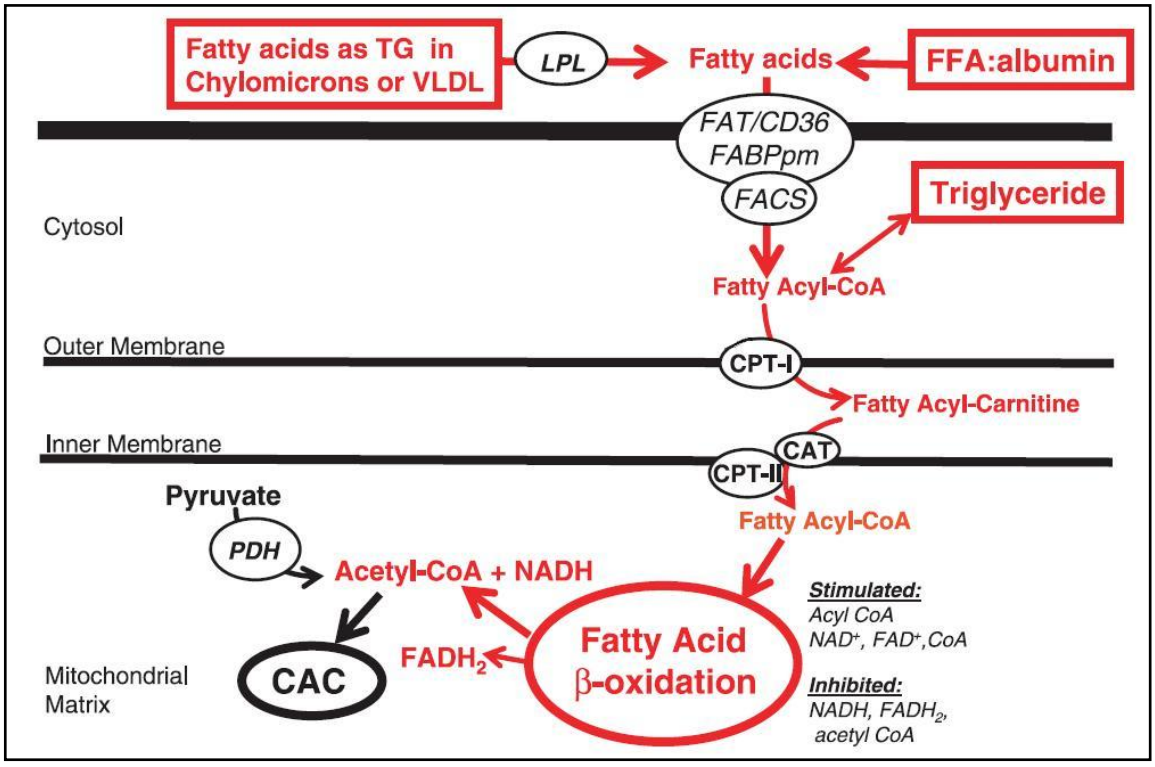

Figure 3.4. Schematic depiction of myocardial fatty acid metabolism (Stanley *et al*., 2005)

Passive diffusion is the absorption of unbound FA in the outer cardiomyocyte membrane, followed by FA translocation toward inner cardiomyocyte membrane and subsequent desorption into cytoplasm. Due to their hydrophobic properties, unbound FA accounts for < 0.01% of the FA present in the blood. Thus, they contribute hardly to the total cardiac FA uptake (Kodde *et al*., 2007).

Albumin receptor acts as a docking place for the albumin-bound FA and it facilitates FA dissociation by comprising FA release near the cardiomyocyte or directly into the outer cardiomyocyte membrane followed by desorption into the cytoplasm (Kodde *et al*., 2007).

Protein mediated transport involves either a fatty acid translocase (FAT) or a plasma membrane fatty acid binding protein (FABPpm) as shown in Figure 3.4 (Stanley *et al*.,

2005). Once transported across the sarcolemma the nonesterified fatty acids bind to FABP and are then activated by esterification to fatty acyl-CoA synthase (Stanley *et al.*, 2005).

Table 3.5. Fatty acid transport and activation reactions

Reaction Name	**Enzyme**	**Reaction**	**Type**	**E.C. #**
TRANS 04		ei-ca[e] -> ei-ca[c]	Uptake	
TRANS 05		hd-ca[e] -> hd-ca[c]	Uptake	
TRANS 06		od-ca[e] -> od-ca[c]	Uptake	
TRANS 07		td-ca[e] -> td-ca[c]	Uptake	
TRANS 08		dd-ca[e] -> dd-ca[c]	Uptake	
TRANS 09		d-ca[e] -> d-ca[c]	Uptake	
TRANS 10		o-ca[e] -> o-ca[c]	Uptake	
TRANS 11		pd-ca[e] -> pd-ca[c]	Uptake	
TRANS 12		od9-ca[e] -> od9-ca[c]	Uptake	
TRANS 13		od9-12-ca[e] -> od9-12-ca[c]	Uptake	
TRANS 14		hd9-ca[e] -> hd9-ca[c]	Uptake	
TRANS 15		tcs-ca[e] -> tcs-ca[c]	Uptake	
TRANS 16		dcs-ca[e] -> dcs-ca[c]	Uptake	
BOX 01	fatty-acid-CoA ligase (eicosanoate, C20:0)	[c]: atp + coa + ei-ca <=> amp + ei-coa + ppi	Activation	6.2.1.3
BOX 09	fatty-acid-CoA ligase (octadecanoate, C18:0)	[c]: atp + coa + od-ca <=> amp + od-coa + ppi	Activation	6.2.1.3
BOX 17	fatty-acid-CoA ligase (hexadecanoate, C16:0)	[c]: atp + coa + hd-ca <=> amp + hd-coa + ppi	Activation	6.2.1.3
BOX 25	fatty-acid-CoA ligase (tetradecanoate, C14:0)	[c]: atp + coa + td-ca <=> amp + td-coa + ppi	Activation	6.2.1.3
BOX 33	fatty-acid-CoA ligase (dodecanoate, C12:0)	[c]: atp + coa + dd-ca <=> amp + dd-coa + ppi	Activation	6.2.1.3

Table 3.5. Fatty acid transport and activation reactions - continued

BOX 41	fatty-acid-CoA ligase (decanoate, C10:0)	[c]: atp + coa + d-ca <=> amp + d-coa + ppi	Activation	6.2.1.3
BOX 49	fatty-acid-CoA ligase (decanoate, C8:0)	[c]: atp + coa + o-ca <=> amp + o-coa + ppi	Activation	6.2.1.3
O-BOX 01	fatty-acid-CoA ligase (pentadecanoate, C15:0)	[c]: atp + coa + pd-ca <=> amp + pd-coa + ppi	Activation	6.2.1.3
U-BOX 01	fatty-acid-CoA ligase (octadecenoate, C18:1 n-9)	[c]: atp + coa + od9-ca <=> amp + od9-coa + ppi	Activation	6.2.1.3
U-BOX 18	fatty-acid-CoA ligase (octadecadienoate, C18:2 n-9,12,12)	[c]: atp + coa + od9-12-ca <=> amp + od9-12-coa + ppi	Activation	6.2.1.3
U-BOX 41	fatty-acid-CoA ligase (hexadecenoate, C16:1 n-9)	[c]: atp + coa + hd9-ca <=> amp + hd9-coa + ppi	Activation	6.2.1.3

3.5.2. Acyl-CoA Formation

Once the fatty acids enter the cytoplasm, they are converted to long-chain acyl-CoA by acyl-CoA synthase, presented as “Activation” reactions in Table 3.5.

3.5.3. L-Carnitine

To enter β-oxidation, long-chain acyl-CoA has to be transported into the mitochondria. To overcome mitochondrial membrane impermeability, long-chain acyl-CoA import requires a special transport mechanism: the carnitine palmitoyltransferase system (Table 3.6). It enables the cell to move the required long-chain acyl-CoA moieties between the compartments, while keeping the acyl-CoA pools in mitochondria and cytoplasm at the required quantities. The system comprises two transfer proteins and two additional proteins. Carnitine palmitoyltransferase 1 and 2 (CPT1 and CPT2, respectively) are responsible for transfer of the acyl moiety. A plasma membrane carnitine transporter ensures proper intracellular L-carnitine levels, and a carnitine acylcarnitine translocase shuttles acylcarnitine and free carnitine between CPT1 and CPT2 (Kodde *et al.*, 2007).

CPT1 is a transmembrane enzyme of the mitochondrial outer membrane that catalyzes the transfer of the long-chain acyl moiety from long-chain acyl-CoA to carnitine, to form long-chain acylcarnitine. The carnitine derivative is subsequently transported into the intermembrane space by CPT1. Carnitine acylcarnitine translocase transports LC acylcarnitine across the inner membrane towards CPT2. CPT2 transfers the acyl group of

LC acylcarnitine to CoA, forming LC acyl-CoA and releasing carnitine (Figure 3.4). The latter returns to the shuttle, while long-chain acyl-CoAwill enter the β-oxidation (Kodde *et al*., 2007).

Table 3.6. Reactions of carnitine palmitoyltransferase system

Reaction Name	**Enzyme**	**Reaction**	**Type**	**E.C. #**
BOX 02	carnitine eicosanoyltransferase	[c]: crn + ei-coa <=> ei-crn + coa	Transport into Mitochondria	2.3.1.21
BOX 03		ei-crn[c] -> ei-crn[m]	Transport into Mitochondria	
BOX 04	carnitine eicosanoyltransferase II	[m]: ei-crn + coa <=> crn + ei-coa	Transport into Mitochondria	2.3.1.21
BOX 10	carnitine octadecanoyltransferase	[c]: crn + od-coa <=> od-crn + coa	Transport into Mitochondria	2.3.1.21
BOX 11		od-crn[c] -> od-crn[m]	Transport into Mitochondria	
BOX 12	carnitine octadecanoyltransferase II	[m]: od-crn + coa <=> crn + od-coa	Transport into Mitochondria	2.3.1.21
BOX 18	carnitine O-palmitoyltransferase	[c]: crn + hd-coa <=> hd-crn + coa	Transport into Mitochondria	2.3.1.21
BOX 19		hd-crn[c] -> hd-crn[m]	Transport into Mitochondria	
BOX 20	carnitine O-palmitoyltransferase II	[m]: hd-crn + coa <=> crn + hd-coa	Transport into Mitochondria	2.3.1.21
BOX 26	carnitine tetradecanoyltransferase	[c]: crn + td-coa <=> td-crn + coa	Transport into Mitochondria	2.3.1.21
BOX 27		td-crn[c] -> td-crn[m]	Transport into Mitochondria	
BOX 28	carnitine tetradecanoyltransferase II	[m]: td-crn + coa <=> crn + td-coa	Transport into Mitochondria	2.3.1.21
BOX 34	carnitine dodecanoyltransferase	[c]: crn + dd-coa <=> dd-crn + coa	Transport into Mitochondria	2.3.1.21
BOX 35		dd-crn[c] -> dd-crn[m]	Transport into Mitochondria	
BOX 36	carnitine dodecanoyltransferase II	[m]: dd-crn + coa <=> crn + dd-coa	Transport into Mitochondria	2.3.1.21
BOX 42	carnitine decanoyltransferase	[c]: crn + d-coa <=> d-crn + coa	Transport into Mitochondria	2.3.1.21
BOX 43		d-crn[c] -> d-crn[m]	Transport into Mitochondria	
BOX 44	carnitine decanoyltransferase II	[m]: d-crn + coa <=> crn + d-coa	Transport into Mitochondria	2.3.1.21
BOX 50	carnitine decanoyltransferase	[c]: crn + o-coa <=> o-crn + coa	Transport into Mitochondria	2.3.1.21
BOX 51		o-crn[c] -> o-crn[m]	Transport into Mitochondria	
BOX 52	carnitine decanoyltransferase II	[m]: o-crn + coa <=> crn + o-coa	Transport into Mitochondria	2.3.1.21
O-BOX 02		[c]: crn + pd-coa <=> pd-crn + coa	Transport into Mitochondria	2.3.1.21
O-BOX 03	carnitine pentadecanoyltransferase	pd-crn[c] -> pd-crn[m]	Transport into Mitochondria	
O-BOX 04		[m]: pd-crn + coa <=> crn + pd-coa	Transport into Mitochondria	2.3.1.21
U-BOX 02		[c]: crn + od9-coa <=> od9-crn + coa	Transport into Mitochondria	2.3.1.21

Table 3.6. Reactions of carnitine palmitoyltransferase system - continued

Reaction Name	Enzyme	Reaction	Type	E.C. #
U-BOX 03	carnitine 9-cis-octadecenoyltransferase	od9-crn[c] -> od9-crn[m]	Transport into Mitochondria	
U-BOX 04		[m]: od9-crn + coa <=> crn + od9-coa	Transport into Mitochondria	2.3.1.21
U-BOX 19		[c]: crn + od9-12-coa <=> od9-12-crn + coa	Transport into Mitochondria	2.3.1.21
U-BOX 20	carnitine 9,12-cis-octadecadiecenoyltransferase	od9-12-crn[c] -> od9-12-crn[m]	Transport into Mitochondria	
U-BOX 21		[m]: od9-12-crn + coa <=> crn + od9-12-coa	Transport into Mitochondria	2.3.1.21
U-BOX 42		[c]: crn + hd9-coa <=> hd9-crn + coa	Transport into Mitochondria	2.3.1.21
U-BOX 43	carnitine 9-cis-octadecenoyltransferase	hd9-crn[c] -> hd9-crn[m]	Transport into Mitochondria	
U-BOX 44		[m]: hd9-crn + coa <=> crn + hd9-coa	Transport into Mitochondria	2.3.1.21

3.5.4. β-Oxidation

Once taken up by the mitochondria, fatty acids undergo β-oxidation, a process that repeatedly cleaves off two carbon acetyl-CoA units, generating NADH and $FADH_2$ in the process (Figure 3.5). The β-oxidation process involves four reactions, with specific enzymes for each step, and each reaction has specific enzymes for long-, medium-, and shortchain length fatty intermediates (Stanley *et al.*, 2005).

Table 3.7. Reactions of β-oxidation of saturated fatty acids

Reaction Name	Enzyme	Reaction	E.C. #
BOX 05	acyl-CoA dehydrogenase (eicosanoyl-CoA, C20:0CoA)	[m]: ei-coa + fad -> t-ei-coa + fadh2	1.3.99.13
BOX 06	3-hydroxyacyl-CoA dehydratase (3-hydroxyeicosanoyl-CoA, C18:0CoA)	[m]: t-ei-coa + h2o <=> 3h-ei-coa	4.2.1.17
BOX 07	3-hydroxyacyl-CoA dehydrogenase (3-oxoeicosanoyl-CoA C18:0CoA)	[m]: 3h-ei-coa + nad <=> 3o-ei-coa + nadh + h	1.1.1.35
BOX 08	acetyl-CoA C-acyltransferase (octadecanoyl-CoA C18:0CoA)	[m]: 3o-ei-coa + coa <=> od-coa + accoa	2.3.1.16
BOX 13	acyl-CoA dehydrogenase (Stearyl-CoA, C18:0CoA)	[m]: od-coa + fad -> t-od-coa + fadh2	1.3.99.13
BOX 14	3-hydroxyacyl-CoA dehydratase (3-hydroxyoctadecanoyl-CoA, C18:0CoA)	[m]: t-od-coa + h2o <=> 3h-od-coa	4.2.1.17
BOX 15	3-hydroxyacyl-CoA dehydrogenase (3-oxooctadecanoyl-CoA C18:0CoA)	[m]: 3h-od-coa + nad <=> 3o-od-coa + nadh + h	1.1.1.35
BOX 16	acetyl-CoA C-acyltransferase (palmitoyl-CoA C16:0CoA)	[m]: 3o-od-coa + coa <=> hd-coa + accoa	2.3.1.16
BOX 21	acyl-CoA dehydrogenase (hexadecanoyl-CoA C16:0CoA)	[m]: hd-coa + fad -> t-hd-coa + fadh2	1.3.99.13
BOX 22	3-hydroxyacyl-CoA dehydratase (3-hydroxyhexadecanoyl-CoA)	[m]: t-hd-coa + h2o <=> 3h-hd-coa	4.2.1.17

Table 3.7. Reactions of β-oxidation of saturated fatty acids

Reaction Name	Enzyme	Reaction	E.C. #
BOX 23	3-hydroxyacyl-CoA dehydrogenase (3-oxohexadecanoyl-CoA)	[m]: 3h-hd-coa + nad <=> 3o-hd-coa + nadh + h	1.1.1.35
BOX 24	acetyl-CoA C-acyltransferase (tetradecanoyl-CoA)	[m]: 3o-hd-coa + coa <=> td-coa + accoa	2.3.1.16
BOX 29	acyl-CoA dehydrogenase (tetradecanoyl-CoA)	[m]: td-coa + fad -> t-td-coa + fadh2	1.3.99.13
BOX 30	3-hydroxyacyl-CoA dehydratase (3-hydroxytetradecanoyl-CoA)	[m]: t-td-coa + h2o <=> 3h-td-coa	4.2.1.17
BOX 31	3-hydroxyacyl-CoA dehydrogenase (3-oxotetradecanoyl-CoA)	[m]: 3h-td-coa + nad <=> 3o-td-coa + nadh + h	1.1.1.35
BOX 32	acetyl-CoA C-acyltransferase (dodecanoyl-CoA)	[m]: 3o-td-coa + coa <=> dd-coa + accoa	2.3.1.16
BOX 37	acyl-CoA dehydrogenase (dodecanoyl-CoA C12:0CoA)	[m]: dd-coa + fad -> t-dd-coa + fadh2	1.3.99.13
BOX 38	3-hydroxyacyl-CoA dehydratase (3-hydroxydodecanoyl-CoA)	[m]: t-dd-coa + h2o <=> 3h-dd-coa	4.2.1.17
BOX 39	3-hydroxyacyl-CoA dehydrogenase (3-oxododecanoyl-CoA)	[m]: 3h-dd-coa + nad <=> 3o-dd-coa + nadh + h	1.1.1.35
BOX 40	acetyl-CoA C-acyltransferase (decanoyl-CoA)	[m]: 3o-dd-coa + coa <=> d-coa + accoa	2.3.1.16
BOX 45	acyl-CoA dehydrogenase (decanoyl-CoA C10:0CoA)	[m]: d-coa + fad -> t-d-coa + fadh2	1.3.99.13
BOX 46	3-hydroxyacyl-CoA dehydratase (3-hydroxydecanoyl-CoA)	[m]: t-d-coa + h2o <=> 3h-d-coa	4.2.1.17
BOX 47	3-hydroxyacyl-CoA dehydrogenase (3-oxodecanoyl-CoA)	[m]: 3h-d-coa + nad <=> 3o-d-coa + nadh + h	1.1.1.35
BOX 48	acetyl-CoA C-acyltransferase (octanoyl-CoA)	[m]: 3o-d-coa + coa <=> o-coa + accoa	2.3.1.16
BOX 53	acyl-CoA dehydrogenase (octanoyl-CoA C8:0CoA)	[m]: o-coa + fad -> t-o-coa + fadh2	1.3.99.13
BOX 54	3-hydroxyacyl-CoA dehydratase (3-hydroxyoctanoyl-CoA)	[m]: t-o-coa + h2o <=> 3h-o-coa	4.2.1.17
BOX 55	3-hydroxyacyl-CoA dehydrogenase (3-oxooctanoyl-CoA)	[m]: 3h-o-coa + nad <=> 3o-o-coa + nadh + h	1.1.1.35
BOX 56	acetyl-CoA C-acyltransferase (hexanoyl-CoA)	[m]: 3o-o-coa + coa <=> h-coa + accoa	2.3.1.16
BOX 57	acyl-CoA dehydrogenase (hexanoyl-CoA C6:0CoA)	[m]: h-coa + fad -> t-h-coa + fadh2	1.3.99.13
BOX 58	3-hydroxyacyl-CoA dehydratase (3-hydroxyhexanoyl-CoA)	[m]: t-h-coa + h2o <=> 3h-h-coa	4.2.1.17
BOX 59	3-hydroxyacyl-CoA dehydrogenase (3-oxohexanoyl-CoA)	[m]: 3h-h-coa + nad <=> 3o-h-coa + nadh + h	1.1.1.35
BOX 60	acetyl-CoA C-acyltransferase (butanoyl-CoA)	[m]: 3o-h-coa + coa <=> but-coa + accoa	2.3.1.16
BOX 61	acyl-CoA dehydrogenase (butanoyl-CoA C4:0CoA)	[m]: but-coa + fad -> t-but-coa + fadh2	1.3.99.13
BOX 62	3-hydroxyacyl-CoA dehydratase (3-hydroxybutanoyl-CoA)	[m]: t-but-coa + h2o <=> 3h-but-coa	4.2.1.17
BOX 63	3-hydroxyacyl-CoA dehydrogenase (3-oxobutanoyl-CoA)	[m]: 3h-but-coa + nad <=> acaccoa + nadh + h	1.1.1.35
BOX 64	acetyl-CoA C-acyltransferase (acetyl-CoA)	[m]: acaccoa + coa <=> (2) accoa	2.3.1.16

The enzymatic reactions of β-oxidation (Table 3.7) are performed by a highly organized single enzymatic complex known as the mitochondrial trifunctional protein (MTP) associated with the mitochondrial inner membrane. Recent studies have indicated

that an entirely different set of enzymes responsible for the β-oxidation of medium and short-chain fatty acids is present in the mitochondrial matrix (Marin-Garcia and Goldenthal, 2002).

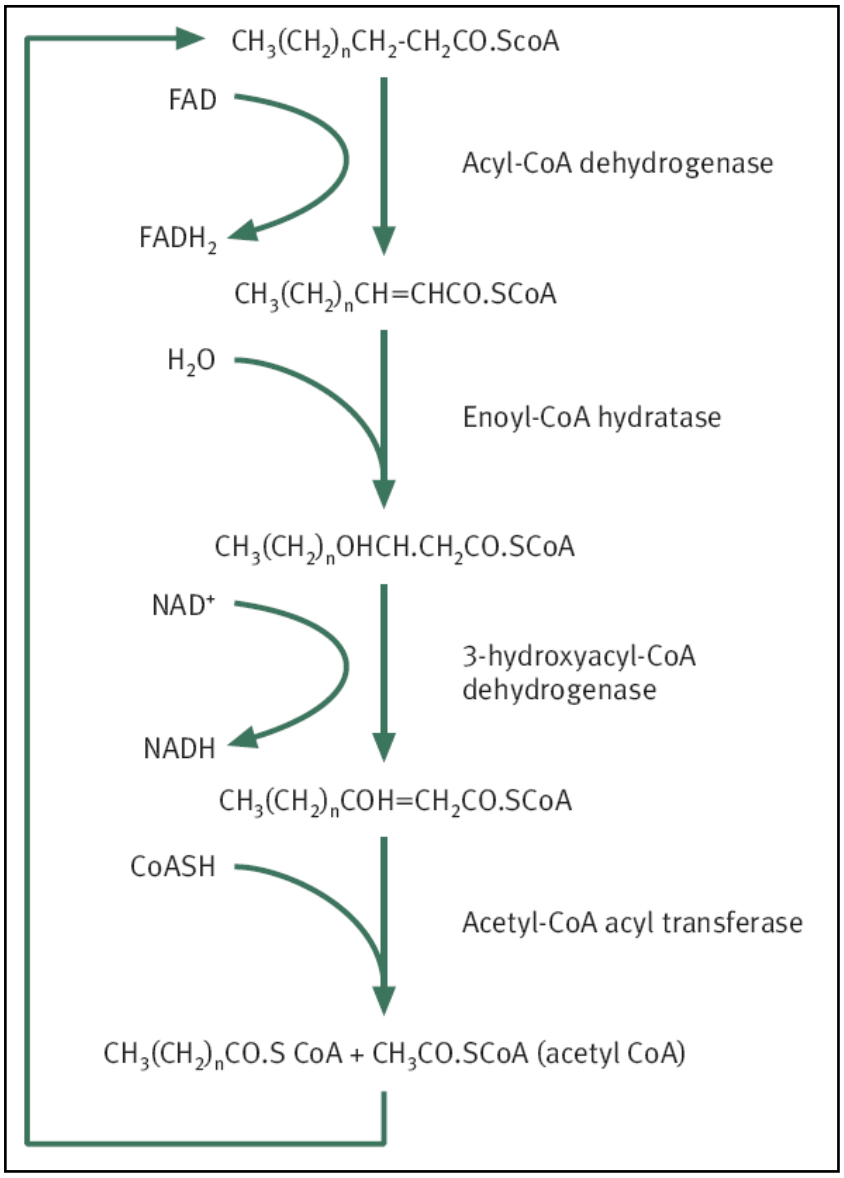

Figure 3.5. β-oxidation (Quinn and Pagano, 2004)

The first step is catalyzed by acyl-CoA dehydrogenase (BOX 05), followed by 2-enoyl-CoA hydratase (BOX 06), and then 3-hydroxyacyl-CoA dehydrogenase (BOX 07). The final step is 3-ketoacyl-CoA thiolase (3-KAT), which regenerates acyl-CoA for another round of β-oxidation and releases acetyl-CoA for the citric acid cycle (BOX 08). Acyl-CoA dehydrogenase and 3-hydroxyacyl-CoA dehydrogenase generate $FADH_2$ and

NADH, respectively, and the acetyl-CoA formed from β-oxidation generates more NADH and $FADH_2$ in the TCA (Stanley *et al*., 2005).

The acetyl-CoA, the end product of each round of β-oxidation, enters the TCA cycle, where it is further oxidized to CO_2 with the concomitant generation of NADH, $FADH_2$ and ATP. The NADH and $FADH_2$ generated during the fat oxidation and acetyl-CoA oxidation in the TCA cycle will subsequently enter the respiratory pathway for the production of ATP. Consequently, the oxidation of fatty acids yields more energy per carbon atom than does the oxidation of carbohydrates. However, while fatty acids produce more ATP during complete aerobic oxidation than glucose, this occurs at the expense of a higher rate of oxygen consumption. The supply of oxygen can be an important determinant of myocardial fuel utilization (Marin-Garcia and Goldenthal, 2002).

3.5.5. Oxidation of unsaturated and odd-chain fatty acids

Unsaturated fatty acids, which usually contain cis- doube bonds, are also degraded by β-oxidation. However, their double bonds must either be removed or moved during the degradation process. All double bonds found in unsaturated acids can be classified either as double bonds extending from odd-numbered carbon atoms, like the 9-cis double bond present in oleic acid, or as double bonds extending from even numbered carbon atoms like the 12-cis double bond of linoleic acid. Since both classes of double bonds are present in linoleic acid, its degradation exemplifies the breakdown of all unsaturated fatty acids (Vance and Vance, 1991).

The double bonds in fatty acids as linoleic acid pose three problems for the β-oxidation pathway that are solved through the actions of four additional enzymes:

- Enoyl-CoA isomerase
- 2,4-dienoyl-CoA reductase
- 3,2-enoyl-CoA isomerase
- 3,5-2,4-dienoyl-CoA isomerase (Voet *et al.*, 2006)

The reactions of the oxidation of linoleic acid (od9-12-ca) are presented in Table 3.8. Linoleic acid, after conversion to its CoA thioester (od9-12-coa), undergoes three cycles of β-oxidation (U-BOX 22-33) to yield 3-cis,6-cis-dodecadienoy-CoA (cis-3-6-dd-coa), which is the isomerized to 2-trans,6-cis-dodecadienoyl-CoA (t-2-6-dd-coa) by 3-cis,2-trans-enoyl-CoA isomerase. 2-trans,6-cis-dodecadienoyl-CoA can pass through the cycle (U-BOX 35-37) to yield 4-cis-decenoyl-CoA (d4-coa), which is dehydrogenated to 2-trans,4-cis-decadienoyl-CoA (d2-4-coa) by acyl-CoA dehydrogenase (U-BOX 38). 2-trans,4-cis-decadienoyl-CoA cannot be directly β-oxidized, but first is reduced by NADPH in a reaction catalyzed by 2,4-dienoyl-CoA reductase (U-BOX 39). The product of this reaction , 3-trans-decenoyl-CoA (cis-d-coa) is isomerized by 3-cis,2-trans-enoyl-CoA isomerase to 2-trans-decenoyl-CoA (t-d-coa) (U-BOX 40),which can be completely degraded by passing four times through the β-oxidation (Vance and Vance, 1991).

Table 3.8. Reactions of β-oxidation of unsaturated fatty acids

Reaction Name	**Enzyme**	**Reaction**	**E.C. #**
U-BOX 05	acyl-CoA dehydrogenase (octadecenoyl-CoA,C18:1CoA, n-9)	[m]: od9-coa + fad -> t-od9-coa + fadh2	1.3.99.13
U-BOX 06	3-hydroxyacyl-CoA dehydratase (3-hydroxyoctadecenoyl-CoA, C18:1CoA, n-9)	[m]: t-od9-coa + h2o <=> 3h-od9-coa	4.2.1.17
U-BOX 07	3-hydroxyacyl-CoA dehydrogenase (3-oxooctadecenoyl-CoA C18:1CoA, n-9)	[m]: 3h-od9-coa + nad <=> 3o-od9-coa + nadh + h	1.1.1.35
U-BOX 08	acetyl-CoA C-acyltransferase (hexadecenoyl-CoA C16:1CoA, n-7)	[m]: 3o-od9-coa + coa <=> hd7-coa + accoa	2.3.1.16
U-BOX 09	acyl-CoA dehydrogenase (hexadecenoyl-CoA, C16:1CoA, n-7)	[m]: hd7-coa + fad -> t-hd7-coa + fadh2	1.3.99.13
U-BOX 10	3-hydroxyacyl-CoA dehydratase (3-hydroxyhexadecenoyl-CoA, C16:1CoA, n-7)	[m]: t-hd7-coa + h2o <=> 3h-hd7-coa	4.2.1.17
U-BOX 11	3-hydroxyacyl-CoA dehydrogenase (3-oxohexadecenoyl-CoA C16:1CoA, n-7)	[m]: 3h-hd7-coa + nad <=> 3o-hd7-coa + nadh + h	1.1.1.35
U-BOX 12	acetyl-CoA C-acyltransferase (tetradecenoyl-CoA C14:1CoA, n-5)	[m]: 3o-hd7-coa + coa <=> td5-coa + accoa	2.3.1.16
U-BOX 13	acyl-CoA dehydrogenase (tetradecenoyl-CoA, C14:1CoA, n-5)	[m]: td5-coa + fad -> t-td5-coa + fadh2	1.3.99.13
U-BOX 14	3-hydroxyacyl-CoA dehydratase (3-hydroxytetradecenoyl-CoA, C14:1CoA, n-5)	[m]: t-td5-coa + h2o <=> 3h-td5-coa	4.2.1.17
U-BOX 15	3-hydroxyacyl-CoA dehydrogenase (3-oxotetradecenoyl-CoA C14:1CoA, n-5)	[m]: 3h-td5-coa + nad <=> 3o-td5-coa + nadh + h	1.1.1.35
U-BOX 16	acetyl-CoA C-acyltransferase (dodecenoyl-CoA C12:1CoA, n-3)	[m]: 3o-td5-coa + coa <=> cisdd-coa + accoa	2.3.1.16

Table 3.8. Reactions of β-oxidation of unsaturated fatty acids - continued

Reaction Name	Enzyme	Reaction	E.C. #
U-BOX 17	Δ3-cis-Δ2-trans-enoyl-CoA isomerase	[m]: cisdd-coa <=> t-dd-coa	5.3.3.8
U-BOX 22	acyl-CoA dehydrogenase (octadecadienoyl-CoA,C18:2CoA, n-9,12)	[m]: od9-12-coa + fad -> t-od9-12-coa + fadh2	1.3.99.13
U-BOX 23	3-hydroxyacyl-CoA dehydratase (3-hydroxyoctadecadienoyl-CoA, C18:2CoA, n-9,12)	[m]: t-od9-12-coa + h2o <=> 3h-od9-12-coa	4.2.1.17
U-BOX 24	3-hydroxyacyl-CoA dehydrogenase (3-oxooctadecadienoyl-CoA C18:2CoA, n-9,12)	[m]: 3h-od9-12-coa + nad <=> 3o-od9-12-coa + nadh + h	1.1.1.35
U-BOX 25	acetyl-CoA C-acyltransferase (hexadecadienoyl-CoA C16:2CoA, n-7,10)	[m]: 3o-od9-12-coa + coa <=> hd-7-10-coa + accoa	2.3.1.16
U-BOX 26	acyl-CoA dehydrogenase (hexadecadienoyl-CoA, C16:2CoA, n-7,10)	[m]: hd-7-10-coa + fad -> t-hd-7-10-coa + fadh2	1.3.99.13
U-BOX 27	3-hydroxyacyl-CoA dehydratase (3-hydroxyhexadecadienoyl-CoA, C16:2CoA, n-7,10)	[m]: t-hd-7-10-coa + h2o <=> 3h-hd-7-10-coa	4.2.1.17
U-BOX 28	3-hydroxyacyl-CoA dehydrogenase (3-oxohexadecadienoyl-CoA C16:2CoA, n-7,10)	[m]: 3h-hd-7-10-coa + nad <=> 3o-hd-7-10-coa + nadh + h	1.1.1.35
U-BOX 29	acetyl-CoA C-acyltransferase (tetradecadienoyl-CoA C14:2CoA, n-5,8)	[m]: 3o-hd-7-10-coa + coa <=> td-5-8-coa + accoa	2.3.1.16
U-BOX 30	acyl-CoA dehydrogenase (tetradecadienoyl-CoA, C14:2CoA, n-5,8)	[m]: td-5-8-coa + fad -> t-td-5-8-coa + fadh2	1.3.99.13
U-BOX 31	3-hydroxyacyl-CoA dehydratase (3-hydroxytetradecadienoyl-CoA, C14:2CoA, n-5,8)	[m]: t-td-5-8-coa + h2o <=> 3h-td-5-8-coa	4.2.1.17
U-BOX 32	3-hydroxyacyl-CoA dehydrogenase (3-oxotetradecadienoyl-CoA C14:2CoA, n-5,8)	[m]: 3h-td-5-8-coa + nad <=> 3o-td-5-8-coa + nadh + h	1.1.1.35
U-BOX 33	acetyl-CoA C-acyltransferase (dodecadienoyl-CoA C12:2CoA, n-3,6)	[m]: 3o-td-5-8-coa + coa <=> cis-3-6-dd-coa + accoa	2.3.1.16
U-BOX 34	Δ3-cis-Δ2-trans-enoyl-CoA isomerase	[m]: cis-3-6-dd-coa <=> t-2-6-dd-coa	5.3.3.8
U-BOX 35	3-hydroxyacyl-CoA dehydratase (3-hydroxydodecadienoyl-CoA, C12:2CoA, n-2,6)	[m]: t-2-6-dd-coa + h2o <=> 3h-2-6-dd-coa	4.2.1.17
U-BOX 36	3-hydroxyacyl-CoA dehydrogenase (3-oxododecadienoyl-CoA C12:2CoA, n-2,6)	[m]: 3h-2-6-dd-coa + nad <=> 3o-2-6-dd-coa + nadh + h	1.1.1.35
U-BOX 37	acetyl-CoA C-acyltransferase (decenoyl-CoA C10:1CoA, n-4)	[m]: 3o-2-6-dd-coa + coa <=> d4-coa + accoa	2.3.1.16
U-BOX 38	acyl-CoA dehydrogenase (decenoyl-CoA,C10:1CoA, n-4)	[m]: d4-coa + fad -> d2-4-coa + fadh2	1.3.99.13
U-BOX 39	2,4-Dienoyl-CoA reductase	[m]: d2-4-coa + nadph + h <=> cis-d-coa + nadp	
U-BOX 40	Δ3-cis-Δ2-trans-enoyl-CoA isomerase	[m]: cis-d-coa <=> t-d-coa	
U-BOX 45	acyl-CoA dehydrogenase (hexadecenoyl-CoA, C16:1CoA, n-9)	[m]: hd9-coa + fad -> t-hd9-coa + fadh2	1.3.99.13

Table 3.8. Reactions of β-oxidation of unsaturated fatty acids - continued

Reaction Name	Enzyme	Reaction	E.C. #
U-BOX 46	3-hydroxyacyl-CoA dehydratase (3-hydroxyhexadecenoyl-CoA, C16:1CoA, n-9)	[m]: t-hd9-coa + h2o <=> 3h-hd9-coa	4.2.1.17
U-BOX 47	3-hydroxyacyl-CoA dehydrogenase (3-oxohexadecenoyl-CoA C16:1CoA, n-9)	[m]: 3h-hd9-coa + nad <=> 3o-hd9-coa + nadh + h	1.1.1.35
U-BOX 48	acetyl-CoA C-acyltransferase (tetradecenoyl-CoA C14:1CoA, n-7)	[m]: 3o-hd9-coa + coa <=> td7-coa + accoa	2.3.1.16
U-BOX 49	acyl-CoA dehydrogenase (tetradecenoyl-CoA, C14:1CoA, n-7)	[m]: td7-coa + fad -> t-td7-coa + fadh2	1.3.99.13
U-BOX 50	3-hydroxyacyl-CoA dehydratase (3-hydroxytetradecenoyl-CoA, C14:1CoA, n-7)	[m]: t-td7-coa + h2o <=> 3h-td7-coa	4.2.1.17
U-BOX 51	3-hydroxyacyl-CoA dehydrogenase (3-oxotetradecenoyl-CoA C14:1CoA, n-7)	[m]: 3h-td7-coa + nad <=> 3o-td7-coa + nadh + h	1.1.1.35
U-BOX 52	acetyl-CoA C-acyltransferase (dodecenoyl-CoA C12:1CoA, n-5)	[m]: 3o-td7-coa + coa <=> dd5-coa + accoa	2.3.1.16
U-BOX 53	acyl-CoA dehydrogenase (dodecenoyl-CoA,C12:1CoA, n-5)	[m]: dd5-coa + fad -> t-dd5-coa + fadh2	1.3.99.13
U-BOX 54	3-hydroxyacyl-CoA dehydratase (3-hydroxydodecenoyl-CoA, C12:1CoA, n-5)	[m]: t-dd5-coa + h2o <=> 3h-dd5-coa	4.2.1.17
U-BOX 55	3-hydroxyacyl-CoA dehydrogenase (3-oxododecenoyl-CoA C12:1CoA, n-5)	[m]: 3h-dd5-coa + nad <=> 3o-dd5-coa + nadh + h	1.1.1.35
U-BOX 56	acetyl-CoA C-acyltransferase (decenoyl-CoA C10:1CoA, n-3)	[m]: 3o-dd5-coa + coa <=> cisd-coa + accoa	2.3.1.16
U-BOX 57	Δ3-cis-Δ2-trans-enoyl-CoA isomerase	[m]: cisd-coa <=> t-d-coa	5.3.3.8

The oxidation of fatty acids with odd-number of carbons (Table 3.9) proceeds by β-oxidation and yields, in addition to acetyl-CoA, one mole of propionyl-CoA per mole of fatty acid (O-BOX 29).

Table 3.9. Reactions of β-oxidation of odd-chain fatty acids

Reaction Name	Enzyme	Reaction	E.C. #
O-BOX 05	acyl-CoA dehydrogenase (pentadecanoyl-CoA)	[m]: pd-coa + fad -> t-pd-coa + fadh2	1.3.99.13
O-BOX 06	3-hydroxyacyl-CoA dehydratase (3-hydroxypentadecanoyl-CoA)	[m]: t-pd-coa + h2o <=> 3h-pd-coa	4.2.1.17
O-BOX 07	3-hydroxyacyl-CoA dehydrogenase (3-oxopentadecanoyl-CoA)	[m]: 3h-pd-coa + nad <=> 3o-pd-coa + nadh + h	1.1.1.35
O-BOX 08	acetyl-CoA C-acyltransferase (tridecanoyl-CoA)	[m]: 3o-pd-coa + coa <=> trd-coa + accoa	2.3.1.16
O-BOX 09	acyl-CoA dehydrogenase (tridecanoyl-CoA)	[m]: trd-coa + fad -> t-trd-coa + fadh2	1.3.99.13
O-BOX 10	3-hydroxyacyl-CoA dehydratase (3-hydroxytridecanoyl-CoA)	[m]: t-trd-coa + h2o <=> 3h-trd-coa	4.2.1.17

Table 3.9. Reactions of β-oxidation of odd-chain fatty acids - continued

Reaction Name	Enzyme	Reaction	E.C. #
O-BOX 11	3-hydroxyacyl-CoA dehydrogenase (3-oxotridecanoyl-CoA)	[m]: 3h-trd-coa + nad <=> 3o-trd-coa + nadh + h	1.1.1.35
O-BOX 12	acetyl-CoA C-acyltransferase (endecanoyl-CoA)	[m]: 3o-trd-coa + coa <=> ed-coa + accoa	2.3.1.16
O-BOX 13	acyl-CoA dehydrogenase (endecanoyl-CoA)	[m]: ed-coa + fad -> t-ed-coa + fadh2	1.3.99.13
O-BOX 14	3-hydroxyacyl-CoA dehydratase (3-hydroxyendecanoyl-CoA)	[m]: t-ed-coa + h2o <=> 3h-ed-coa	4.2.1.17
O-BOX 15	3-hydroxyacyl-CoA dehydrogenase (3-oxoendecanoyl-CoA)	[m]: 3h-ed-coa + nad <=> 3o-ed-coa + nadh + h	1.1.1.35
O-BOX 16	acetyl-CoA C-acyltransferase (nonanoyl-CoA)	[m]: 3o-ed-coa + coa <=> n-coa + accoa	2.3.1.16
O-BOX 17	acyl-CoA dehydrogenase (nonanoyl-CoA)	[m]: n-coa + fad -> t-n-coa + fadh2	1.3.99.13
O-BOX 18	3-hydroxyacyl-CoA dehydratase (3-hydroxynonanoyl-CoA)	[m]: t-n-coa + h2o <=> 3h-n-coa	4.2.1.17
O-BOX 19	3-hydroxyacyl-CoA dehydrogenase (3-oxononanoyl-CoA)	[m]: 3h-n-coa + nad <=> 3o-n-coa + nadh + h	1.1.1.35
O-BOX 20	acetyl-CoA C-acyltransferase (heptanoyl-CoA)	[m]: 3o-n-coa + coa <=> hpd-coa + accoa	2.3.1.16
O-BOX 21	acyl-CoA dehydrogenase (heptanoyl-CoA)	[m]: hpd-coa + fad -> t-hpd-coa + fadh2	1.3.99.13
O-BOX 22	3-hydroxyacyl-CoA dehydratase (3-hydroxyheptanoyl-CoA)	[m]: t-hpd-coa + h2o <=> 3h-hpd-coa	4.2.1.17
O-BOX 23	3-hydroxyacyl-CoA dehydrogenase (3-oxoheptanoyl-CoA)	[m]: 3h-hpd-coa + nad <=> 3o-hpd-coa + nadh + h	1.1.1.35
O-BOX 24	acetyl-CoA C-acyltransferase (pentanoyl-CoA)	[m]: 3o-hpd-coa + coa <=> p-coa + accoa	2.3.1.16
O-BOX 26	acyl-CoA dehydrogenase (pentanoyl-CoA)	[m]: p-coa + fad -> t-p-coa + fadh2	1.3.99.13
O-BOX 27	3-hydroxyacyl-CoA dehydratase (3-hydroxypentanoyl-CoA)	[m]: t-p-coa + h2o <=> 3h-p-coa	4.2.1.17
O-BOX 28	3-hydroxyacyl-CoA dehydrogenase (3-oxopentanoyl-CoA)	[m]: 3h-p-coa + nad <=> 3o-p-coa + nadh + h	1.1.1.35
O-BOX 29	acetyl-CoA C-acyltransferase (propanoyl CoA)	[m]: 3o-p-coa + coa <=> prop-coa + accoa	2.3.1.16
O-BOX 30	Propionyl-CoA carboxylase mitochondrial	[m]: atp + co2 + prop-coa -> adp + mmcoa-S + pi	6.4.1.3
O-BOX 31	methylmalonyl-CoA epimerase mitochondrial	[m]: mmcoa-S <=> mmcoa-R	5.1.99.1
O-BOX 32	R-methylmalonyl-CoA mutase mitochondrial	[m]: mmcoa-R -> succoa	5.4.99.2

3.5.6. Peroxisomal β-Oxidation

In mammalian cell the bulk of β-oxidation occurs in mitochondria, but peroxisomes also oxidize fatty acids, particularly those with very long (>22) chains or branced chains.

Very long fatty acids are transported into peroxisomes by a mechanism that does not require carnitine (PBOX 01 and PBOX 07), and activated by acyl-CoA synthetase (PBOX

02 and PBOX 08). Peroxisomal β-oxidation results in the same chemical changes to fatty acids as in the mitochondrial pathway but only requires three enzymes:

- Acyl-coa oxidase
- Enoyl-coa +3-L-hydroxyacyl-coa (on a single polypeptide)
- Peroxisomal thiolase

Table 3.10. Reactions of peroxisomal β-oxidation

Reaction Name	**Enzyme**	**Reaction**	**E.C. #**
PBOX 01	ABCD1/ABCD3 homodimer	tcs-coa[c] -> tcs-coa[p]	
PBOX 02	fatty-acid-CoA ligase (Tetracosanoic acid, C24:0)	[c]: atp + coa + tcs-ca <=> amp + tcs-coa + ppi	6.2.1.3
PBOX 03	acyl-CoA oxidase (docosanoyl-CoA, C24:0CoA)	[p]: tcs-coa + o2 <=> t-tcs-coa + h2o2	1.3.99.13
PBOX 04	Trifunctional enzyme	[p]: t-tcs-coa + h2o <=> 3h-tcs-coa	
PBOX 05	Trifunctional enzyme	[p]: 3h-tcs-coa + nad <=> 3o-tcs-coa + nadh + h	
PBOX 06	acetyl-CoA C-acyltransferase (docosanoyl-CoA C22:0CoA)	[p]: 3o-tcs-coa + coa <=> dcs-coa + accoa	2.3.1.16
PBOX 07		dcs-coa[c] -> dcs-coa[p]	
PBOX 08	fatty-acid-CoA ligase (Docosanoate, C22:0)	[c]: atp + coa + dcs-ca <=> amp + dcs-coa + ppi	6.2.1.3
PBOX 09	acyl-CoA oxidase (docosanoyl-CoA, C22:0CoA)	[p]: dcs-coa + o2 <=> t-dcs-coa + h2o2	1.3.99.13
PBOX 10	Trifunctional enzyme	[p]: t-dcs-coa + h2o <=> 3h-dcs-coa	
PBOX 11	Trifunctional enzyme	[p]: 3h-dcs-coa + nad <=> 3o-dcs-coa + nadh + h	
PBOX 12	acetyl-CoA C-acyltransferase (eicosanoyl-CoA C20:0CoA)	[p]: 3o-dcs-coa + coa <=> ei-coa + accoa	2.3.1.16
PBOX 13		ei-coa[p] -> ei-coa[c]	
PBOX 14	acyl-CoA oxidase (eicosanoyl-CoA, C20:0CoA)	[p]: ei-coa + o2 <=> t-ei-coa + h2o2	1.3.99.13
PBOX 15	Trifunctional enzyme	[p]: t-ei-coa + h2o <=> 3h-ei-coa	
PBOX 16	Trifunctional enzyme	[p]: 3h-ei-coa + nad <=> 3o-ei-coa + nadh + h	
PBOX 17	acetyl-CoA C-acyltransferase (octadecanoyl-CoA C18:0CoA)	[p]: 3o-ei-coa + coa <=> od-coa + accoa	2.3.1.16
PBOX 18		od-coa[p] -> od-coa[c]	
PBOX 19	acyl-CoA oxidase (Stearyl-CoA, C18:0CoA)	[p]: od-coa + o2 <=> t-od-coa + h2o2	1.3.99.13
PBOX 20	Trifunctional enzyme	[p]: t-od-coa + h2o <=> 3h-od-coa	
PBOX 21	Trifunctional enzyme	[p]: 3h-od-coa + nad <=> 3o-od-coa + nadh + h	

Table 3.10. Reactions of peroxisomal β-oxidation - continued

Reaction Name	Enzyme	Reaction	E.C. #
PBOX 22	acetyl-CoA C-acyltransferase (palmitoyl-CoA C16:0CoA)	[p]: 3o-od-coa + coa <=> hd-coa + accoa	2.3.1.16
PBOX 23		hd-coa[p] -> hd-coa[c]	
PBOX 24	acyl-CoA oxidase (hexadecanoyl-CoA C16:0CoA)	[p]: hd-coa + o2 <=> t-hd-coa + h2o2	1.3.99.13
PBOX 25	Trifunctional enzyme	[p]: t-hd-coa + h2o <=> 3h-hd-coa	
PBOX 26	Trifunctional enzyme	[p]: 3h-hd-coa + nad <=> 3o-hd-coa + nadh + h	
PBOX 27	acetyl-CoA C-acyltransferase (tetradecanoyl-CoA)	[p]: 3o-hd-coa + coa <=> td-coa + accoa	2.3.1.16
PBOX 28		td-coa[p] -> td-coa[c]	
PBOX 29	acyl-CoA oxidase (tetradecanoyl-CoA)	[p]: td-coa + o2 <=> t-td-coa + h2o2	1.3.99.13
PBOX 30	Trifunctional enzyme	[p]: t-td-coa + h2o <=> 3h-td-coa	
PBOX 31	Trifunctional enzyme	[p]: 3h-td-coa + nad <=> 3o-td-coa + nadh + h	
PBOX 32	acetyl-CoA C-acyltransferase (dodecanoyl-CoA)	[p]: 3o-td-coa + coa <=> dd-coa + accoa	2.3.1.16
PBOX 33		dd-coa[p] -> dd-coa[c]	
PBOX 34	acyl-CoA oxidase (dodecanoyl-CoA C12:0CoA)	[p]: dd-coa + o2 <=> t-dd-coa + h2o2	1.3.99.13
PBOX 35	Trifunctional enzyme	[p]: t-dd-coa + h2o <=> 3h-dd-coa	
PBOX 36	Trifunctional enzyme	[p]: 3h-dd-coa + nad <=> 3o-dd-coa + nadh + h	
PBOX 37	acetyl-CoA C-acyltransferase (decanoyl-CoA)	[p]: 3o-dd-coa + coa <=> d-coa + accoa	2.3.1.16
PBOX 38		d-coa[p] -> d-coa[c]	
PBOX 39	acyl-CoA oxidase (decanoyl-CoA C10:0CoA)	[p]: d-coa + o2 <=> t-d-coa + h2o2	1.3.99.13
PBOX 40	Trifunctional enzyme	[p]: t-d-coa + h2o <=> 3h-d-coa	
PBOX 41	Trifunctional enzyme	[p]: 3h-d-coa + nad <=> 3o-d-coa + nadh + h	
PBOX 42	acetyl-CoA C-acyltransferase (octanoyl-CoA)	[p]: 3o-d-coa + coa <=> o-coa + accoa	2.3.1.16
P-BOX 43		o-coa[p] -> o-coa[c]	
P-BOX 44		accoa[p] -> accoa[c]	
P-BOX 45		accoa[c] + crn[c] -> accrn[c] + coa[c]	
P-BOX 46		accrn[c] -> accrn[m]	
P-BOX 47		[m]: accrn + coa -> accoa + crn	

3.6. Triglyceride Metabolism

Triacylglycerols play an important role in energy storage in animals. Most of the triacylglycerols are deposited in the adipose tissue. However, triacylglycerols can be deposited in liver, heart and skeletal muscle under several conditions of metabolic stress when the supply of fatty acids from adipose tissue exceeds the need, or the capacity of the cell to oxidize them.

Table 3.11. Reactions of triglyceride metabolism

Reaction Name	Enzyme	Reaction	E.C. #
TRIGLY 00	glycerol-3-phosphate dehydrogenase	[c]: dhap + nadh <=> glyc3p + nad	1.1.1.8
TRIGLY 01	glycerate kinase	[c]: 3pg + adp <=> atp + glycrt	2.7.1.13
TRIGLY 02	aldehyde dehydrogenase	[c]: glycrt + nadh + h <=> glyc-ald + nad + h2o	1.2.1.3
TRIGLY 03	aldehyde reductase	[c]: glyc-ald + nadph + h <=> glyc + nadp	1.1.1.21 1.1.1.2
TRIGLY 04	aldehyde reductase	[c]: glyc-ald + nadh + h <=> glyc + nad	1.1.1.21 1.1.1.2
TRIGLY 05	glycerol kinase	[c]: glyc + atp -> glyc3p + adp	2.7.1.30
TRIGLY 06	glycerol-3-phosphate acyltransferase, mitochondrial	[c]: glyc3p + fa-coa -> lpa + coa	2.3.1.15
TRIGLY 07	1-acylglycerol-3-phosphate O-acyltransferase 1	[c]: lpa + fa-coa -> pda + coa	2.3.1.51
TRIGLY 08	phosphatidic acid phosphatase type 2A	[c]: pda + h2o -> 12glyc + pi	3.1.3.4
TRIGLY 09	diacylglycerol O-acyltransferase	[c]: 12glyc + fa-coa -> triglyc + coa	2.3.1.20
TRIGLY 10	lipoprotein lipase	[c]: triglyc -> glyc + fa	3.1.1.34
TRIGLY 11	triacylglycerol lipase	[c]: triglyc + h2o -> 12glyc + fa	3.1.1.3
TRIGLY 12	diacylglycerol kinase	[c]: 12glyc + atp -> pda + adp	2.7.1.107
TRIGLY 13	carboxyl ester lipase	[c]: 12glyc + h2o -> aglyc + fa	3.1.1.3
TRIGLY 14	monoglyceride lipase	[c]: aglyc + h2o -> glyc + fa	3.1.1.23
TRIGLY 15	acylglycerol kinase	[c]: atp + aglyc -> adp + lpa	2.7.1.94

Table 3.11. Reactions of triglyceride metabolism - continued

Reaction Name	Enzyme	Reaction	E.C. #
TRANS 24		triglyc[e] <=> triglyc[c]	
TRIGLY 16	Average fatty acid of heart mitochondria	[c]: (0.03) td-coa + (0.37) hd-coa + (0.03) hd9-coa + (0.23) od9-coa + (0.16) od9-12-coa + (0.15) od-coa <=> fa-coa	
TRIGLY 17	Average fatty acid of heart mitochondria	[c]: fa <=> (0.03) td-ca + (0.37) hd-ca + (0.03) hd9-ca + (0.23) od9-ca + (0.16) od9-12-ca + (0.15) od-ca	

3.7. Ketone Body Metabolism

The liver releases acetoacetate and β-hydroxybutyrate, which are carried by bloodstream to the peripheral tissues for use as alternative fuels. There these products are converted to acetyl-CoA. Acetoacetate is first converted to acetoacetyl-CoA (KETONE 01) and then to acetyl-CoA by reaction BOX 64 given in Table 3.7. (Voet *et al.*, 2006).

Table 3.12. Reactions of ketone bodies

Reaction Name	Enzyme	Reaction	E.C. #
TRANS 16		acac[e] -> acac[c]	
I-TRANS		acac[c] -> acac[m]	
KETONE 01	3-oxoacid CoA transferase	[m]: acac + coa + atp -> acaccoa + adp + pi	2.8.3.5

3.8. TCA Cycle

Acetyl CoA (from β- and glucose oxidation) participates in a series of reactions within the mitochondrial matrix near the inner mitochondrial membrane. The metabolism of acetyl CoA in turn generates NADH and $FADH_2$ for the electron transport chain. NADH and $FADH_2$ (from the tricarboxylic acid cycle and that generated and transported into the mitochondria from the cytoplasm) are made available for the electron transport chain (Quinn and Pagano, 2004).

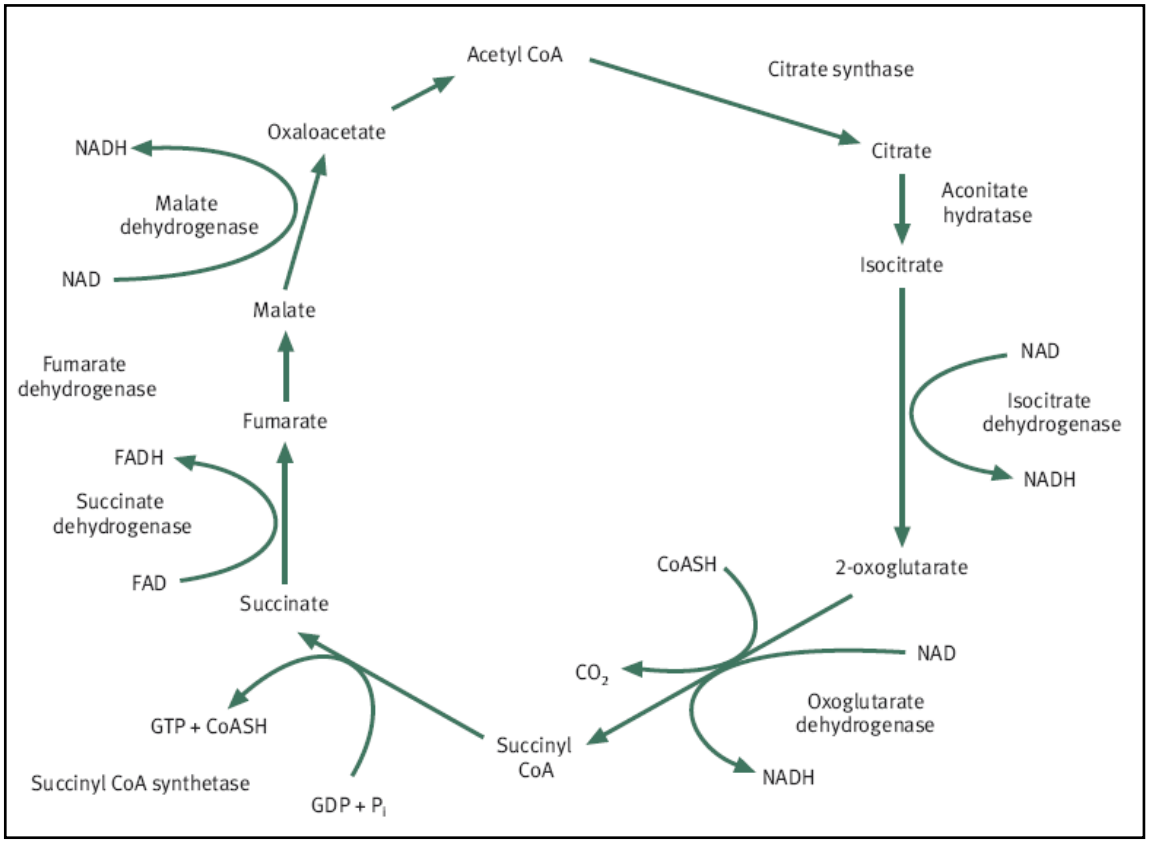

Figure 3.6. TCA Cycle (Quinn and Pagano, 2004)

In eukaryotes, all the enzymes of citric acid cycle are located in mitochondrion, so all the substrates including NAD and GDP must be generated or transported into mitochondria from cytosol. Similarly all products of TCA cycle must be consumed or transported into cytosol (Voet *et al.*, 2006).

The result of one cycle (Table 3.12) is the oxidation of one acetyl group to 2 CO_2, which requires the transfer of four pairs of electrons (The reduction of 3 NAD to 3 NADH accounts for three pairs of electrons, the reduction of FAD to $FADH_2$ accounts for the fourth pair) (Voet *et al*., 2006).

The Krebs cycle (Figure 3.6) is perhaps the best example for the paradigm of efficient energy transfer through metabolic cycles, which includes the recycling of CO_2 and H_2O. Under normoxic conditions, pyruvate is not only decarboxylated but also carboxylated to oxaloacetate and malate. This mechanism allows both a "refeeding" of Krebs cycle intermediates and a recycling of CO_2 produced from the action of

dehydrogenases. Fixation of CO_2 is particularly important during prolonged oxidation of fatty acids and ketone bodies, which can "unspan" the Krebs cycle by the sequestration of coenzyme A. The potential contribution of substrates to anaplerosis has given rise to the distinction between glucose and lactate, which produce both acetyl-CoA and oxaloacetate, and fatty acids or ketone bodies, which produce only acetyl-CoA. The need for anaplerosis may explain why glucose uptake is never completely inhibited in hearts perfused with fatty acids (Depre *et al.*, 1999).

Table 3.13. Reaction of TCA cycle

Reaction Name	Enzyme	Reaction	E.C. #
TCA 01	citrate synthase	[m]: accoa + h2o + oaa -> cit + coa	2.3.3.1
TCA 02	aconitase 2	[m]: cit <=> cacon + h2o	4.2.1.3
TCA 03	aconitase 2	[m]: cacon + h2o <=> icit	4.2.1.3
TCA 04	isocitrate dehydrogenase 3 (NAD+)	[m]: icit + nad -> akg + co2 + nadh + h	1.1.1.41
TCA 05	2-oxoglutarate dehydrogenase, mitochondrial	[m]: akg + coa + nad -> co2 + nadh + succoa	
TCA 06	succinate-CoA ligase	[m]: gdp + pi + succoa <=> gtp + succ + coa	6.2.1.4
TCA 07	succinate-CoA ligase	[m]: adp + pi + succoa <=> atp + succ + coa	6.2.1.4
TCA 08	succinate dehydrogenase complex	[m]: succ + fad <=> fum + fadh2	1.3.5.1
TCA 09	fumarate hydratase	[m]: fum + h2o <=> mal-L	4.2.1.2
TCA 10	malate dehydrogenase 2, NAD	[m]: mal-L + nad -> oaa + nadh + h	1.1.1.37

3.9. Malate-Aspartate Shuttle

Irrespective of the source, NADH generated within the cytoplasm must be transported to the mitochondrial matrix to donate electrons to the electron transport chain. A malate– aspartate metabolic shuttle (Figure 3.7) achieves this by using cytoplasmic oxaloacetate to accept a proton from NADH and synthesize malate (MAL-ASP 04, given in Table 3.13) (Quinn and Pagano, 2004).

Cytosolic accumulation of NADH (e.g. with increased glycolysis) shifts the activity of malate dehydrogenase (MDH) in the direction of malate formation from oxaloacetate (MAL-ASP 04). Malate crosses the mitochondrial membrane in exchange for a-ketoglutarate (MAL-ASP 06), and is reconverted to oxaloacetate by mitochondrial MDH. NADH is thus regenerated in the mitochondria and can enter the respiratory chain. In addition, oxaloacetate replenishes the TCA cycle, combining with acetyl-CoA to form citrate. Oxaloacetate can also combine with glutamate to form α-ketoglutarate and

aspartate (MAL-ASP 02). α-ketoglutarate drives the entry of malate, as aspartate exits the cell in exchange for glutamate (MAL-ASP 07).

In the cytosol, the α-ketoglutarate and aspartate recombine to form oxaloacetate and glutamate. There is thus an overall shift of malate into the mitochondria, and aspartate out of the organelle when cytosolic NADH increases (King and Opie, 1998).

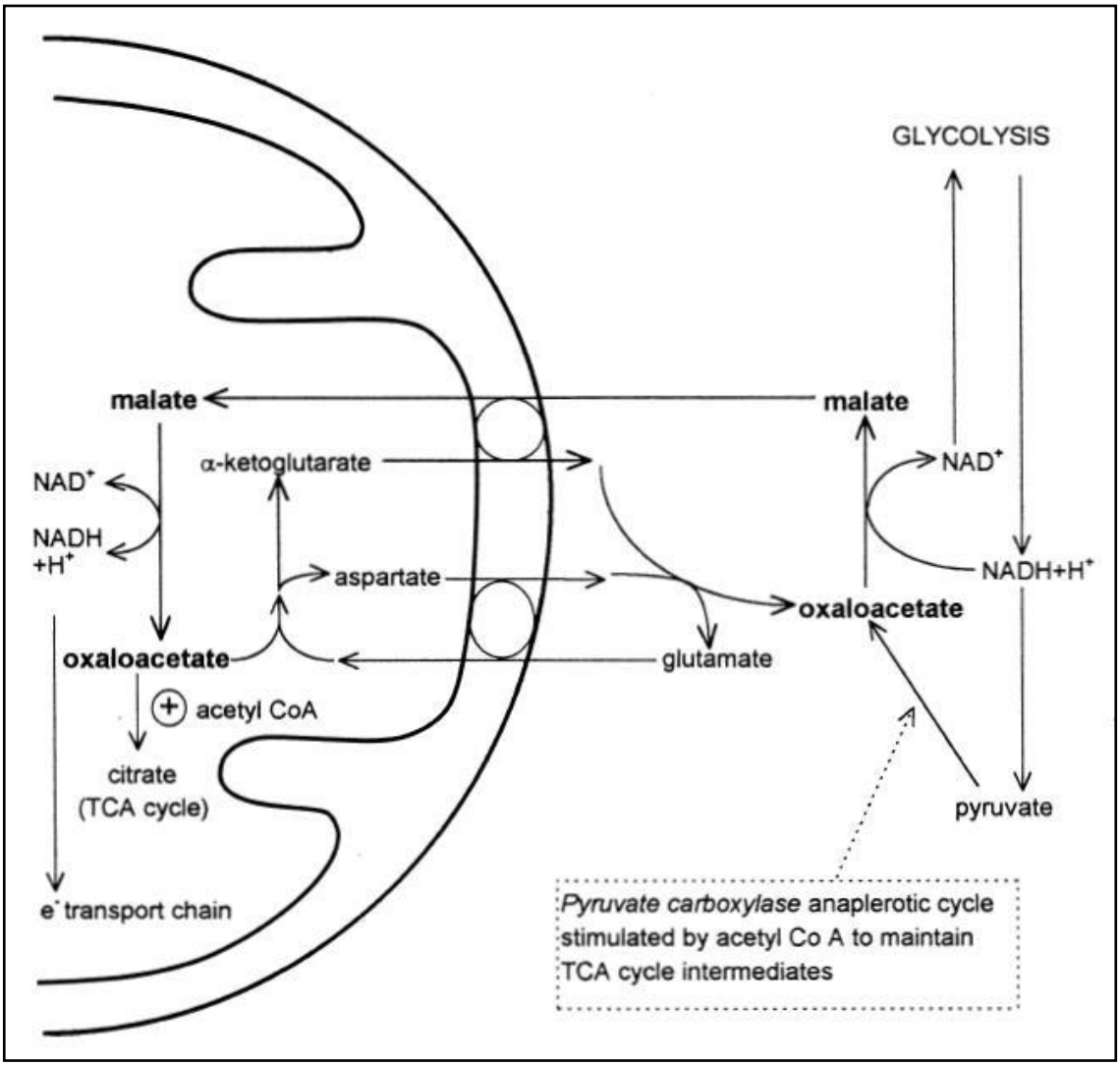

Figure 3.7. The malate-aspartate shuttle.

The whole shuttle can reverse, such that malate is transported out of the mitochondria, converted to oxaloacetate, and then to pyruvate. Pyruvate can also contribute to oxaloacetate formation via pyruvate carboxylase, or to malate by malic enzyme. These

mechanisms, and the malate-aspartate shuttle, result in the anaplerotic contributions of pyruvate (King and Opie, 1998).

Its direction is determined by the cytosolic to mitochondrial NADH/NAD+, such that a higher cytosolic ratio drives NADH transport into the mitochondria. This transfer does not utilise energy, but allows production of ATP by oxidative phosphorylation. If oxygen is limiting, NADH accumulates in the mitochondria, and then in the cytosol. This may affect redox-dependent reactions including glycolysis. The malate-aspartate shuttle can be reversed if NADH levels rise in the mitochondria, with the formation of malate. Malate is then transported out of the mitochondria, and converted to pyruvate by NADP-dependent malic enzyme, or to oxaloacetate by MDH (King and Opie, 1998).

Table 3.14. Reactions of malate-aspartate shuttle

Reaction Name	**Enzyme**	**Reaction**	**E.C. #**
MAL-ASP 01	mitochondrial carrier; dicarboxylate transporter	mal-L[m] + pi[c] <=> mal-L[c] + pi[m]	
MAL-ASP 02	aspartate transaminase	[c]: akg + asp-L <=> glu-L + oaa	2.6.1.1
MAL-ASP 03	aspartate transaminase	[m]: glu-L + oaa <=> akg + asp-L	2.6.1.1
MAL-ASP 04	malate dehydrogenase	[c]: oaa + h + nadh -> mal-L + nad	1.1.1.37
MAL-ASP 06	mitochondrial carrier; oxoglutarate carrier	mal-L[m] + akg[c] <=> mal-L[c] + akg[m]	
MAL-ASP 07	mitochondrial aspartate glutamate carrier	asp-L[m] + glu-L[c] -> asp-L[c] + glu-L[m]	

4. ENZYME DEFICIENCIES IN CARDIOMYOCYTES

4.1. HMG-CoA Synthase Deficiency

Ketogenesis is a mitochondrial process by which acetyl-CoA, mostly derived from the β-oxidation of fatty acids, is converted through four reactions, usually known as the HMG-CoA pathway, into acetoacetate, β-hydroxybutyrate and acetone, all of which are commonly called ketone bodies (Hegart, 1999). Ketone bodies are essential vectors of energy transfer from liver to extrahepatic tissues like brain, heart, and kidneys (Bouchard *et al*., 2001). Factors that induce ketogenesis are (in addition to diabetes) fasting and intense lipolysis. In the transition from the fed to the fasted condition, carbohydrate utilization and fatty acid synthesis in the liver cease and are replaced by the oxidation of fatty acids and the induction of ketogenesis (Hegart, 1999).

The availability of ketone bodies depends almost exclusively on hepatic ketogenesis. Failure of ketogenesis are typically manifested by hypoglycemia, which results from the inadequate supply of alternative substrate (ketones). Other clinical features are more variable and may include myopathy, cardiomyopathy, hepatocellular damage, and neuropathies (Thompson *et al*., 1997).

Fasting is accompanied by a decrease in the availability of glucose for energy use in peripheral tissues and, consequently, an increased reliance of these tissues on the availability of ketone bodies and fatty acids for energy. Ketone bodies (3-hydroxybutyrate and acetoacetate) are important fuels during fasting, both for the brain and for peripheral tissues.

During fasting, acetyl-CoA produced by mitochondrial β-oxidation of fatty acids in the liver is largely directed towards production of ketones, with minimal use of the tricarboxylic acid cycle, so that the vast majority of the two-carbon units produced by fatty acid oxidation are directed through HMG-CoA synthase to the production of ketone bodies (Thompson *et al*., 1997).

Mitochondrial HMG-CoA synthase (EC 4.1.3.5) is a key enzyme in the control of ketogenesis and mediates the first and rate-limiting step of ketone body synthesis, the condensation of acetoacetyl-CoA and acetyl-CoA to form HMG-CoA (Bouchard *et al*., 2001).

Clinical data obtained from patients of HMG-CoA synthase deficiency show that the plasma ketone concentrations are about 10% of the minimum normal values and the HMG-CoA synthase activity is about 10-17% compared to normal subjects during fasting (Thompson *et al*., 1997).

The diagnosis of mitochondrial HMG-CoA synthase deficiency is not straightforward. Like other defects of fatty-acid oxidation, this condition should be considered in any patient with coma induced by fasting or a life-threatening event from the newborn period through infancy to middle childhood (Thompson *et al*., 1997).

4.2. Mitochondrial Complex I Deficiency (NADH-CoQ reductase deficiency)

Oxidative phosphorylation has a prominent role in energy metabolism of the cell. Oxidative phosphorylation deficiencies manifest as a broad clinical spectrum. Complex I, the biggest and most complicated enzyme complex of the OXPHOS system, has been subjected to thorough investigation in recent years (Janssen *et al*, 2006).

NADH:ubiquinone oxidoreductase (complex I; EC 1.6.5.3), the first and largest (and most complicated) of the five complexes, is one of the two entry points of the oxidative phosphorylation system, complex II (EC 1.3.5.1) being the other (Janssen *et al*, 2006).

Complex I is a large multiprotein assembly and its main function is transport of electrons from NADH to ubiquinone with simultaneous shunting of protons across the inner mitochondrial membrane to the intermembrane space (Loeffen *et al*, 2000).

The first clinical symptoms of complex I deficiency, presenting either at birth or in early childhood, seem to result in brain dysfunction, sometimes combined with defects in

other energy-consuming organs, such as the skeletal muscle and the heart (Smeitink and van der Heulen, 1999).

At least theoretically, a dysfunction of dehydrogenases, like complex I, which dehydrogenates NADH to NAD+ plus H+, may disturb the cellular NAD pool giving rise to an altered redox state of the cell. Briefly, the aerobic oxidation of glucose by the glycolytic pathway, pyruvate dehydrogenase complex and citric acid cycle results in the reduction of NAD+ to NADH (Smeitink *et al*, 2004). Mean enzyme activity was found to be 16.7% of the normal value in patients with complex I deficiency (Koga *et al*, 1988).

4.3. Primary Carnitine Deficiency

L-Carnitine (b-hydroxy-g-trimethylaminobutyric acid) is an essential component in the transport of long chain fatty acids into mitochondria, where they undergo β-oxidation. Carnitine serves two roles in this process. First, through the enzyme carnitine palmityl transferase (CPT-I), carnitine reacts with long chain fatty acids to make long chain acyl carnitine esters. The second role of carnitine is to shuttle free carnitine and long chain acyl carnitine across the inner mitochondrial membrane. Inside the mitochondrial matrix, long chain acyl carnitine is converted back to free carnitine and long chain fatty acids via CPT-II. Since, the normal heart obtains approximately 60% of its total energy production from fatty acid oxidation, this function of carnitine is thought to be of major importance. Because of these functions of carnitine and since a number of case reports have shown that some patients with carnitine deficiency will exhibit cardiomyopathy, it is believed that adequate levels of carnitine are required for normal energy metabolism and contractile function of the heart (Paulson, 1998).

It is expected that glucose oxidation would be increased in a carnitine deficient heart in order to compensate for the decrease in fatty acid oxidation. However, it is uncertain whether the increase in glucose oxidation would completely compensate for the decrease in fatty acid oxidation, such that total ATP production by the heart would be maintained. Another mechanism that may account for the deleterious effects of carnitine deficiency is that the impaired fatty acid transport into mitochondria may lead to the cytosolic

accumulation of lipid intermediates such as long chain acyl carnitine and acyl CoA, which have been shown to inhibit a number of key enzymes (Paulson, 1998).

Deficiencies of carnitine are classified as either primary or secondary. Primary carnitine deficiencies may arise from a genetic disorder resulting in one or more of the following: (1) a defect in carnitine synthesis; (2) abnormal renal handling of carnitine; (3) alterations in cellular mechanisms for carnitine transport affecting uptake and/or release of carnitine from tissues; (4) excessive degradation of carnitine; or (5) defective intestinal absorption of carnitine. A number of case reports have established that primary carnitine deficiency is associated with cardiomyopathy. This form of carnitine deficiency is relatively severe with muscle and plasma carnitine being reported as low as 10% of normal values (Paulson, 1998).

4.4. Fabry Disease

Fabry disease is an X-linked, hereditary, lysosomal storage disease caused by deficiency of the enzyme α-galactosidase A (Clarke, 2007). This enzymatic defect leads to the progressive accumulation of glycosphingolipids, predominantly globotriaosylceramide, throughout the body, particularly in the skin, kidney, nervous system, eye, and heart (Nakao *et al*, 1995).

The pathophysiology of cardiomyopathy in Fabry disease is poorly understood. Although glycosphingolipid has been shown to accumulate in cardiomyocytes, the amount is too small to account for the massive increase in left ventricular size. Failure of left ventricular hypertrophy to respond well to enzyme replacement therapy in some patients, despite apparent clearance of glycosphingolipid globotriaosylceramide, suggests that some other process is contributing to the cardiomyopathy in the disease, perhaps increased levels of a circulating growth-promoting factor (Clarke, 2007).

Recently, several cases of an atypical variant of Fabry's disease, with manifestations limited to the heart, have been reported. In patients with this type of Fabry's disease, the diagnosis was made by the pathological study of endomyocardial-biopsy specimens or autopsy specimens of the heart. These patients had left ventricular hypertrophy as a result

of the deposition of globotriaosylceramide in the cardiomyocytes. However, there has been only a single report of the incidence of Fabry's disease among patients with cardiac symptoms; in that study the disease was found by endomyocardial biopsy (Nakao *et al*, 1995).

4.5. Tangier Disease

Tangier disease is a rare recessive disorder characterized by a severe deficiency or absence of high density lipoprotein (HDL) in plasma and an accumulation of cholesteryl esters in macrophages and other reticuloendothelial cells in many tissues. The prevalence of coronary heart disease in patients with Tangier disease is not as high as one might expect from the very low plasma HDL cholesterol levels, as only 44% of these patients over 35 years of age have been reported to have clinical manifestations of cardiovascular disease (Bertolini *et al*, 2000).

Furthermore, there is no increase in concentration of any of the tissue phospholipids or sphingolipids. A modest increase in triglycerides has been present in a few isolated tissues from patients with Tangier disease but this is not a consistent abnormality. Most work on the biochemical defect has centered around the peculiar changes in plasma lipoproteins (Ferrans and Fredrickson, 1975).

5. Ischemia

The mechanical performance of myocardium is highly dependent on oxidative energy production, that is, on the respiratory function of myocardial mitochondria. In cardiomyocytes, a long lasting lack of oxygen leads to loss of energy reserves and alterations in ion homeostasis, which contribute to structural damage. Lack of oxygen not only impairs ATP synthesis within the mitochondria, but may also induce a condition where mitochondria consume ATP, thus contributing to the depletion of energy reserves (Bosetti *et al*, 2000).

The myocardial response to ischemia is regulated to protect the structural and functional integrity of the cardiac myocyte. Ischemia tampers myocardial energy metabolism by slowing aerobic metabolism and by accelerating anaerobic. Glucose assumes a central role for energy production in the ischemic heart, when lack of oxygen induces a shift to anaerobic metabolism with rapid stimulation of glucose uptake, glycogenolysis and glycolytic flux (Depre and Taegtmeyer, 2000).

Myocardial substrate metabolism during ischemia is highly dependent upon the severity of ischemia. Complete elimination or very severe reduction of blood flow produces depletion of high energy phosphates, lactate accumulation, glycogen breakdown, and severe contractile dysfunction. Myocardial ischemia causes a decrease of substrate flux through PDH, as shown by a decreased rate of glucose oxidation and a switch from net lactate uptake to net lactate production. Decreased flux through PDH could be due to PDH inhibition by its products, NADH and acetyl-CoA. During mild to moderate ischemia the fatty acid oxidation rate decreases but still remains an important source of energy (Calvani *et al*, 2000).

The reduced oxygen supply in ischemic heart severely impairs mitochondrial oxidation of fatty acids. Under ischemic conditions, residual fatty acids extracted from the extracellular compartment are mainly incorporated into triacylglycerols (Shaap *et al*, 1998).

6. METHODS

6.1. Flux Balance Analysis

A metabolic network is constrained by the imposition of stoichiometric constraints that correspond to the mass balance around each metabolite. When the metabolic network has a steady state distribution of fluxes, the constraints are described by a system of linear equations as shown below:

$$S \cdot v = 0 \tag{6.1}$$

where S is the mxn stoichiometric matrix of all the reactions in the metabolic network, m is the number of metabolites, n is the number of fluxes (reaction rates), and v is the flux vector of the metabolic network. In addition to these linear constraints, there exist thermodynamic constraints on reactions that may restrict the directional flow of the reaction along with capacity constraints that provide potential upper limits to the flux levels of the reactions. A typical objective function used for the simulation of microbial genome-scale metabolic networks has been the growth rate as represented by a reaction draining biomass components. The Linear Programming (LP) problem that is solved is summarized below:

$$\text{Max } f^T v \tag{6.2}$$

$$\text{s.s. } S \cdot v = 0 \tag{6.3}$$

$$0 \leq v \leq v_{max} \tag{6.4}$$

where f is the objective function vector and v_{max} is the vector containing the maximum capacities of the fluxes. Maximum measured uptake rates are used to constrain the exchange fluxes (Mahadevan and Schilling, 2003). Linear programming problems are solved by the MATLAB Optimization Toolbox.

6.2. Flux Variability Analysis

In this LP-based approach, the emphasis is on determining the maximum and minimum values of all the fluxes that will satisfy the constraints and allow for the same optimal objective value. It must be noted that this approach does not identify all possible alternate optimal solutions, but rather the range of flux variability that is possible within any given solution (Mahadevan and Schilling, 2003).

The approach begins with determining the base/wildtype value of the objective function by solving the LP problem outlined in equations 6.2-6.4. From this solution, the range of variability that can exist in each flux in the network due to alternate optimal solutions can be calculated through a series of LP problems, wherein the value of the original objective is fixed and each reaction in the network is maximized and subsequently minimized to determine the feasible range of flux values for each reaction. The mathematical formulation of this approach is described below:

- Case 1

$$\text{Max } v_i \tag{6.5}$$

$$\text{s.s. } S \cdot v = 0 \tag{6.6}$$

$$f^T v = Z_{obj} \tag{6.7}$$

$$0 \leq v \leq v_{max} \quad \text{for } i = 1, \dots, n \tag{6.8}$$

- Case 2

$$\text{Min } v_i \tag{6.9}$$

$$\text{s.s.} \quad S \cdot v = 0 \tag{6.10}$$

$$f^T v = Z_{obj} \tag{6.11}$$

$$0 \leq v \leq v_{max} \quad \text{for } i = 1, \ldots, n \tag{6.12}$$

where Z_{obj} is the value of the objective function calculated previously from equation 6.2, and n is the number of fluxes. The solution of the 2n LP problems outlined in equations 6.5-6.12 determines the upper and lower bounds of every reaction flux that will result in the same value for the original objective function (Mahadevan and Schilling, 2003). Linear programming problems are solved using the MATLAB Optimization Toolbox.

6.3. Flux Coupling Analysis

The Flux Coupling Finder (FCF) procedure is used for finding coupled reaction sets and blocked reactions in genome-scale metabolic systems. The set of blocked reactions for a given network is identified by maximizing each particular flux subject to the network stoichiometry. If the maximum possible value of a particular flux is zero, then the reaction is said to be unusable or blocked because it cannot carry any flux. Similarly, linear fractional programming is employed to identify the maximum and minimum flux ratios (i.e., max v_1/v_2, min v_1/v_2) for every pair of metabolic fluxes. Comparison of flux ratios allows one to determine whether any two fluxes, v_1 and v_2, share any of the following types of coupling:

- Directional coupling ($v_1 \rightarrow v_2$), if a non-zero flux for v_1 implies a non-zero flux for *v2* but not necessarily the reverse.
- Partial coupling ($v_1 \leftrightarrow v_2$), if a non-zero flux for v_1 implies a non-zero, though variable, flux for v_2 and vice versa.
- Full coupling ($v_1 \Leftrightarrow v_2$), if a non-zero flux for v_1 implies not only a non-zero but also a fixed flux for v_2 and vice versa (Burgard *et al.*, 2004).

Reaction pairs not falling into one of these categories are classified as *uncoupled*. Reactions, which are mutually partially and/or fully coupled to one another, are grouped into *coupled reaction sets* (Burgard *et al.,* 2004).

6.3.1. Blocked Reactions

Blocked reactions are defined as reactions incapable of carrying flux under steady-state conditions. They are classified by identifying fluxes whose maximum and minimum values are zero for a particular uptake scenario. The maximization of a particular flux v_i for a steady-state metabolic network comprised of a set N = {1,…, *N*} of metabolites and a set M = {1,…, *M*} of reactions is expressed mathematically as the following linear programming (LP):

$$\text{Maximize} \quad v_j \tag{6.13}$$

$$\text{Subject to} \quad \sum_{j=1}^{M} S_{ij}\, v_j = 0 \quad \forall\, i \in N \tag{6.14}$$

$$v_j^{uptake} \leq v_j^{uptake,max} \quad \forall\, j \in N \tag{6.15}$$

$$v_j \geq 0 \tag{6.16}$$

where *Sij* is the stoichiometric coefficient of metabolite *i* in reaction *j*. Reversible reactions are expressed as two irreversible reactions in opposite directions (i.e., $v_j = v_j^{\,f} - v_j^{\,b}$), thus constraining all fluxes to positive values. The optimization problem can be easily modified to examine not only the effects of changing which metabolites are internal or external, but more specifically changing which metabolites can be taken up, secreted, or both. Constraint (6.15) limits the uptake of resources (i.e., carbon, oxygen, etc.) to the network, and the maximum uptake of any metabolite absent from the external medium is set to zero. Transport mechanisms for metabolites out of the cell can be blocked by changing the inequality in constraint (6.16) to an equality. All isozymes catalyzing a given reaction are lumped into a single flux, eliminating duplicate reactions. The set of blocked reactions is identified by solving the above linear programming problem once for every flux. If the

maximum value of the flux is zero, then the reaction is said to be unusable or blocked (Burgard *et al.,* 2004).

The identified blocked reactions may have either biological meaning, such as the reaction being a part of an incomplete pathway at an intermediate stage of evolution, or they could signify errors/omissions in the metabolic reconstruction. It is important to note that the results depend upon the steady-state assumption, imposed uptake/secretion scenarios, growth requirements, and energy production requirements (Burgard *et al.,* 2004).

6.3.2. Coupled Reactions

The identification of all coupled reactions and corresponding coupled reaction sets hinges upon the calculation of the upper and lower limits of all flux ratios (i.e., R_{max} = max v_1/v_2, R_{min} = min v_1/v_2). The calculation of these ratios originally gives rise to nonlinear optimization problems, which is computed by the MATLAB Optimization Toolbox (Burgard *et al.,* 2004).

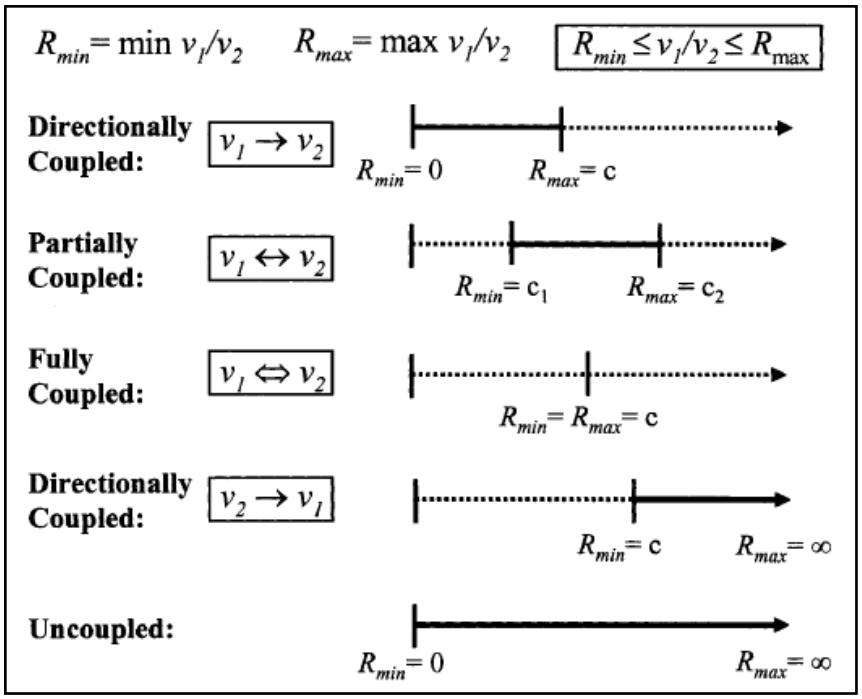

Figure 6.1. Various outcomes for the maximum and minimum flux ratios (Burgard *et al.,* 2004)

Various outcomes for the maximum and minimum flux ratios are presented in Figure 6.1. The first case occurs whenever R_{min} is equal to zero and R_{max} is equal to some finite value c. The fluxes are directionally coupled ($v_1 \rightarrow v_2$) because the activity of v_1 implies v_2 (i.e., $v_2 \geq v_1/c$). Similarly, if R_{min} is equal to a finite constant c and R_{max} is unbounded, then the fluxes are directionally coupled in the opposite direction ($v_2 \rightarrow v_1$), as v_2 implies v_1 (i.e., $v_1 \geq v_2/c$). Two fluxes can also be partially coupled ($v_1 \leftrightarrow v_2$) if R_{max} and R_{min} are both finite and unequal, or fully coupled ($v_1 \Leftrightarrow v_2$) if R_{max} is finite and equal to R_{min}. The final case occurs whenever the two fluxes are completely uncoupled and is encountered if their ratio can vary freely from zero to infinity (Burgard *et al.*, 2004).

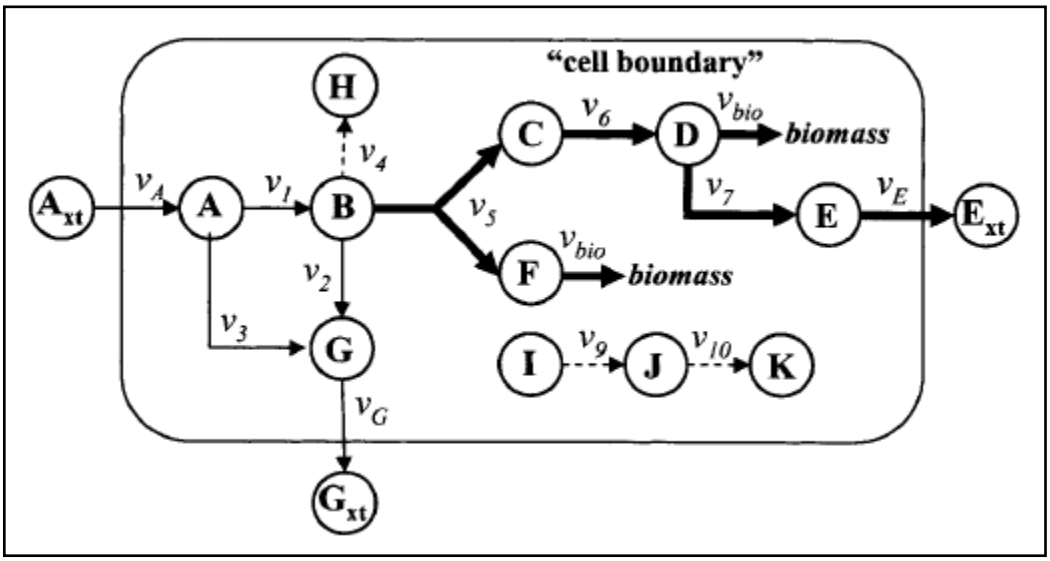

Figure 6.2. Fully coupled reaction set (Burgard *et al.*, 2004)

Figure 6.2 shows an example of a fully coupled reaction set. The partial and/or full coupling of reactions is a transitive property (i.e., $v_1 \leftrightarrow v_2$ and $v_2 \leftrightarrow v_3$ imply that $v_1 \leftrightarrow v_3$), complete coupled reaction sets can be subsequently inferred from the maximum and minimum flux ratios. Directional coupling, unlike partial and full coupling, can capture the one way type of connectivity between metabolic reactions. This information enables the global identification of *equivalent knockouts* defined as the set of all possible reactions whose deletion forces the flux through a particular reaction to zero, and sets of *affected reactions* defined as all reactions whose fluxes are forced to zero if a particular reaction is deleted. These concepts are illustrated in Figure 6.3 where the reactions v_1, v_2, and v_3 all

imply reaction *v**. This means that if any of these fluxes assumes a non-zero value, then *v** must also attain a non-zero value. Therefore, knocking out reaction *v** from the network forces the fluxes through reactions v_1, v_2, and v_3 to zero. Thus, one refers to reactions v_1, v_2, and v_3 as the set of reactions *affected* by the removal of *v**. Similarly, a non-zero flux through *v** implies that the fluxes through v_4, v_5, and v_6 are also non-zero. This means that removing any of v_4, v_5, or v_6 from the network forces the flux through *v** to zero. Reactions v_4, v_5, and v_6 are thus referred to as *equivalent knockouts* for *v**. Note that although the sets of reactions affected by each of the equivalent knockouts may differ, the directionality of coupling for partially/fully coupled reactions remains the same (Burgard *et al.*, 2004).

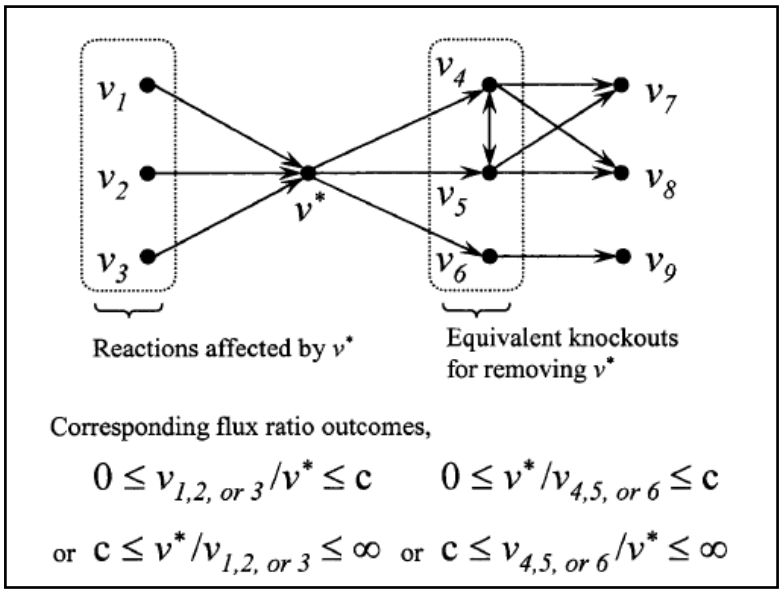

Figure 6.3. Examples of affected reaction sets and equivalent knockouts for reaction *v** (Burgard *et al.*, 2004)

6.4. Self-Organizing Maps

Self-organizing maps (SOM) is a type of mathematical cluster analysis that is particularly well suited for recognizing and classifying features in complex, multidimensional data. The method has been implemented in a publicly available computer package, GENECLUSTER, that performs the analytical calculations and provides easy data visualization. GENECLUSTER is used to produce and display SOMs of gene expression data (Tamayo *et al*., 1999).

SOM has a set of nodes with a simple topology (e.g., two-dimensional grid) and a distance function $d(N_1, N_2)$ on the nodes. Nodes are iteratively mapped into *k*-dimensional ‘‘gene expression’’ space (in which the i^{th} coordinate represents the expression level in the i^{th} sample). The position of node N at iteration *i* is denoted $f_i(N)$. The initial mapping f_0 is random. On subsequent iterations, a data point P is selected and the node N_P that maps nearest to P is identified. The mapping of nodes is then adjusted by moving points toward P by the formula:

$$f_{i+1}(N) = f_i(N) + \tau(d(N, N_P), i)\big(P - f_i(N)\big) \tag{6.16}$$

The learning rate τ decreases with distance of node N from N_P and with iteration number *i*. The point P used at each iteration is determined by random ordering of the *n* data points generated once and recycled as needed. The function τ is defined by

$$\tau(x, i) = 0.02/(T + 100i) \quad for \quad x = \rho(i) \tag{6.17}$$

and $\tau(x, i)$ otherwise, where radius r(*i*) decreases linearly with *i* ($\rho(0) = 53$), and eventually becomes zero and T is the maximum number of iterations (Tamayo *et al.*, 1999).

7. RESULTS and DISCUSSION

Many reactions take place in myocytes and together they build up the metabolism in the heart. In the present study, these reactions are used to form a stochiometric model of the cardiomyocyte metabolism by literature survey.

Flux balance analysis is applied to the reconstructed network to obtain the flux distribution of the cardiomyocyte at several system conditions of healthy and disease cases. Together with flux balance analysis, flux variability analysis, flux coupling analysis and self-organizing maps are also applied to characterize the metabolic steady-state flux solution and the behaviour of the energy metabolism at different physiological conditions.

7.1. Network Reconstruction

A reaction network of myocyte is reconstructed using literature information and the databases of Kyoto Encyclopedia of Genes and Genomes (KEGG) and Reactome as explained in section 3. In the construction of the network, all reactions and metabolites have been compartmentalized. Three compartments, cytoplasm ([c]), mitochondria ([m]) and peroxisome ([p]) constitute the intracellular space of the myocyte, and the extracellular space ([e]) represents the plasma or blood.

The reconstructed reaction network includes carbohydrate metabolism (glycolysis, glycogenesis, glycogenolysis, pentose phosphate pathway and pyruvate metabolism), fatty acid metabolism (β-oxidation of saturated, unsaturated, odd-chain and long-chain fatty acids, triglyceride synthesis and degradation), ketone body metabolism, TCA Cycle, electron transport chain, malate-aspartate shuttle, nucleotide and transport reactions. This network is investigated using the tools of Metabolic Engineering, i.e. Flux Balance Analysis is employed to obtain the flux distribution in cardiac muscle cell at different metabolic and physiological states.

To complete the network, transport reactions and some other reactions must be added for modeling purposes (Table A.1). Glucose, lactate, acetate and fatty acids are taken from

the plasma as the substrates for their corresponding energy metabolisms. Each of these metabolites has its own transport reactions. Oxygen and carbondioxide which are used and produced in the electron transport chain are also transported across the cell membrane. Water, which freely diffuses across the cell membrane, has a reversible transport reaction. Hydrogen is let to pass freely across the cell membrane and phosphate is transported across the compartments with the expense of an hydrogen ion.

Triglycerides and glycogen are two metabolites which are produced and stored in myocytes. To keep the steady state balance of the myocyte, two transport reactions are added such that these two metabolites can be freely secreted out of the cell to match the production rate and uptaken from the plasma to match the degradation rate from the stores in the cell.

For triglyceride production and degradation an overall fatty acid metabolite “fa-coa” is added to the network. This metabolite presents an average fatty acid content and is constituted from the fatty acid fractions in the triglyceride pool. The fraction values used in the calculations are obtained from literature (Table 7.1.).

Table 7.1. Fatty Acid Fractions in the Triglyceride Pool

Fatty Acid	Thiele, 2004	van der Vusse, 1982	O'Donnell, 2002
C14:0	-	0.02	0.03
C15:0	-	-	0.01
C16:0	0.20	0.22	0.37
C16:1	-	0.05	0.03
C17:0	-	-	0.01
C18:0	0.20	0.10	0.15
C18:1	0.10	0.41	0.23
C18:2	0.20	0.17	0.16
C18:3	-	-	0.01
C20:4	0.25	0.01	-
C22:6	0.05	-	-

The values used in the work of Thiele *et al.*, 2004 are not considered to be reliable because they do not match with the experimental values of the fatty acids given in various references, both in terms of quantity and content. The works of van der Vusse *et al.*, 1982 and O’Donnell *et al.*, 2002 are compared and they seem to match moderately. Pentadecanoic acid (C15:0), heptadecanoic acid (C17:0) and linoleneate (C18:3) are

eliminated since they seem to be either missing or in negligible amounts. Finally, the values from O'Donnell *et al*., 2002 are used to have a continuity in data.

All the reactions used in the flux balance analysis are given in Tables 3.1-3.12.

7.2. Flux Balance Analysis

7.2.1. Objective Function

The objective function chosen for FBA is the ATP hydrolysis reaction in the cytoplasm similar to the works of Thiele *et al.*, 2004, Salem *et al.*, 2002 and Zhou *et al*, 2005. This objective function is a common choice since normal cardiac function is dependent on constant resynthesis of ATP by oxidative phosphorylation in the mitochondria and the chemical energy that fuels cardiac contractile work and relaxation is derived from ATP hydrolysis (Stanley and Chandler, 2002). ATP hydrolysis reaction represents both the contractile and ion hemostatis reactions overall since the ATP produced in the mitochondria is transported to cytoplasm and used in these two systems.

7.2.2. Flux Distribution in Myocyte: Healthy Case

A literature survey was done to obtain flux data for various reaction and transport values at the normoxic steady state for different organisms. Values for human are primarily preferred if available. Alternate organisms are all chosen from mammals (rat, pig, mice, rabbit and dog).

7.2.2.1. Constraints: Transport and uptake values for glucose, glycogen, lactate, fatty acids, triglycerides and oxygen were obtained from literature. The glucose uptake rate is limited to the range of 0.43-0.56 μmol/min/g wet weight according to the data of Iozzo *et al.*, 2002, Kofoed *et al.*, 2002 and Meyer *et al*, 1997. Glycogen transport is taken as 0.20 μmol/min/g wet weight to match the synthesis and degradation rates of Wisneski *et al.*, 1987.

Table 7.2. Transport and flux values for glucose and glycogen (μmol/min/g wet weight)

Flux	Reaction	Value	Reference
Glucose Uptake	TRANS 01	0.560	Iozzo, 2002
Glucose Uptake	TRANS 01	0.510	Kofoed, 2002
Glucose Uptake	TRANS 01	0.430	Meyer, 1997
Glycogen Breakdown	GLCGN 04	0.200	Wisneski, 1985
Glycogen Synthesis	GLCGN 03	0.200	Wisneski, 1985

Total fatty acid uptake rate is adjusted to the range between 0.20-0.05 μmol/min/g wet weight to span a variety of data from literature (Table 7.3.). The fatty acid fractions are obtained from van der Vusse *et al.*, 1982 and their corresponding values are calculated from these fractions (Table 7.4.)

Table 7.3. Fatty acid uptake rates obtained from literature (μmol/min/g wet weight)

Fatty Acid Utilization	0.121	Bergmann, 1995
Fatty Acid Oxidation	0.050-0.100	van der Vusse, 1992
Palmitate Oxidation	0.200-0.140	O'Donnell, 2002
Palmitate Oxidation	0.090	O'Donnell, 2002
Fatty Acid Uptake	0.001 - 0.484	Bergmann, 1995
Fatty Acid Uptake	0.066	van der Vusse, 1982
Fatty Acid Uptake	0.026 - 0.312	Thiele, 2004

Table 7.4. Fatty acid uptake fractions and rates

	van der Vusse, 1982			
Fatty Acid	**Uptake**	**%**	**lb**	**Ub**
C14:0	0.001	1.6	0.001	0.003
C16:0	0.013	19.0	0.009	0.038
C16:1	0.007	10.6	0.005	0.021
C18:0	0.005	7.7	0.004	0.015
C18:1	0.032	45.8	0.023	0.092
C18:2	0.009	13.5	0.007	0.027

The overall flux distribution of an healthy cardiomyocyte is presented in Figure 7.1. All the external metabolites (glucose, lactate and fatty acids) are taken into the cell and the intracellular pools of glycogen and triglycerides are used to maximize the ATP production.

7.2.2.2. Carbohydrate metabolism: G6p that will be used by glycolysis is generated from the sources of glucose and glycogen. The flux of g6p entering glycolysis is calculated as 0.760 μmol/min/g wet weight and it is derived from glucose (0.560 μmol/min/g wet weight) and glycogen (0.200 μmol/min/g wet weight), which are the upper bounds set for glucose and glycogen uptake (Table 7.2).

Anaerobic oxidation of glycogen and glucose (glycolysis) only supplies about 2% of total ATP (1.780 μmol/min/g wet weight) directly (except the by-product NADH that enters ETC to yield more ATP) and about 80% of the pyruvate, which is then converted to acetyl-CoA. The rest of the pyruvate production is supplied by the lactate dehydrogenation (0.413 μmol/min/g wet weight) and converted to accoa to enter the TCA cycle for further NADH production.

7.2.2.3. Fatty acid metabolism: The fatty acid pool in the cell is supplied both from the triglyceride reserves and from the fatty acid uptake. The production of accoa (3.190 μmol/min/g wet weight) and the coenzymes NADH and $FADH_2$ (2.446 and 2.175 μmol/min/g wet weight, respectively) from the β-oxidation of fatty acids is greater than those supplied by glycolysis (Figure 7.1).

7.2.2.4. TCA Cycle: Most of the coenzymes NADH and $FADH_2$ are produced in the TCA cycle (Table 7.5). Also 5.183 μmol/min/g wet weight ATP is produced by this metabolism.

Table 7.5. Comparison of coenzyme and ATP production rates for healthy case (μmol/min/g wet weight)

Pathway	**NADH**	**$FADH_2$**	**ATP**
Glycolysis	1.520	-	1.780
Lactate dehydrogenation.	0.413	-	-
β-oxidation	2.446	2.175	-
TCA cycle	15.699	5.183	5.183

7.2.2.5. Electron Transfer Chain: NADH and $FADH_2$, produced from glycolysis, lactate dehydrogenation, β-oxidation and TCA cycle, enter the electron transfer chain and oxidative phosphorylation to yield most of the ATP produced (90 μmol/min/g wet weight).

7.2.2.6. ATP Hydrolysis: As the result of FBA, the maximum ATP hydrolysis rate is found to be 37.759 μmol/min/g wet weight when the constraints and parameters given in Tables 7.2-7.4 are used. This value is close to the ATP hydrolysis rate of 30 μmol/min/g wet weight during normal physical conditions (Opie, 1999). Under these conditions not all of the external metabolites available for the cell are used at the maximum rate. To illustrate the maximum energy production capacity of the cardiomyocyte, another FBA was applied with unbounded oxygen state and the ATP hydrolysis rate increased to 96.045 μmol/min/g wet weight.

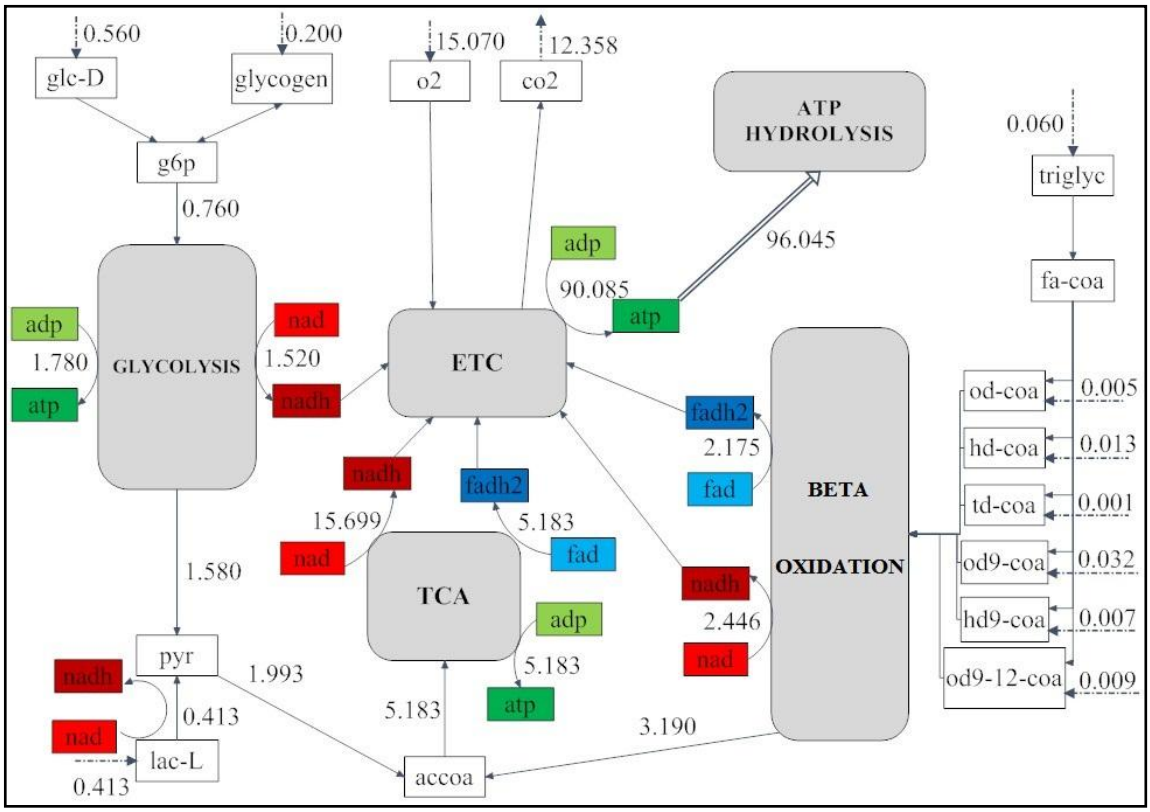

Figure 7.1. Flux distribution for healthy case (unbounded oxygen)

In the well-perfused heart, 60-90 % of the total energy production comes from β-oxidation of fatty acids and 10-40 % comes from the oxidation of pyruvate that is derived

from glycolysis and lactate oxidation (Stanley *et al*., 2005). The results of the flux balance analysis suggests that fatty acids supply most of the ATP, followed by glucose and lactate.

7.3. Enzyme Deficiencies in Cardiomyocytes

Cardiomyopathies are diseases of the myocardium and most of them are genetic. There is about 8.2 million individuals suffering from heart disease in the world. The prevalence rate of cardiomyopathy is about 0.02% in USA and 0.06% in Turkey. The deficiencies of the enzymes in the cardiomyocytes are reported to lead to the malfunctioning of myocardium, thus cardiomyopathies.

7.3.1. HMG-CoA Synthase Deficiency

Since HMG-CoA synthase is a hepatic enzyme and has no detectable activity in cardiomyocytes, its deficiency does not affect the heart directly. This deficiency manifests itself with impared ketogenesis, hence low concentration levels of ketone bodies in plasma. Ketone bodies are an important source of energy for the cardiomyocytes only during starvation.

As HMG-CoA synthase deficiency deficiency does not affect the heart at normoxic conditions, an alternative scenario simulating the starvation case is used in the present study. A fasting state for the heart is created. Fasting is accompanied by a decrease in the availability of glucose for energy use in peripheral tissues and an increased reliance of these tissues on the availability of ketone bodies and fatty acids for energy (Bouchard *et al*, 2001). Two cases with and without the deficiency together with fasting are compared to see the effects of this deficiency on cardiomyocytes.

7.3.1.1. Constraints: According to the work of Kaijser *et al.*, 1972, the myocardial uptake rates of free fatty acids and acetoacetate (representative ketone body in the reconstructed cardiac network) are positively correlated to their respective arterial concentrations. In the present study, the uptake values of these metabolites are adjusted according to the increase in the free fatty acid and acetoacetate fractions in the arterial concentrations obtained from the work of Owen *et al.*, 1990. In the case of HMG-CoA deficiency, acetoacetate uptake

rates are reduced by 90% (Table 7.6) according to the plasma concentration and enzyme activity values obtained from literature (Thompson *et al*, 1997).

Table 7.6. Uptake values for fasting (Thompson *et al*, 1997)
(μmol/min/g wet weight)

	lb	**ub**
C14:0 Uptake	0	0.007
C16:0 Uptake	0.021	0.086
C16:1 Uptake	0.012	0.048
C18:0 Uptake	0.009	0.035
C18:1 Uptake	0.052	0.206
C18:2 Uptake	0.015	0.061
Glucose Uptake	0.072	0.093
Acetoacetate Uptake	0	0.08

7.3.1.2. Carbohydrate Metabolism: Table 7.7 presents the flux values for the most diversified reactions at fasting state. The effect of the decrease in glucose availibility can be seen as the decrease of glucose uptake (from 0.560 to 0.093 μmol/min/g wet weight) and the decrease in the flux through glycolysis to 60% that of the healthy state.

Table 7.7. Flux values for healthy and fasting states (μmol/min/g wet weight)

Reaction Name	**Healthy**	**Fasting**	**% Change**
BOX 10-16	0.000	0.012	-
BOX 18-20	0.000	0.029	-
BOX 21-24	0.000	0.041	-
BOX 26-28	0.000	0.002	-
BOX 29-32	0.000	0.043	-
BOX 37	0.000	0.043	-
BOX 38-40	0.009	0.100	985.8
BOX 45-63	0.012	0.131	956.6
BOX 64	0.012	0.211	1601.7
GLY 01	0.560	0.093	83.4
GLY 02	0.760	0.293	61.4
GLY 05-07	0.760	0.293	61.4
GLY 08-09	1.520	0.586	61.4
GLY 10-12	1.500	0.608	59.5

Table 7.7. Flux values for healthy and fasting states (μmol/min/g wet weight) - continued

Reaction Name	Healthy	Fasting	% Change
KETONE 01	0.000	0.080	-
PYR 01	0.258	0.066	74.4
PYR 03	1.758	0.674	61.7
TRANS 01 (glc-D)	0.560	0.093	83.4
TRANS 03 (lac-L)	0.258	0.066	74.4
TRANS 12 (od9-ca)	0.023	0.052	126.1
TRANS 13 (od-9-12-ca)	0.010	0.015	56.3
TRANS 14 (hd9-ca)	0.005	0.012	140.0
TRANS 16 (acac)	0.000	0.080	-
TRANS 24 (triglyc)	-0.020	0.022	208.3
TRIGLY 01	0.020	-0.022	208.3
TRIGLY 02	0.020	-0.022	208.3
TRIGLY 03	-1.580	-0.534	66.2
TRIGLY 04	1.600	0.513	68.0
TRIGLY 05-09	0.020	0.000	100.0
TRIGLY 10,17	0.000	0.022	-
TRIGLY 16	0.060	0.000	100.0
U-BOX 02-17 (od9-coa)	0.009	0.057	519.4
U-BOX 19-40	0.000	0.018	-
U-BOX 42-57 (hd9-coa)	0.003	0.013	295.3

7.3.1.3. Fatty Acid Metabolism: The HMG-CoA synthase deficiency manifests itself mostly in the metabolism of fatty acids (β-oxidation of saturated and unsaturated fatty acids and triglyceride metabolism) (Figure 7.3). Increased fatty acid uptake from 0.071 to 0.110 μmol/min/g wet weight, gives rise to increased β-oxidation rates and increased fatty acid pool.

Increased fatty acid pool causes the triglyceride metabolism to switch to the production (0.022 μmol/min/g wet weight) rather than the depletion (0.022 μmol/min/g wet weight) observed in the healthy state.

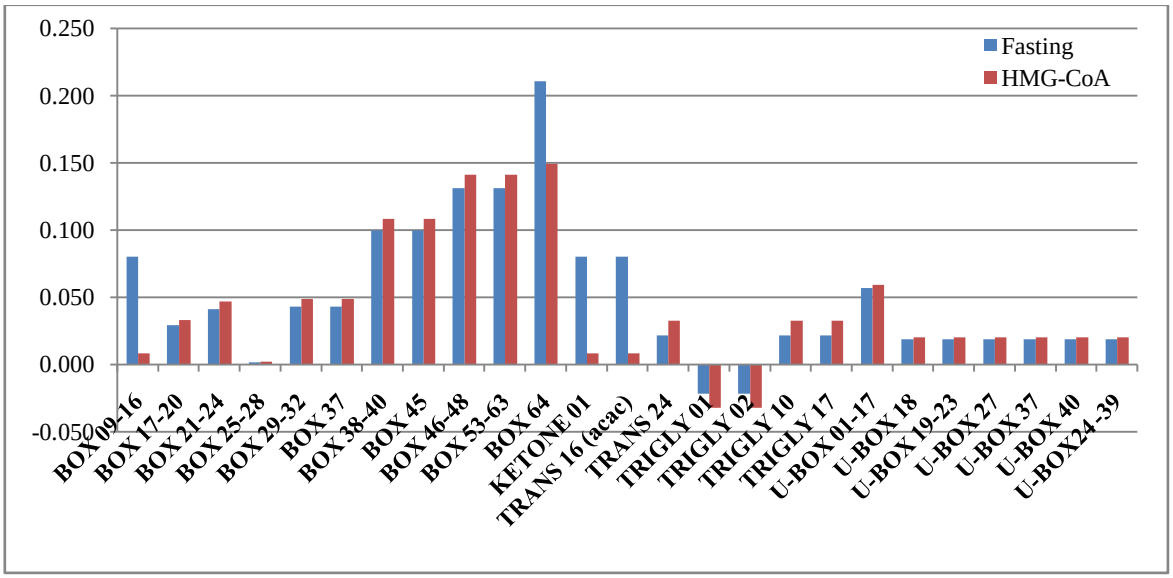

Figure 7.2. Flux comparison of fasting state vs. HMG-CoA deficiency

7.3.1.4. Ketone Body Metabolism: A significant change occurs in the reaction BOX 64, which is the production of acetyl-CoA from acetoacetyl-CoA, the entry point of ketone bodies in the energy metabolism. Figure 7.2 presents the changes in the flux values. A 10% decrease in HMG-CoA synthase activity results in decrease of flux values through ketone metabolism.

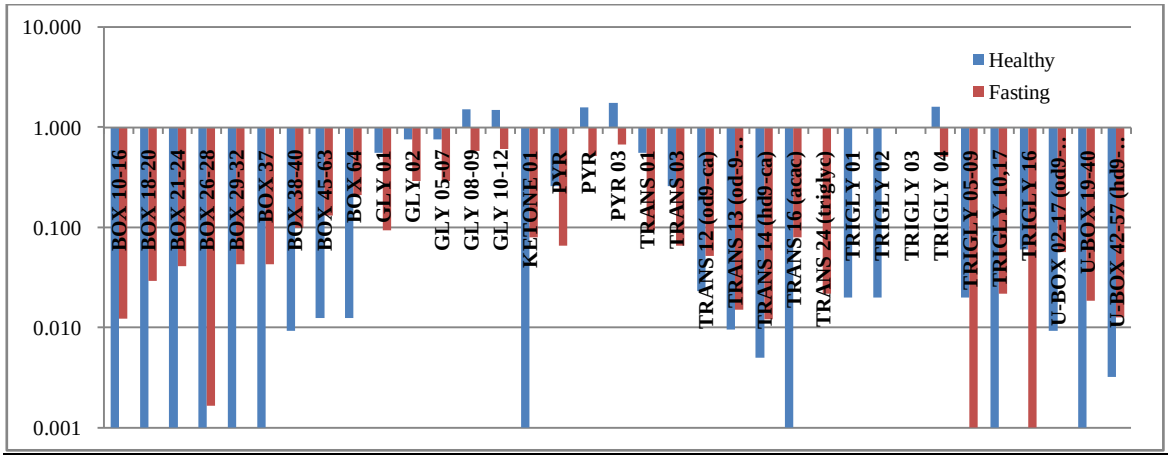

Figure 7.3. Flux comparison of healthy vs. fasting state (logarithmic scale)

Table 7.8. Flux values fasting state with and without HMG-CoA synthase deficiency (μmol/min/g wet weight)

	Fasting	HMG-CoA deficient fasting	% Change
BOX 09-16	0.080	0.008	13.0
BOX 17-20	0.029	0.033	13.6
BOX 21-24	0.041	0.047	13.4
BOX 25-28	0.002	0.002	19.4
BOX 29-32	0.043	0.049	13.6
BOX 37	0.043	0.049	13.6
BOX 38-40	0.100	0.108	8.3
BOX 45	0.100	0.108	8.3
BOX 46-48	0.131	0.141	7.9
BOX 53-63	0.131	0.141	7.9
BOX 64	0.211	0.149	29.2
KETONE 01	0.080	0.008	90.0
TRANS 16 (acac)	0.080	0.008	90.0
TRANS 24 (triglyc)	0.022	0.032	49.1
TRIGLY 01	-0.022	-0.032	49.1
TRIGLY 02	-0.022	-0.032	49.1
TRIGLY 10	0.022	0.032	49.1
TRIGLY 17	0.022	0.032	49.1
U-BOX 01-17	0.057	0.059	4.3
U-BOX 18	0.018	0.020	9.2
U-BOX 19-23	0.018	0.020	9.2
U-BOX 27	0.018	0.020	9.2
U-BOX 37	0.018	0.020	9.2
U-BOX 40	0.018	0.020	9.2
U-BOX24 -39	0.018	0.020	9.2

7.3.1.5. ATP Hydrolysis: Despite the decrease in the glucose uptake, increased fatty acid uptake during fasting seems to meet the deficit of decreased glucose concentrations, and the ATP production rate of 35.177 μmol/min/g wet weight (Figure 7.4) seems to be close to the experimental value of 30 μmol/min/g wet weight reported by Opie *et al*, 1999.

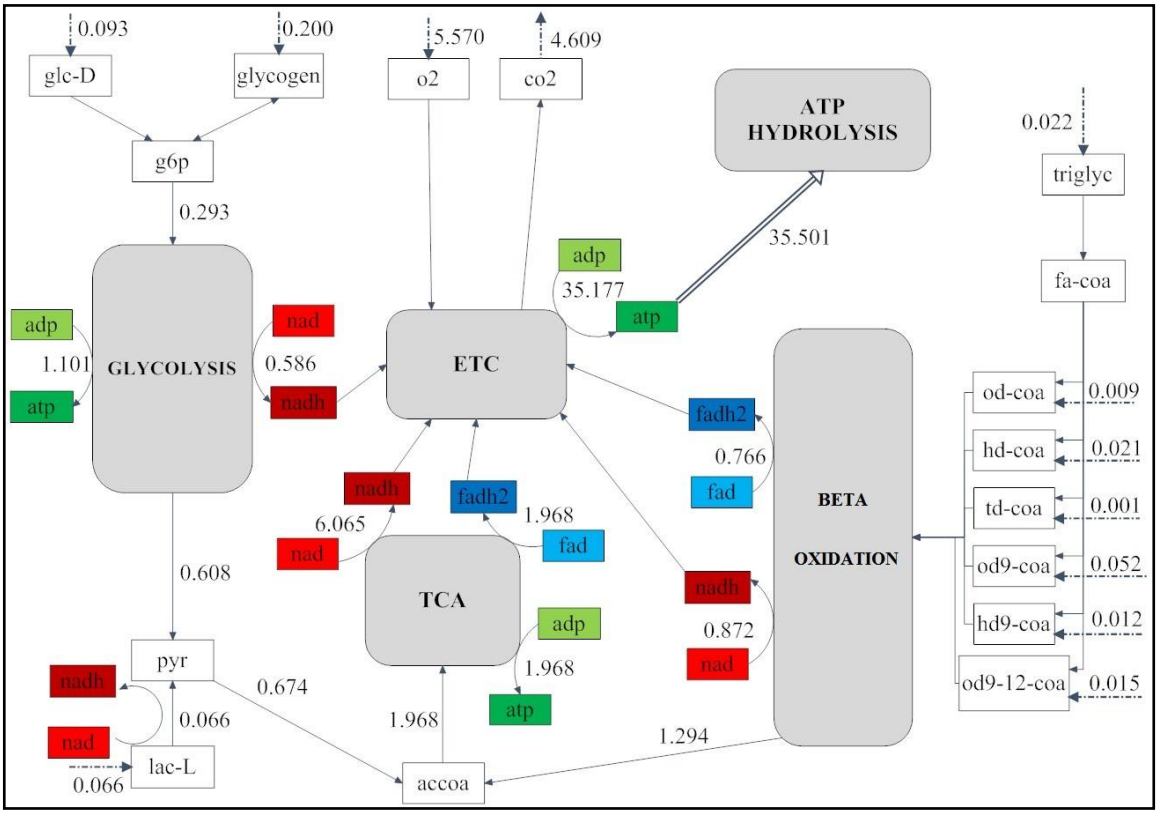

Figure 7.4. Flux distribution for fasting

The FBA results for the fasting with and without HMG-CoA synthase deficiency senario yield similar ATP hyrolysis rates of 35.177 and 33.252 µmol/min/g wet weight, respectively (Figure 7.4 and 7.5). There is not any significant difference between these values because of the low concentrations of ketone bodies, used for ATP production. The deficiency of HMG-CoA synthase does not seem to critically affect the energy metabolism of the cardiomyocyte.

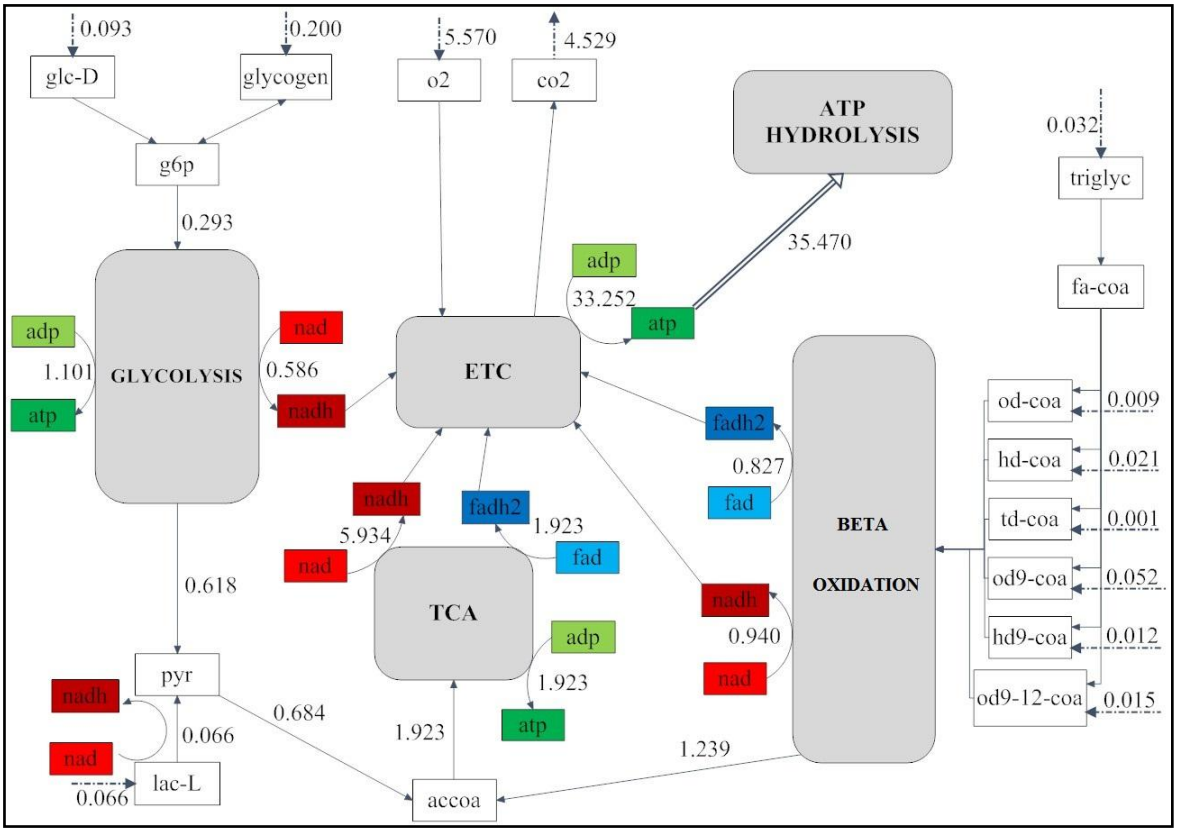

Figure 7.5. Flux distribution for fasting with HMG-CoA synthase deficiency

7.3.2. Mitochondrial Complex I Deficiency (NADH-CoQ reductase deficiency)

Complex I is one of the entry points of the oxidative phosphorylation system, which plays an important role in the energy metabolism of the cardiomyocyte. A dysfunction of complex I, which dehydrogenates NADH to NAD and H^+, may disturb the cellular NAD pool and oxidative phosphorylation, hence ATP production. In patients with complex I deficiency, high lactate concentrations and a severely increased NADH/NAD ratio are observed as a result of impared electron transfer chain (Smeitink *et al*, 2004).

7.3.2.1. Constraints: For the Complex I Deficiency, the experimental enzymatic activity of complex I is limited to 16.7% (Koga *et al*, 1988) of the normal value (8.988 μmol/min/g wet weight) obtained from the FBA of the normoxic case. All the uptake values are kept the same as the normoxic case.

Table 7.9. Uptake values for Complex I Deficiency

Reaction Name	Reaction	Healthy	Complex I
TRANSPORT 01	glc-D[e] -> glc-D[c]	0.560	0.444
TRANSPORT 02	glycogen[c] <=> glycogen[e]	-0.200	-0.036
TRANSPORT 03	lac-L[e] + h[e] <=> lac-L[c] + h[c]	0.258	-0.960
TRANSPORT 05	hd-ca[e] -> hd-ca[c]	0.022	0.009
TRANSPORT 06	od-ca[e] -> od-ca[c]	0.009	0.004
TRANSPORT 07	td-ca[e] -> td-ca[c]	0.002	0.001
TRANSPORT 12	od9-ca[e] -> od9-ca[c]	0.023	0.023
TRANSPORT 13	od9-12-ca[e] -> od9-12-ca[c]	0.010	0.007
TRANSPORT 14	hd9-ca[e] -> hd9-ca[c]	0.005	0.005
TRANSPORT 16	acac[e] -> acac[c]	0.000	0.001
TRANSPORT 24	triglyc[e] <=> triglyc[c]	-0.020	-0.002

7.3.2.2. Carbohydrate Metabolism: An important issue in the case of complex I deficiency is the reduced glycogen consumption and glucose uptake as well as the lactate production. Since the regeneration of NAD by the electron transfer chain is hindered, the performance of glycolysis decreases by 36% of the healthy case NAD flux and consequently the glycogen uptake also decreases. Lactate production rather than consumption occurs at the maximum extent (0.960 μmol/min/g wet weight) to generate NAD, which the cell lacks, from NADH.

7.3.2.3. Fatty Acid Metabolism: In case of complex I deficiency, due to the limited electron transfer chain performance, the uptake values of the fatty acids decrease and the accumulating excess fatty acids are converted to triglycerides as can be seen in Table 7.9.

7.3.2.4. Electron Transfer Chain: The effect of impaired oxidative phosphorylation can be seen in the change of flux values through electron transfer chain reactions given in Table 7.10. The 16.7% limitation of complex I resulted in about 80% decrease of the oxidative phosphorylation flux (ETC 01-04).

Table 7.10. Flux values of healthy state and complex I deficiency (μmol/min/g wet weight)

Reaction Name	Healthy	Complex I	% Change
ATP	37.759	7.649	79.7
BOX 09	0.009	0.004	55.6
BOX 10-16	0.000	0.003	-
BOX 17	0.022	0.009	59.5
BOX 18-20	0.000	0.007	-
BOX 21-32 (hd-coa)	0.000	0.011	-
BOX 26-28	0.000	0.001	-
BOX 37	0.000	0.011	-
BOX 46-63	0.012	0.045	259.1
ETC 01	9.190	1.501	83.7
ETC 02	1.950	0.698	64.2
ETC 03	11.140	2.199	80.3
ETC 04	5.570	1.100	80.3
GLYCGN 01	-0.200	-0.036	81.9
GLYCGN 04	0.200	0.036	81.9
PYR 01 (lac)	0.258	-0.960	472.4
TCA 01-04	1.866	0.389	79.2
TCA 05	1.866	0.389	79.2
TCA 06	0.658	0.155	76.5
TCA 07	1.208	0.234	80.6
TCA 08-09	1.866	0.389	79.2
TCA 10	2.024	0.560	72.3
TRANS 02 (glycogen)	-0.200	-0.036	81.9
TRANS 03 (lac)	0.258	-0.960	472.4
TRANS 05 (hd-ca)	0.022	0.009	59.5
TRANS 06 (od-ca)	0.009	0.004	55.6
TRANS 16 (acac)	0.000	0.001	-
TRANS 17 (co2)	-5.490	-0.778	85.8
TRANS 18 (o2)	5.570	1.100	80.3
TRANS 24 (triglyc)	-0.020	-0.002	92.3
TRIGLY 03	-1.580	0.173	111.0
TRIGLY 04	1.600	-0.172	110.7
TRIGLY 16	0.060	0.005	92.3
TRIGLYC 01-09	0.020	0.002	92.3
U-BOX 02-17	0.009	0.022	138.5
U-BOX 19-40 (od9-12-coa)	0.000	0.006	-
U-BOX 42-57 (hd9-coa)	0.003	0.005	51.9

7.3.2.5. TCA Cycle: The impaired oxidation of NADH to NAD by the electron transfer chain causes the flux through the TCA cycle to decrease about 80%, too (Figure 7.6).

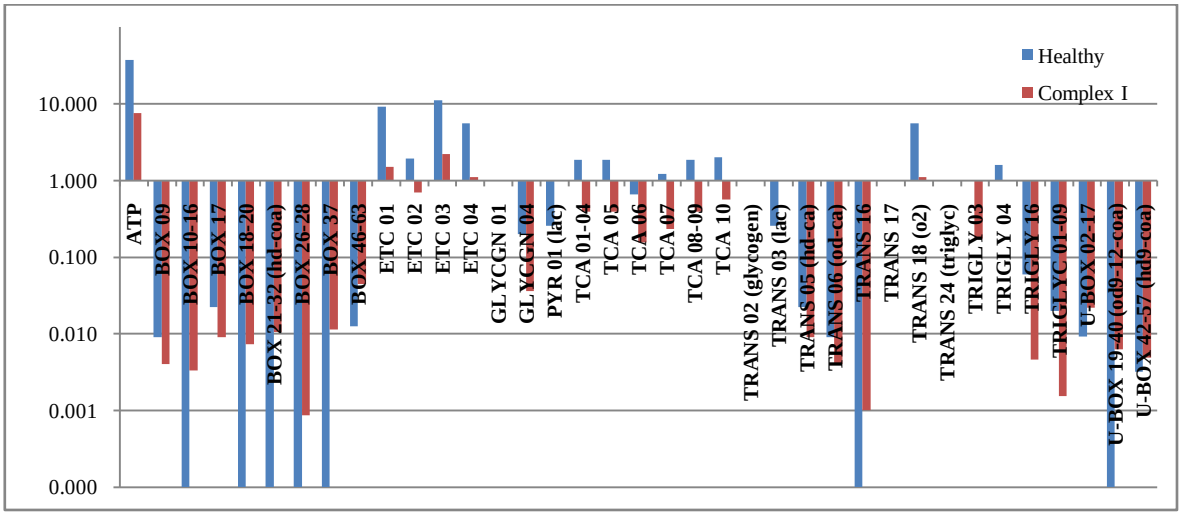

Figure 7.6. Flux comparison of healthy state vs. complex I deficiency (logarithmic scale)

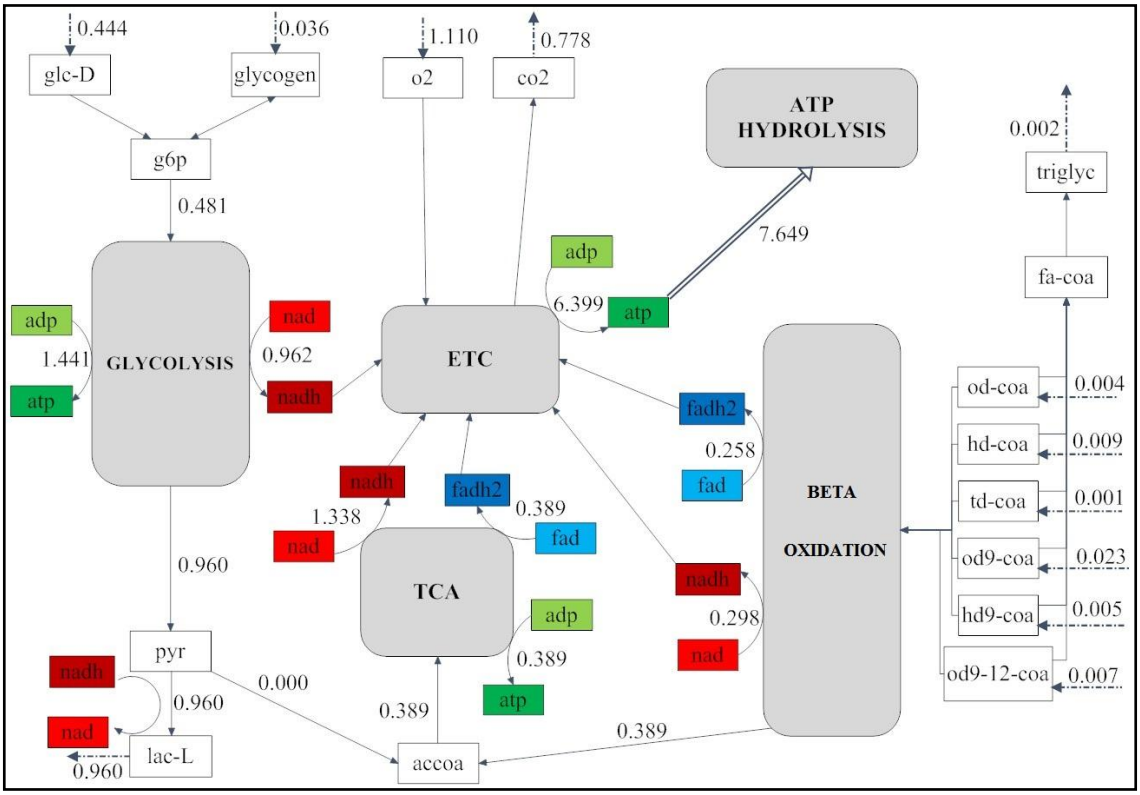

Figure 7.7. Flux distribution for complex I deficiency

7.3.2.6. ATP Hydrolysis: The ATP hydrolysis flux is found to be 7.649 μmol/min/g wet weight, which is about 20% of the normal healthy value. So a decrease about 80% of the oxidative phosphorylation directly affects the ATP production about the same proportion. Such low values may inhibit the sodium-potassium pump and the contraction of the cardiomyocyte.

It can be seen in Figure 7.7 that the anaerobic oxidation of glycolytic pathway improved its role in ATP production. The contribution of glycolysis to ATP production increases from 4% to 19%.

7.3.3. Primary Carnitine Deficiency

The main issue with the primary carnitine deficiency is that the transport of the fatty acid molecules from the cytoplasm to the mitochondria is impaired. For this deficiency, the reduced experimental concentration of the carnitine in tissue samples is used to limit the enzymatic activity of the carnitine-associated enzymes.

7.3.3.1. Constraints: The maximum activity of the carnitine palmitoyltransferase enzyme (transport rate) is limited to the 10% of the maximum acceptable values indicated in the healthy case scenario for each fatty acid molecule. The reactions with limited CPT rate are given in Table 7.11.

Table 7.11. List of carnitine palmiotyl transferase reactions

Reaction Name	Reaction
BOX 02	[c]: crn + ei-coa <=> ei-crn + coa
BOX 10	[c]: crn + od-coa <=> od-crn + coa
BOX 18	[c]: crn + hd-coa <=> hd-crn + coa
BOX 26	[c]: crn + td-coa <=> td-crn + coa
BOX 34	[c]: crn + dd-coa <=> dd-crn + coa
BOX 42	[c]: crn + d-coa <=> d-crn + coa
BOX 50	[c]: crn + o-coa <=> o-crn + coa
O-BOX 02	[c]: crn + pd-coa <=> pd-crn + coa
U-BOX 02	[c]: crn + od9-coa <=> od9-crn + coa
U-BOX 19	[c]: crn + od9-12-coa <=> od9-12-crn + coa
U-BOX 42	[c]: crn + hd9-coa <=> hd9-crn + coa

7.3.3.2. Carbohydrate Metabolism: Since glucose and glycogen are imported into the cell at the maximum rate, the only metabolite remaining for energy production other than the fatty acids is lactate. The present FBA results indicate a 30% increase in the lactate consumption of the cell in case of primary carnitine deficiency.

7.3.3.3. Fatty Acid Metabolism: It can be seen in Figure 7.8 that carnitine deficiency directly affects the reactions concerning fatty acids, which are β-oxidation reactions, triglyceride metabolism and transport reactions for fatty acids.

Since the transport of fatty acids into the mitochondria is hindered during carnitine deficiency, the fatty acids (fatty acyl-CoA) accumulation is expected. However, due to the fact that the cell is at steady state condition, fatty acids that are used for triglyceride production during healthy state, are now used for β-oxidation (Table 7.12). The fluxes through β-oxidation (BOX 09, 17, 25, 38-40, 45-64) and triglyceride metabolism show the most remarkable changes with respect to the healthy flux distribution.

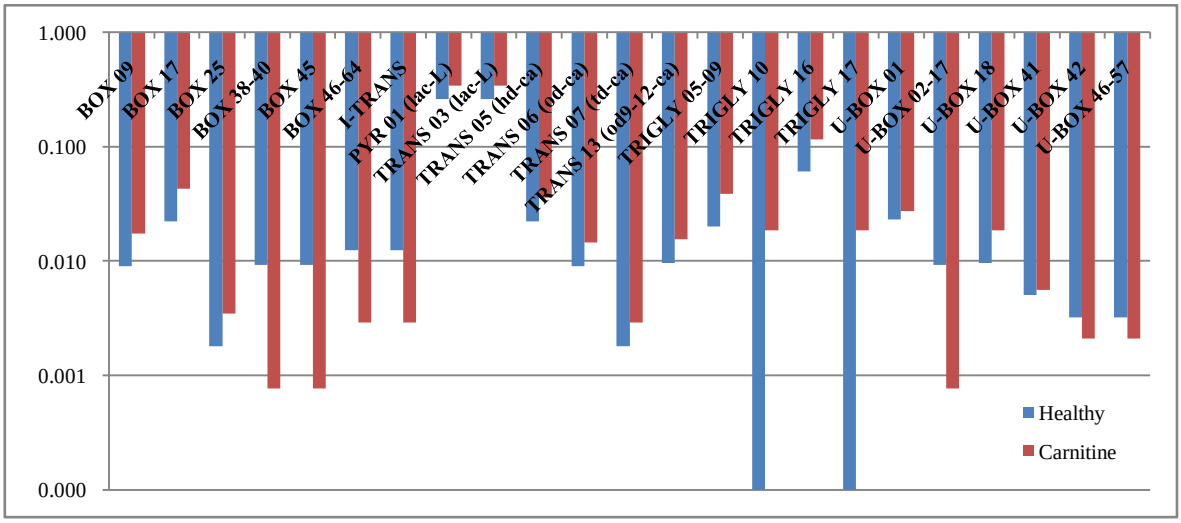

Figure 7.8. Flux comparison of healthy state vs. primary carnitine deficiency (logarithmic scale)

Table 7.12. Flux values for healthy state and primary carnitine deficiency (μmol/min/g wet weight)

Reaction Name	Healthy	Carnitine Def.	% Change
BOX 09	0.009	0.017	91.7
BOX 17	0.022	0.043	91.7
BOX 25	0.002	0.003	91.7
BOX 38-40	0.009	0.001	91.7
BOX 45	0.009	0.001	91.7
BOX 46-64	0.012	0.003	76.9
I-TRANS (crn)	0.012	0.003	76.9
PYR 01 (lac-L)	0.258	0.338	31.0
TRANS 03 (lac-L)	0.258	0.338	31.0
TRANS 05 (hd-ca)	0.022	0.036	61.1
TRANS 06 (od-ca)	0.009	0.014	61.1
TRANS 07 (td-ca)	0.002	0.003	61.1
TRANS 13 (od9-12-ca)	0.010	0.015	61.1
TRIGLY 05-09	0.020	0.038	91.7
TRIGLY 10	0.000	0.018	-
TRIGLY 16	0.060	0.115	91.7
TRIGLY 17	0.000	0.018	-
U-BOX 01	0.023	0.027	18.3
U-BOX 02-17	0.009	0.001	91.7
U-BOX 18	0.010	0.018	91.7
U-BOX 41	0.005	0.006	11.0
U-BOX 42	0.003	0.002	34.4
U-BOX 46-57	0.003	0.002	34.4

7.3.3.4. ATP Hydrolysis: The flux distribution in Figure 7.9 shows that glucose replaces fatty acids for the continuity of ATP production, since the decreased rates of accoa and NADH produced by β-oxidation cause the overall fraction of those supplied by glycolysis to increase, though they remain the same in quantity. Although the maximum ATP hydrolysis rate is 37.742 μmol/min/g wet weight, the cell is still dependent on the supplies of triglyceride and glycogen. In the long run, glucose only may not be enough for the sustenance of energy production, and the cell may experience problems.

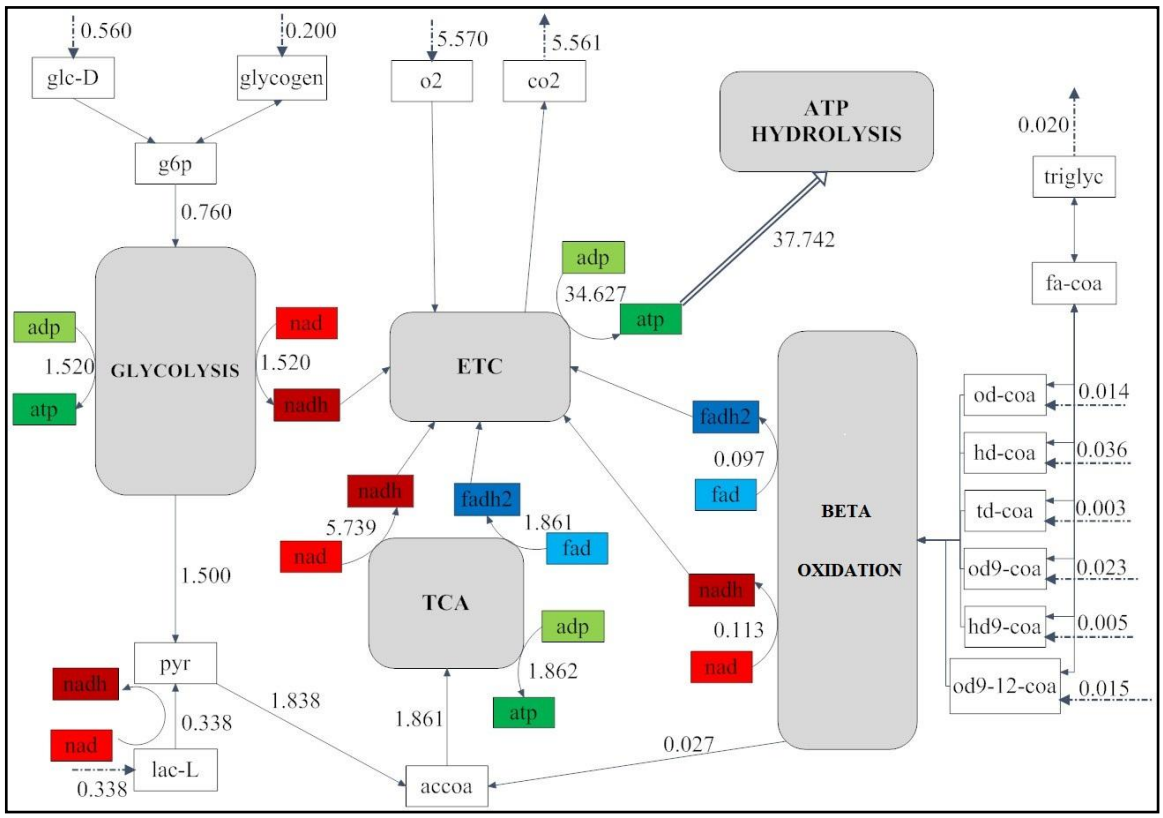

Figure 7.9. Flux distribution for primary carnitine deficiency

7.3.4. Fabry Disease

Fabry disease affects the sphingolipid metabolism of the cells and results in the accumulation of the glycosphingolipid globotriaosylceramide in the cell. Since metabolic effects of this disease only manifest themselves in the structural lipid metabolism of the cell and not the lipids which are associated with the energy metabolism, and the corresponding lipid products are not included in the constructed network, this case is not applicable for the flux balance analysis with the present network and objective function.

7.3.5. Tangier Disease

Tangier disease affects the cholesterol transport system of the cells and results in the accumulation of the high density lipoproteins in the cell. The experimental data show that no accumulation of triglycerides or phospholipids occur in the cell. Since the metabolic effects of this disease only manifest themselves in the structural lipid metabolism of the cell and not the lipids which are associated with the energy metabolism, and the

corresponding lipid products are not included in the constructed network, this case is not applicable for the flux balance analysis with the present network and objective function.

7.4. Ischemia

Reduced blood flow in ischemia manifests itself mainly as reduced oxygen supply for the cell. Hence, the case for ischemia is investigated by limiting the oxygen supply by 70%, a moderate ischemia state.

7.4.1.1. Carbohydrate Metabolism: Lactate production occurs (0.413 μmol/min/g wet weight consumption in healthy case vs. 0.960 μmol/min/g wet weight production in ischemia) as it can be seen in Figure 7.11.

7.4.1.2. Fatty Acid Metabolism: The reactions of β-oxidation (BOX 09, 17, 25 38-40, 45-64) and triglyceride metabolism are also among the most affected ones (Figure 7.10) since the impaired oxidative metabolism hinders β-oxidation and shifts fatty acids to triglyceride production increasing the triglyceride reserves of the cell.

7.4.1.3. Electron Transfer Chain: It can be seen in Table 7.13 that the electron transfer chain is directly affected by the limited oxygen supply. The flux through oxidative phosphorylation (ETC 01-04) decreases about the same rate as the oxygen consumption.

7.4.1.4. ATP Hydrolysis: Since fatty acids are the major source for energy production, impaired oxygen supply affects the energy metabolism severely. A maximum ATP hydrolysis rate of 12.181 μmol/min/g wet weight can be achieved, which is about 1/3 of the normal need of a cardiomyocyte.

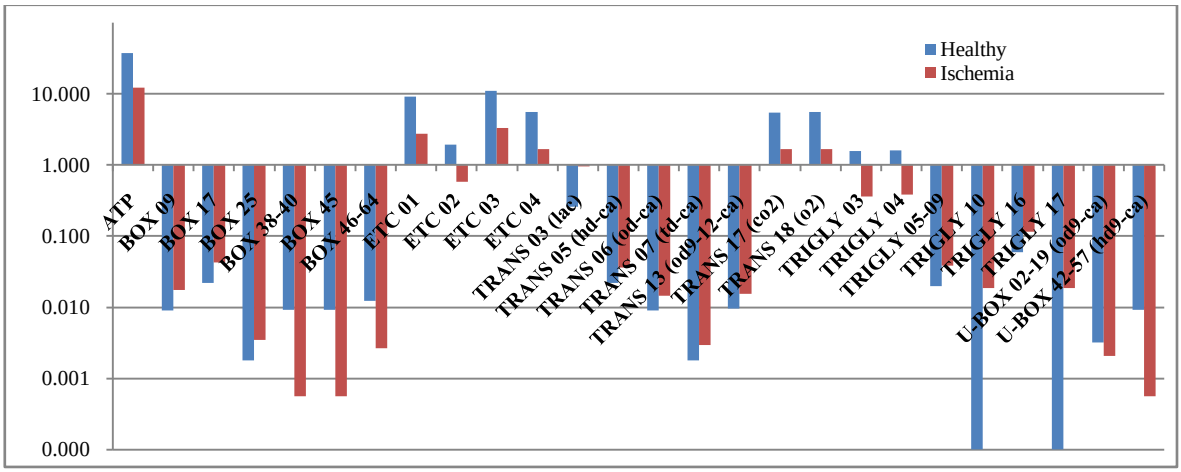

Figure 7.10. Flux comparison of healthy vs. ischemic state (logarithmic scale)

Table 7.13. Flux values for healthy and ischemic states (μmol/min/g wet weight)

Reaction Name	Healthy	Ischemia	% Change
ATP	37.759	12.181	67.7
BOX 09	0.009	0.017	93.9
BOX 17	0.022	0.043	93.9
BOX 25	0.002	0.003	93.9
BOX 38-40	0.009	0.001	93.9
BOX 45	0.009	0.001	93.9
BOX 46-64	0.012	0.003	78.7
ETC 01	9.190	2.764	69.9
ETC 02	1.950	0.578	70.4
ETC 03	11.140	3.342	70.0
ETC 04	5.570	1.671	70.0
TRANS 03 (lac)	0.258	0.960	272.4
TRANS 05 (hd-ca)	0.022	0.036	62.6
TRANS 06 (od-ca)	0.009	0.015	62.6
TRANS 07 (td-ca)	0.002	0.003	62.6
TRANS 13 (od9-12-ca)	0.010	0.016	62.6
TRANS 17 (co2)	5.490	1.663	69.7
TRANS 18 (o2)	5.570	1.671	70.0
TRIGLY 03	1.580	0.362	77.1
TRIGLY 04	1.600	0.382	76.1
TRIGLY 05-09	0.020	0.039	93.9
TRIGLY 10	0.000	0.019	-
TRIGLY 16	0.060	0.116	93.9
TRIGLY 17	0.000	0.019	-
U-BOX 02-19 (od9-ca)	0.003	0.002	35.2
U-BOX 42-57 (hd9-ca)	0.009	0.001	93.9

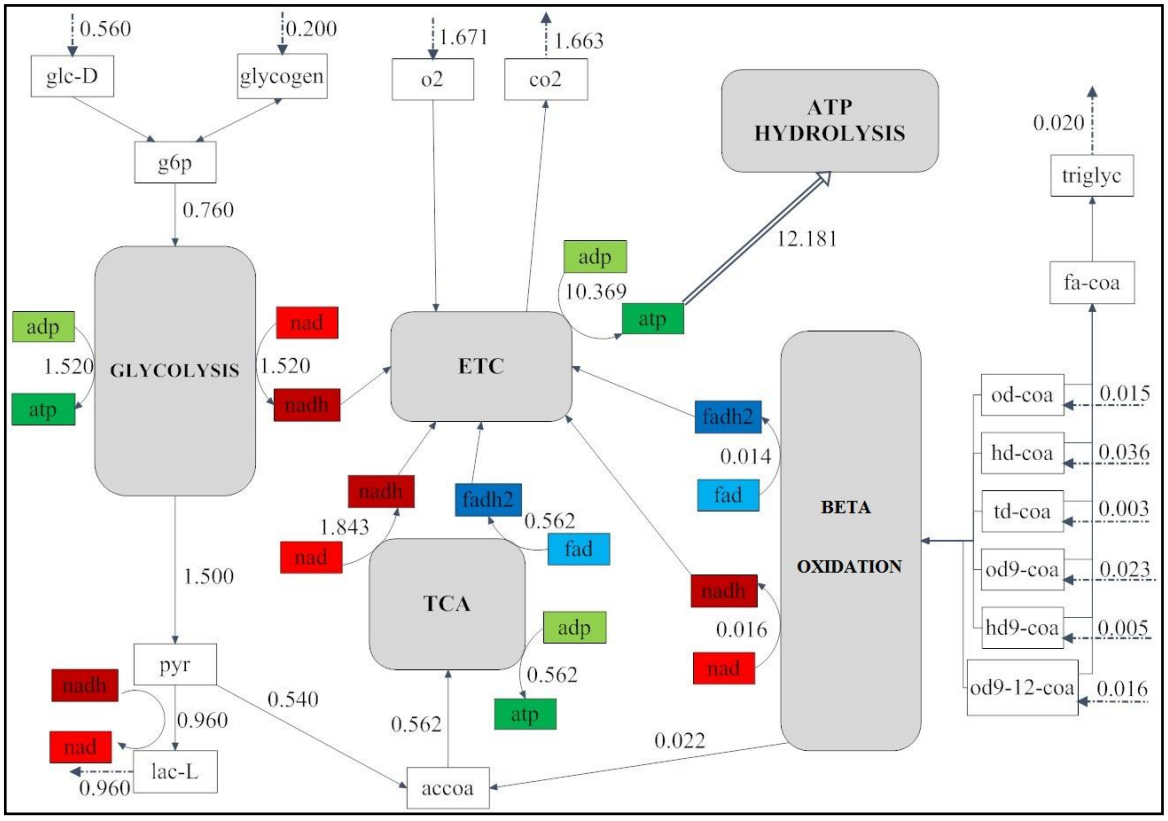

Figure 7.11. Flux distribution for ischemia

7.5. Flux Variability Analysis

Flux variability analysis is performed to obtain the range for each flux by maximizing and minimizing each reaction separately as the objective function in the FBA. This method was only applied to the healthy case. When the previously obtained ATP hydrolysis rates were used for the variability analysis of the disease cases, an optimization by linear programming could not be done for most of the reactions in the network.

For the healthy case, all of the flux values remained constant when the maximum ATP hydrolysis rate of 37.759 μmol/min/g wet weight was fixed. Therefore, the experimental value of 30 μmol/min/g wet weight is used in the flux variability analysis and the results are given in Table D.2. The calculated values of flux ranges are compared to various data obtained from literature (Table 7.14) to substantiate the constraints and parameters used.

Table 7.14. Flux range comparisons

Reaction	Name	Flux Range	Lit. Value	Reference
Fatty Acid Utilization (C14:0)	BOX 27	0-0.008	0.001	Bergmann, 1995
Fatty Acid Utilization (C16:0)	BOX 19	0-0.105	0.027	Bergmann, 1995
Fatty Acid Utilization (C16:1)	U-BOX 43	0.002-0.026	0.011	Bergmann, 1995
Fatty Acid Utilization (C18:0)	BOX 11	0-0.042	0.009	Bergmann, 1995
Fatty Acid Utilization (C18:1)	U-BOX 03	0-0.133	0.053	Bergmann, 1995
Fatty Acid Utilization (C18:2)	U-BOX 20	0-0.056	0.020	Bergmann, 1995
Glucose Uptake	TRANS 01	0.430-0.560	0.510	Kofoed, 2002
Lactate Formation	PYR 01	0-0.916	0.180	Stanley, 1994
Mitochondrial Respiration	ETC 04	4.386-5.570	4.000-5.500	Mootha, 1997
Palmitate Oxidation	BOX 19	0-0.105	0.200-0.140	O'Donnell, 2002
Pyruvate Dehydrogenase	PYR 03	0-1.993	1.260	Stanley, 1997
Oxygen Consumption	TRANS 18	4.386-5.570	2.340	O'Donnell, 2002
Palmitate Oxidation	BOX 19	0-0.105	0.090	O'Donnell, 2002
TCA Flux	TCA 01	1.432-5.183	0.870	O'Donnell, 2002
Aspartate shuttle	MAL-ASP 02	0-0.200	0.290	O'Donnell, 2002

The fluxes are next classified according to their activity in the metabolism as ‘never been used’, ‘having constant flux values’ or ‘having variable flux values’ (Voet al., 2004). There are no fluxes with constant values and 90 reactions out of a total of 287 have never been used (Tables 7.14 and D.1). However all of these “never been used” reactions belong to the very-long fatty acid molecules of ei-ca, tcs-ca and dcs-ca, that have been eliminated from the network because of their very low uptake rates relative to the other fatty acid molecules, and their corresponding β-oxidation reactions.

Table 7.15. Flux classes of flux variability analysis

“never been used”	“having constant flux values”	“having variable flux values”
90	0	197

The flux ranges obtained from the flux variability analysis are ranked according to their magnitude and plotted on Figure 7.12. The most variable fluxes are those that belong to pyruvate, glycogen and triglyceride metabolism. Pyruvate metabolism is directly linked to malate-aspartate shuttle, hence it has a wide range.

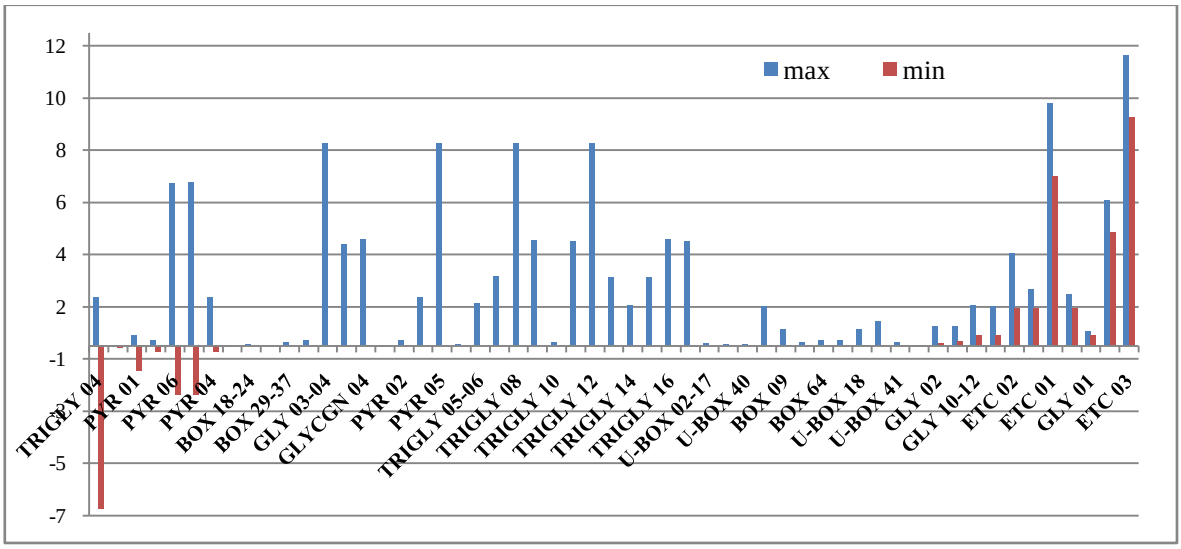

Figure 7.12. Flux ranges for flux variability analysis

Glycogen and triglycerides are the cells internal deposits, and they can be either produced or used, thus these two metabolisms are quiet flexible in their flux values.

Since the main source of energy of cardiomyocytes is the oxidative phosphorylation, ATP hydrolysis and oxidative phosphorylation are directly related. Thus, the least flexible range in the flux variability analysis belongs to the fluxes of electron transfer chain as seen in Figure 7.12. The fixed objective function of ATP hydrolysis causes the oxidative phosphorylation to be the least variable group in the network as well.

7.6. Flux Coupling Analysis

The Flux Coupling analysis is used for finding coupled reaction sets and blocked reactions in genome-scale metabolic systems. The set of blocked reactions for a given network is identified by maximizing each particular flux subject to the stoichiometric matrix. If the maximum possible value of a particular flux is zero, then the reaction is said to be unusable or blocked because it cannot carry any flux. Linear fractional programming is employed to identify the maximum and minimum flux ratios (i.e., max v_1/v_2, min v_1/v_2) for every pair of metabolic fluxes (Burgard *et al.*, 2004).

In the present study, in order to analyze the reaction network, the reversible reactions were first separated as two irreversible reactions. Then to this newly constructed

stoichiometric matrix, flux maximization was applied to obtain the blocked reactions. The set of blocked reactions were the same as the “never been used” set obtained in the flux variability analysis. These blocked reactions were removed from the matrix and a 229x310 stoichiometric matrix is obtained.

In order to obtain the coupled reactions, the procedure of flux coupling finder was followed. The procedure was performed for all the previously studied cases of healthy and disease conditions. For each case the same constraints and limitations used previously in the flux balance analysis was applied. From this newly constructed reaction set of 310 reactions, there are a total of 47895 coupled reaction sets, which are the 2-combinations of 310 reactions. For the healthy case scenario, 35 fully coupled, 4854 directionally coupled, and 11630 partially coupled reaction sets are obtained (Table 7.16). When the results of the disease cases were investigated, it was observed that the results only contained directionally coupled and un-coupled reaction sets.

Table 7.16. Flux coupling results for healthy case scenario

Type	**#**
Fully coupled	35
Directionally coupled	4854
Partially Coupled	11630
Uncoupled	31376
Total	47895

It should be noticed that for such a big reaction set of 310 reactions there are huge amount of data to be analyzed. These previously mentioned 47895 reaction sets cannot be analyzed individually to obtain a coupling network such as Figure 6.2.

For the healthy case, the reactions in Table 7.17 are found to be fully coupled. Full coupling ($v_1 \Leftrightarrow v_2$) suggest that a non-zero flux for v_1 implies not only a non-zero but also a fixed flux for v_2 and vice versa. This is an expected result for the previously mentioned reversible reaction sets. However, only eight reversible reaction sets highlighted in Table 7.17 are found to be fully coupled. Most of the other reactions are from the β-oxidation pathway that do not suggest a specific group or metabolism, and no plausible results can be obtained from these data.

Table 7.17. Fully Coupled Reactions

Reaction Name #1	Reaction #1	Reaction Name #2	Reaction #2
1	glc-D[e] -> glc-D[c]	glc-D[e]xt	glc-D[e]xt
95	[c]: atp + coa + dd-ca <=> amp + dd-coa + ppi	95rev	[c]: atp + coa + dd-ca <=> amp + dd-coa + ppi
100	[m]: t-dd-coa + h2o -> 3h-dd-coa	101	[m]: 3h-dd-coa + nad -> 3o-dd-coa + nadh + h
102	[m]: 3o-dd-coa + coa -> d-coa + accoa	107	[m]: d-coa + fad -> t-d-coa + fadh2
103	[c]: atp + coa + d-ca <=> amp + d-coa + ppi	103rev	[c]: atp + coa + d-ca <=> amp + d-coa + ppi
108	[m]: t-d-coa + h2o -> 3h-d-coa	110	[m]: 3o-d-coa + coa -> o-coa + accoa
109	[m]: 3h-d-coa + nad -> 3o-d-coa + nadh + h	122	[m]: 3o-h-coa + coa -> but-coa + accoa
110	[m]: 3o-d-coa + coa -> o-coa + accoa	116	[m]: t-o-coa + h2o -> 3h-o-coa
111rev	[c]: atp + coa + o-ca <=> amp + o-coa + ppi	111	[c]: atp + coa + o-ca <=> amp + o-coa + ppi
118	[m]: 3o-o-coa + coa -> h-coa + accoa	122	[m]: 3o-h-coa + coa -> but-coa + accoa
119	[m]: h-coa + fad -> t-h-coa + fadh2	122	[m]: 3o-h-coa + coa -> but-coa + accoa
119	[m]: h-coa + fad -> t-h-coa + fadh3	123	[m]: but-coa + fad -> t-but-coa + fadh2
120	[m]: t-h-coa + h2o -> 3h-h-coa	125	[m]: 3h-but-coa + nad -> acaccoa + nadh + h
123	[m]: but-coa + fad -> t-but-coa + fadh3	125	[m]: 3h-but-coa + nad -> acaccoa + nadh + h
123	[m]: but-coa + fad -> t-but-coa + fadh2	124	[m]: t-but-coa + h2o -> 3h-but-coa
161	[m]: od9-crn + coa -> crn + od9-coa	165	[m]: 3o-od9-coa + coa -> hd7-coa + accoa
166	[m]: hd7-coa + fad -> t-hd7-coa + fadh2	169	[m]: 3o-hd7-coa + coa -> td5-coa + accoa
172	[m]: 3h-td5-coa + nad -> 3o-td5-coa + nadh + h	173	[m]: 3o-td5-coa + coa -> cisdd-coa + accoa
338	o2[e] <=> o2[c]	o2[e]xt	o2[e]xt
177	od9-12-crn[c] -> od9-12-crn[m]	178	[m]: od9-12-crn + coa -> crn + od9-12-coa
178	[m]: od9-12-crn + coa -> crn + od9-12-coa	180	[m]: t-od9-12-coa + h2o -> 3h-od9-12-coa
188	[m]: t-td-5-8-coa + h2o -> 3h-td-5-8-coa	189	[m]: 3h-td-5-8-coa + nad -> 3o-td-5-8-coa + nadh + h
199	[c]: crn + hd9-coa -> hd9-crn + coa	212	[m]: 3h-dd5-coa + nad -> 3o-dd5-coa + nadh + h
203	[m]: t-hd9-coa + h2o -> 3h-hd9-coa	205	[m]: 3o-hd9-coa + coa -> td7-coa + accoa
204	[m]: 3h-hd9-coa + nad -> 3o-hd9-coa + nadh + h	210	[m]: dd5-coa + fad -> t-dd5-coa + fadh2
205	[m]: 3o-hd9-coa + coa -> td7-coa + accoa	210	[m]: dd5-coa + fad -> t-dd5-coa + fadh2
210	[m]: dd5-coa + fad -> t-dd5-coa + fadh2	211	[m]: t-dd5-coa + h2o -> 3h-dd5-coa
316	acac[c] -> acac[m]	acac[e]xt	acac[e]xt
317	[m]: acac + coa + atp -> acaccoa + adp + pi	acac[e]xt	acac[e]xt
330	coa[c] <=> coa[m]	330rev	coa[c] <=> coa[m]
331	glu-L[c] + h[c] <=> glu-L[m] + h[m]	331rev	glu-L[c] + h[c] <=> glu-L[m] + h[m]
334	o2[c] <=> o2[p]	334rev	o2[c] <=> o2[p]
341	[c]: dhap + nadh <=> glyc3p + nad	341rev	[c]: dhap + nadh <=> glyc3p + nad
16	[c]: g6p + nadp -> 6pgl + nadph + h	18	[c]: 6pgc + nadp -> ru5p + co2 + nadph + h
25	[c]: (2) glut-red + h2o2 <=> glut-ox + (2) h2o	25rev	[c]: (2) glut-red + h2o2 <=> glut-ox + (2) h2o

Directional coupling, unlike partial and full coupling, can capture the one way type of connectivity between metabolic reactions. This information enables the global identification of *equivalent knockouts* defined as the set of all possible reactions whose

deletion forces the flux through a particular reaction to zero, and sets of *affected reactions* defined as all reactions whose fluxes are forced to zero if a particular reaction is deleted (Burgard *et al.*, 2004). So a limited reaction such as that of complex I deficiency is expected to be directionally coupled with the affected reactions. However, when the directionally coupled reactions sets of complex I deficiency were investigated, it was observed that the reaction catalyzed by complex I was not directionally coupled with any other reactions. Such results were observed in other cases, so no meaningful result was obtained from the flux coupling analysis.

7.7. Self-Organizing Maps

Self-Organizing Maps (SOM), which is a mathematical cluster method, is used to organize the reactions of the network into biologically relevant clusters and to observe the co-response of fluxes in case of enzyme deficiencies. The self-organizing maps of clusters are computed and from a variety of different grid variations a 7x7 SOM is selected to present the data that cover the whole map with the most significant and plausible clusters. The smaller grid ranges resulted in clusters with no reactions. When nodes are added, distinctive and tight clusters emerge as indicated by Tamayo *et al*, 1999.

The computed clusters and their centroids are presented in Figure 7.13, where the SOM centers of flux values for the reactions are plotted for each cluster. The y-axis of the figure represents the reactions and the x-axis represents the FBA simulations for healthy case, healthy case with unbounded oxygen, primary carnitine deficiency, mitochondrial complex I deficiency, fasting state, fasting together with HMG-CoA synthase deficiency and ischemic state, respectively. The name of each cluster and the number of reactions included are given above each plot. All of the reactions and their corresponding clusters are listed in Table E.1.

C1 is the cluster that represents the ketone body metabolism. The reaction of acetoacetoyl-CoA formation from acetoacetate together with the extracellular and intracellular transport of acetoacetate is included in this cluster. It can be seen that the fifth node that belongs to the fasting state shows an increase of the reactions, relative to other nodes. The nodes of fasting without and with HMG-CoA synthase deficiency (fifth and

sixth nodes in the clusters, respectively) show the same behavior in all the other clusters. It can be deduced that as HMG-CoA synthase deficiency only concerns the ketone body metabolism, the close ATP hydrolysis rates obtained in flux balance analysis in case of enzyme deficient and indeficient fasting states are consequential, as stated in Section 7.3.1.

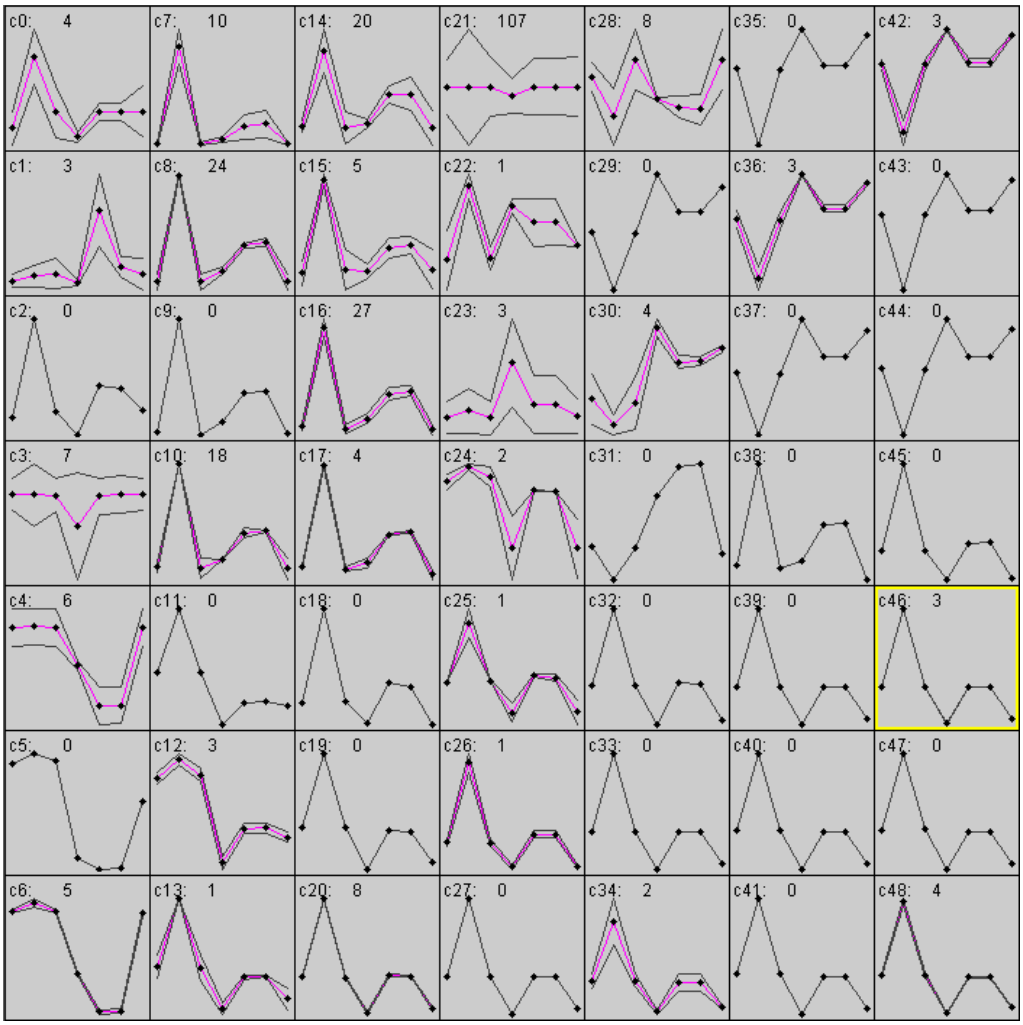

Figure 7.13. Cluster groups of Self-Organizing Maps

TCA cycle is represented by the cluster c20. All reactions of TCA cycle are included in this cluster. In some of the grids smaller than 7x7, these sets of reactions were not grouped in the same cluster. A similar cluster is observed in c24, which includes the transport and dehydrogenation reactions of lactate. Maximum values for this cluster is observed in the second node, the healthy case with unbounded oxygen, where all the metabolites were used at a maximum rate as stated in Section 7.2.2.

The glycolysis reactions together with the import reaction of glucose are divided into two clusters, c4 and c6. The reactions in each cluster form a linear pathway and the division into two clusters implies that a metabolite in the glycolysis pathway is being used/produced by another one. For example, the metabolites 3pg and dhap are either used or produced in the triglyceride metabolism and thus they affect the second part of the glycolysis (c6) according to their contribution to triglyceride metabolism. Nodes 5 and 6, representing the fasting scenarios show rather smaller values that the other cases, due to the decreased glucose levels in the blood during fasting, hence low glucose uptake and glycolysis rates.

C3 and c23 contain reactions of malate-aspartate shuttle and pyruvate transport into mitochondria, together with two interesting reactions of glycogen metabolism. C3 includes the glycogen degradation reaction with the pyruvate transport into mitochondria. Pyruvate is produced during glycolysis and then it has two fates. It may either enter the mitochondria to be converted to acetyl-CoA, which further enters the TCA cycle, or it may be used for lactate production. So cluster c3 suggests that glycogen used in glycolysis is directly used for pyruvate production that will be used in the TCA cycle and not for lactate production. Node 4 shows a different behavior in these two clusters. Since during complex I deficiency the regeneration of NAD by the electron transfer chain is hindered, the NADH and pyruvate produced in the cytoplasm by glycolysis is consumed by the lactate production. Hence, NADH transport to the mitochondria for the electron transfer chain by the malate-aspartate shuttle also decreases.

C7, c8, c10, c14, c15, c16 and c17 concern fatty acid oxidation. These cluster groups link the triglyceride degradation reactions with β-oxidation reactions. It is observed that the fatty acids and their corresponding β-oxidation reactions are usually included in the same clusters, for example, c8 contains β-oxidation of od9-12-coa. C8 also includes a reaction from pyruvate metabolism. Malate is converted to pyruvate for the production of NADPH that will be used by β-oxidation of od9-12-coa. In these clusters nodes belonging to healthy case with unbounded oxygen and the two fasting states have relatively higher values due to the increased fatty acid uptake in these scenarios.

The metabolism of triglyceride synthesis is found in c28. An important point to mention about this cluster is that it was not linked with any of the β-oxidation reactions. Triglyceride is produced under normal conditions for cases of emergency in the cell and when there is excess fatty acid moieties in the cell, so it does not affect any other metabolism.

C46 links the transport of oxygen to oxidative phosphorylation. This phenomena has also been observed in the flux balance analysis of complex I deficiency and the ischemic state. When there is not enough oxygen available to cell, the flux values through electron transfer chain decrease. The opposite is also observed such that when the performance of electron chain is limited, the oxygen uptake is reduced. Hence, nodes 4 and 7, belonging to the mitochondrial complex I deficiency and ischemia, have relatively lower values compared to the other states.

C21 is a huge cluster of 107 reactions, and it includes all of the reactions that were labeled as “never been used” by the flux variability analysis.

8. CONCLUSION and RECOMMENDATIONS

8.1. Conclusions

The constructed reaction network presented in this study seems to be successful as a candidate model for the investigation of normoxic conditions as well as enzyme deficiencies and metabolic stress conditions using the energy metabolism of cardiomyocytes. The network includes all of the key substrates and metabolisms for the energy production.

The objective function, ATP hydrolysis, employed for the analysis of the network covers most of the energy consuming pathways and metabolism in the cardiomyocyte such as contraction and Na-K pumps.

The flux distributions at different physiological conditions are obtained by using flux balance analysis. It is observed that the reconstructed model shows parallel results with the experimental findings and with the symptoms of the healthy and disease states. The results of flux variability analysis indicate that the flux ranges obtained by the model overlap with the experimental flux values. The reactions are organized into biologically relevant clusters and the co-response of fluxes in case of enzyme deficiencies are investigated.

The flux distribution maps show that under healthy conditions the cardiac energy metabolism provides most of the energy primarily from the fatty acids and then from glucose and lactate. Lactate production is observed when the cell is under limitations regarding aerobic oxidation such as ischemia and complex I deficiency.

The ATP production rate decreases under all disease and metabolic stress conditions. To increase the impaired ATP hydrolysis, the cellular reserves of glycogen are used at all conditions. However, triglyceride reserves are not always used like glycogen. In case of impaired or decreased fatty acid oxidation caused by primary carnitine deficiency, complex I deficiency and ischemia, fatty acid metabolism shifts in the direction of triglyceride production.

Although the present model shows promising results with enzyme deficiencies of energy metabolism such as Mitochondrial Complex I deficiency or Primary carnitine deficiency, or metabolic limitations such as fasting and ischemia, enzyme deficiencies of non-energy related metabolisms such as Tangier and Fabry disease cannot be studied with this model. These types of diseases do not create applicable constraints for this stoichiometric (steady state) model, since they result in lipid accumulation, which interrupts the cell physiologically rather than metabolically. Lipid accumulation in the lysosomes of the cell affects the physiological structure of the cell, rather than a metabolic involvement in the reactions.

8.2. Recommendations

The major drawback of this model is that it represents steady state conditions. A better model can be constructed by taking dynamic conditions into consideration. However, a study with dynamic conditions will lead to the parameter estimation problem.

Moreover, the constant contractile behavior of the cardiomyocyte can best be presented under dynamic constraints. Linking this model of energy metabolism with the contraction and Na-K pumps of the cardiac metabolism will shed light to future understanding in cardiac studies.

APPENDIX A

Table A.1. Reactions added for modeling purposes

Reaction Name	**Enzyme**	**Reaction**	**Pathway/Metabolism**	**E.C. #**
ATP		[c]: atp + h2o -> adp + pi + h	ATP hydrolysis	
CONTR 01	muscle contraction, myocyte cytosol	[c]: myoactinADPPi -> adp + myoactin + pi	Contraction	
CONTR 02	myosin-ADP-Pi attachment, myocyte cytosol	[c]: actin + myosinADPPi -> myoactinADPPi	Contraction	
CONTR 03	myosin ATP binding, myocyte cytosol	[c]: atp + myoactin -> actin + myosinATP	Contraction	
CONTR 04	myosin-ATP hydrolysis, myocyte cytosol	[c]: h2o + myosinATP -> h + myosinADPPi	Contraction	
ETC 01	Complex I - NADH:Ubiquinone oxidoreductase	nadh[m] + (5) h[m] + ubq[mim] -> nad[m] + (4) h[mis] + qh2[mim]	Electron Transport Chain	
ETC 02	succinate dehydrogenase cytochrome b	fadh2[m] + ubq[mim] <=> fad[m] + qh2[mim]	Electron Transport Chain	
ETC 03	ubiquinol-cytochrome c reductase	qh2[mim] + (2) h[m] + (2) cytc-o[mim] -> ubq[mim] + (2) cytc-r[mim] + (4) h[mis]	Electron Transport Chain	1.10.2.2
ETC 04	cytochrome c oxidase	o2[m] + (8) h[m] + (4) cytc-r[mim] -> (2) h2o[m] + (4) h[mis] + (4) cytc-o[mim]	Electron Transport Chain	1.9.3.1
I-TRANS		coa[m] <=> coa[p]	Modeling Purpose	
I-TRANS		h2o[c] <=> h2o[p]	Modeling Purpose	
I-TRANS		nad[m] <=> nad[p]	Modeling Purpose	
I-TRANS		nadh[p] <=> nadh[m]	Modeling Purpose	
I-TRANS		h[p] <=> h[m]	Modeling Purpose	
I-TRANS		crn[m] <=> crn[c]	Transport	
I-TRANS		h[c] <=> h[m]	Transport	
I-TRANS	CO_2 transport (diffusion),	co2[c] <=> co2[m]	Transport	
I-TRANS	CoA transporter	coa[c] <=> coa[m]	Transport	
I-TRANS		glu-L[c] + h[c] <=> glu-L[m] + h[m]	Transport	
I-TRANS	H_2O transport, mitochondrial	h2o[c] <=> h2o[m]	Transport	

Table A.1. Reactions added for modeling purposes - continued

Reaction Name	**Enzyme**	**Reaction**	**Pathway/Metabolism**	**E.C. #**
I-TRANS	O_2 transport (diffusion)	o2[c] <=> o2[m]	Transport	
I-TRANS	O_2 transport (diffusion)	o2[c] <=> o2[p]	Transport	
I-TRANS	phosphate transporter, mitochondrial	h[c] + pi[c] <=> h[m] + pi[m]	Transport	
NUCLEO 02	adenylate kinase	[c]: amp + atp <=> (2) adp	Nucleotide	2.7.4.3
NUCLEO 03	ATP synthase	adp[m] + pi[m] + (3) h[mis] -> atp[m] + (3) h[m] + h2o[m]	Nucleotide	3.6.3.14
NUCLEO 04	ADP/ATP translocase homodimer	atp[m] + adp[c] -> atp[c] + adp[m]	Nucleotide	
NUCLEO 05	nucleoside-diphosphate kinase (ATP:GDP)	[m]: atp + gdp <=> adp + gtp	Nucleotide	2.7.4.6
OTHERS	catalase	[p]: (2) h2o2 --> (2) h2o + o2	Others	
OTHERS	pyrophosphatase (inorganic) 1	[c]: ppi + h2o -> (2) pi + h	Others	3.6.1.1
OTHERS	glutathione reductase	[c]: glut-ox + nadph + h -> (2) glut-red + nadp	Others	1.8.1.7
OTHERS	glutathione peroxidase	[c]: (2) glut-red + h2o2 <=> glut-ox + (2) h2o	Others	1.11.1.9
TRANS 17	CO_2 transporter via diffusion	co2[e] <=> co2[c]	Transport to cytosol	
TRANS 18	O_2 transport (diffusion)	o2[e] <=> o2[c]	Transport to cytosol	
TRANS 19	proton diffusion	h[e] <=> h[c]		
TRANS 20	phosphate reversible transport via symport	h[e] + pi[e] <=> h[c] + pi[c]	Transport to cytosol	
TRANS 21		h2o[e] <=> h2o[c]		
TRANS 22		h2o2[e] -> h2o2[c]	Modeling Purpose	
TRANS 23	CoA transporter	coa[e] <=> coa[c]	Transport to cytosol	

APPENDIX B

Table B.1. Compound list

Abbreviation	Name	Kegg Entry	Formula	Mass
12glyc	1,2-Diacyl-sn-glycerol	C00641	C5H6O5R2	
13dpg	3-Phospho-D-glyceroyl phosphate	C00236	C3H8O10P2	265.9593
2pg	2-Phospho-D-glycerate	C00631	C3H7O7P	185.9929
3h-but-coa	(S)-3-Hydroxybutanoyl-CoA; (S)-3-Hydroxybutyryl-CoA	C01144	C25H42N7O18P3S	853.152
3h-d-coa	(S)-Hydroxydecanoyl-CoA; (S)-3-Hydroxydecanoyl-CoA	C05264	C31H54N7O18P3S	937.2459
3h-dd-coa	(S)-3-Hydroxydodecanoyl-CoA	C05262	C33H58N7O18P3S	965.2772
3h-h-coa	(S)-Hydroxyhexanoyl-CoA; (S)-3-Hydroxyhexanoyl-CoA	C05268	C27H46N7O18P3S	881.1833
3h-hd-coa	(S)-3-Hydroxyhexadecanoyl-CoA	C05258	C37H66N7O18P3S	1021.3398
3h-o-coa	(S)-Hydroxyoctanoyl-CoA; (S)-3-Hydroxyoctanoyl-CoA	C05266	C29H50N7O18P3S	909.2146
3h-td-coa	(S)-3-Hydroxytetradecanoyl-CoA	C05260	C35H62N7O18P3S	993.3085
3o-d-coa	3-Oxodecanoyl-CoA	C05265	C31H52N7O18P3S	935.2302
3o-dd-coa	3-Oxododecanoyl-CoA	C05263	C33H56N7O18P3S	963.2615
3o-h-coa	3-Oxohexanoyl-CoA; 3-Ketohexanoyl-CoA	C05269	C27H44N7O18P3S	879.1676
3o-hd-coa	3-Oxopalmitoyl-CoA; 3-Ketopalmitoyl-CoA; 3-Oxohexadecanoyl-CoA	C05259	C37H64N7O18P3S	1019.3241
3o-o-coa	3-Oxooctanoyl-CoA	C05267	C29H48N7O18P3S	907.1989
3o-td-coa	3-Oxotetradecanoyl-CoA	C05261	C35H60N7O18P3S	991.2928
3pg	3-Phospho-D-glycerate	C00197	C3H7O7P	185.9929
6pgc	6-Phospho-D-gluconate	C00345	C6H13O10P	276.0246
6pgl	D-Glucono-1,5-lactone 6-phosphate	C01236	C6H11O9P	258.0141
acac	Acetoacetate	C00164	C4H6O3	102.0317
acaccoa	Acetoacetyl-CoA; Acetoacetyl coenzyme A; 3-Acetoacetyl-CoA	C00332	C25H40N7O18P3S	851.1363
accoa	Acetyl-CoA	C00024	C23H38N7O17P3S	809.1258
adp	Adenosine 5'-diphosphate	C00008	C10H15N5O10P2	427.0294
aglyc	Monoacylglycerol;1-Acylglycerol;Glyceride;	C01885	C4H7O4R	
akg	alpha-Ketoglutaric acid, 2-oxoglutarate	C00026	C5H6O5	146.0215
asp-L	L-Aspartate	C00049	C4H7NO4	133.0375
atp	Adenosine 5'-triphosphate	C00002	C10H16N5O13P3	506.9957
but-coa	Butanoyl-CoA; Butyryl-CoA	C00136	C25H42N7O17P3S	837.1571
cacon	cis-Aconitate	C00417	C6H6O6	174.0164
cit	Citrate	C00158	C6H8O7	192.027
co2	Carbon dioxide	C00011	CO2	43.9898
coa	CoA	C00010	C21H36N7O16P3S	767.1152

Table B.1. Compound list - continued

Abbreviation	Name	Kegg Entry	Formula	Mass
Crn	L-Carnitine	C00318	C7H15NO3	161.1052
cytc-o	Cytochrome c3+	C00125		
cytc-r	Reduced cytochrome c	C00126		
d-coa	Decanoyl-CoA	C05274	C31H54N7O17P3S	921.251
dcs-ca	Docosanoic acid	C08281	C22H44O2	340.3341
dd-coa	Lauroyl-CoA; Lauroyl coenzyme A; Dodecanoyl-CoA	C01832	C33H58N7O17P3S	949.2823
Dhap	Dihydroxyacetone phosphate	C00111	C3H7O6P	169.998
e4p	D-Erythrose 4-phosphate	C00279	C4H9O7P	200.0086
ei-ca	Eicosanoic acid	C06425	C20H40O2	312.3028
f26bp	D-Fructose 2,6-bisphosphate	C00665	C6H14O12P2	339.996
f6p	D-Fructose 6-phosphate	C00085	C6H13O9P	260.0297
Fa	Fatty acid	C00162	CHO2R	
fa-coa	Acyl-CoA	C00040	C22H35N7O17P3SR	
Fad	FAD;Flavin adenine dinucleotide	C00016	C27H33N9O15P2	785.1571
fadh2	FADH2	C01352	C27H35N9O15P2	787.1728
Fbp	D-Fructose 1,6-bisphosphate	C00354	C6H14O12P2	339.996
Fum	Fumarate	C00122	C4H4O4	116.011
g1p	D-Glucose 1-phosphate	C00103	C6H13O9P	260.0297
g3p	D-Glyceraldehyde 3-phosphate	C00118	C3H7O6P	169.998
g6p	alpha-D-Glucose 6-phosphate	C00668	C6H13O9P	260.0297
Gdp	Guanosine 5'-diphosphate	C00035	C10H15N5O11P2	443.0243
glc-D	alpha-D-Glucose	C00267	C6H12O6	180.0634
glu-L	L-Glutamate	C00025	C5H9NO4	147.0532
glut-ox	Oxidized glutathione	C00127	C20H32N6O12S2	612.152
glut-red	Reduced glutathione	C00051	C10H17N3O6S	307.0838
Glyc	Glycerol	C00116	C3H8O3	92.0473
glyc3p	Glycerol-3-phosphate	C00093	C3H9O6P	172.0137
glyc-ald	D-Glyceraldehyde	C00577	C3H6O3	90.0317
Glycrt	D-Glycerate	C00258	C3H6O4	106.0266
Gtp	Guanosine 5'-triphosphate	C00044	C10H16N5O14P3	522.9907
H	H	C00080	H	1.0078
h2o	H2O	C00001	H2O	18.0106
h2o2	Hydrogen peroxide	C00027	H2O2	34.0055
h-coa	Hexanoyl-CoA	C05270	C27H46N7O17P3S	865.1884
hd9-ca	(9Z)-Hexadecenoic acid; Palmitoleic acid	C08362	C16H30O2	254.2246
hd9-coa	Palmitoleoyl-CoA; (9Z)-Hexadecenoyl-CoA		C37H64N7O17P3S	

Table B.1. Compound list - continued

Abbreviation	Name	Kegg Entry	Formula	Mass
hd-ca	Hexadecanoic acid; Hexadecanoate; Hexadecylic acid; Palmitic acid; Palmitate; Cetylic acid	C00249	C16H32O2	256.2402
hd-coa	Palmitoyl-CoA; Hexadecanoyl-CoA	C00154	C37H66N7O17P3S	1005.3449
hd-crn	L-Palmitoylcarnitine	C02990	C23H45NO4	399.3349
lac-L	(S)-Lactate	C00186	C3H6O3	90.0317
lpa	1-Acyl-sn-glycerol 3-phosphate, Lysophosphatidic acid	C00681	C4H8O7PR	
mal-L	(S)-Malate	C00149	C4H6O5	134.0215
nad	NAD+	C00003	C21H28N7O14P2	664.1169
nadh	NADH	C00004	C21H29N7O14P2	665.1248
nadp	Nicotinamide adenine dinucleotide phosphate	C00006	C21H29N7O17P3	744.0833
nadph	NADPH	C00005	C21H30N7O17P3	745.0911
o2	Oxygen	C00007	O2	31.9898
oaa	Oxaloacetate	C00036	C4H4O5	132.0059
o-coa	Octanoyl-CoA	C01944	C29H50N7O17P3S	893.2197
od9-12-ca	Linoleate; 9-cis,12-cis-Octadecadienoic acid	C01595	C18H32O2	280.2402
od9-12-coa	Linoleoyl-CoA; (9Z,12Z)-Octadecadienoyl-CoA	C02050	C39H66N7O17P3S	1029.3449
od9-ca	Oleate; 9-cis-Octadecenoic acid	C00712	C18H34O2	282.2559
od9-coa	Oleoyl-CoA; (9Z)-Octadecenoyl-CoA	C00510	C39H68N7O17P3S	1031.3605
od-ca	Octadecanoic acid	C01530	C18H36O2	284.2715
pda	Phosphatidic acid,1,2-Diacyl-sn-glycerol 3-phosphate	C00416	C5H7O8PR2	
pep	Phosphoenolpyruvate	C00074	C3H5O6P	167.9824
pi	Orthophosphate	C00009	H3PO4	97.9769
ppi	Pyrophosphate	C00013	P2H4O7	177.9432
pyr	Pyruvate	C00022	C3H4O3	88.016
qh2	Ubiquinol	C00390	C14H20O4(C5H8)n	
r5p	D-Ribose 5-phosphate	C00117	C5H11O8P	230.0192
ru5p	D-Ribulose 5-phosphate	C00199	C5H11O8P	230.0192
s7p	Sedoheptulose 7-phosphate	C00281	C7H15O10P	290.0403
succ	Succinate	C00042	C4H6O4	118.0266
succoa	Succinyl-CoA	C00091	C25H40N7O19P3S	867.1313
t-but-coa	Crotonoyl-CoA; Crotonyl-CoA; 2-Butenoyl-CoA; trans-But-2-enoyl-CoA; But-2-enoyl-CoA	C00877	C25H40N7O17P3S	835.1414
tcs-ca	Tetracosanoic acid	C08320	C24H48O2	368.3654
td-ca	Tetradecanoic acid; Myristic acid	C06424	C14H28O2	228.2089
td-coa	Tetradecanoyl-CoA; Myristoyl-CoA	C02593	C35H62N7O17P3S	977.3136
t-d-coa	trans-Dec-2-enoyl-CoA; (2E)-Decenoyl-CoA	C05275	C31H52N7O17P3S	919.2353
td-crn	Myristoylcarnitine			
t-dd-coa	2-trans-Dodecenoyl-CoA; (2E)-Dodec-2-enoyl-CoA; (2E)-Dodecenoyl-CoA	C03221	C33H56N7O17P3S	947.2666

Table B.1. Compound list - continued

Abbreviation	Name	Kegg Entry	Formula	Mass
t-h-coa	trans-Hex-2-enoyl-CoA; (2E)-Hexenoyl-CoA	C05271	C27H44N7O17P3S	863.1727
t-hd-coa	trans-Hexadec-2-enoyl-CoA; trans-2-Hexadecenoyl-CoA; (2E)-Hexadecenoyl-CoA	C05272	C37H64N7O17P3S	1003.3292
t-o-coa	trans-Oct-2-enoyl-CoA; (2E)-Octenoyl-CoA	C05276	C29H48N7O17P3S	891.204
Triglyc	Triacylglycerol	C00422	C6H5O6R3	
t-td-coa	trans-Tetradec-2-enoyl-CoA; (2E)-Tetradecenoyl-CoA	C05273	C35H60N7O17P3S	975.2979
Ubq	Ubiquinone	C00399	C14H18O4(C5H8)n	
Udp	UDP	C00015	C9H14N2O12P2	404.0022
Udpg	UDP-glucose	C00029	C15H24N2O17P2	566.055
Utp	Uridine 5'-triphosphate	C00075	C9H15N2O15P3	483.9685
x5p	D-Xylulose 5-phosphate	C00231	C5H11O8P	230.0192

Table C.1. FBA results and percent changes

Reaction Name	Reaction	Normal	O_2 unlim.	%	carnitine	%	complex I	%	fasting	%	hmg-coa	%	ischemia	%
TRANS 01	glc-D[e] -> glc-D[c]	0.56	0.56	0	0.56	0	0.444	20.6	0.093	83.4	0.093	83.4	0.56	0
TRANS 02	glycogen[c] <=> glycogen[e]	-0.2	-0.2	0	-0.2	0	-0.036	81.9	-0.2	0	-0.2	0	-0.2	0
TRANS 03	lac-L[e] + h[e] <=> lac-L[c] + h[c]	0.258	0.413	60.2	0.338	31	-0.96	472.4	0.066	74.4	0.066	74.4	-0.96	472.4
TRANS 04	ei-ca[e] -> ei-ca[c]	0	0	0	0	-	0	0	0	0	0	0	0	0
TRANS 05	hd-ca[e] -> hd-ca[c]	0.022	0.038	71.2	0.036	61.1	0.009	59.5	0.021	5.4	0.021	5.4	0.036	62.6
TRANS 06	od-ca[e] -> od-ca[c]	0.009	0.015	66.7	0.014	61.1	0.004	55.6	0.009	0	0.009	0	0.015	62.6
TRANS 07	td-ca[e] -> td-ca[c]	0.002	0.003	66.7	0.003	61.1	0.001	44.4	0.001	44.4	0.001	44.4	0.003	62.6
TRANS 08	dd-ca[e] -> dd-ca[c]	0	0	0	0	-	0	0	0	0	0	0	0	0
TRANS 09	d-ca[e] -> d-ca[c]	0	0	0	0	-	0	0	0	0	0	0	0	0
TRANS 10	o-ca[e] -> o-ca[c]	0	0	0	0	-	0	0	0	0	0	0	0	0
TRANS 12	od9-ca[e] -> od9-ca[c]	0.023	0.092	300	0.023	0	0.023	0	0.052	126.1	0.052	126.1	0.023	0
TRANS 13	od9-12-ca[e] -> od9-12-ca[c]	0.01	0.027	181.2	0.015	61.1	0.007	27.1	0.015	56.3	0.015	56.2	0.016	62.6
TRANS 14	hd9-ca[e] -> hd9-ca[c]	0.005	0.021	320	0.005	0	0.005	0	0.012	140	0.012	140	0.005	0
TRANS 15	tcs-ca[e] -> tcs-ca[c]	0	0	0	0	-	0	0	0	0	0	0	0	0
TRANS 16	dcs-ca[e] -> dcs-ca[c]	0	0	0	0	-	0	0	0	0	0	0	0	0
TRANS 16	acac[e] -> acac[c]	0	0.001	-	0	795.9	0.001	-	0.08	-	0.008	-	0	0
TRANS 17	co2[e] <=> co2[c]	-5.49	-12.358	125.1	-5.561	-1.3	-0.778	85.8	-4.609	16	-4.529	17.5	-1.663	69.7
TRANS 18	o2[e] <=> o2[c]	5.57	15.07	170.5	5.57	0	1.1	80.3	5.57	0	5.57	0	1.671	70
TRANS 19	h[e] <=> h[c]	-34.663	-89.853	159.2	-34.695	-0.1	-6.386	81.6	-33.257	4.1	-33.271	4	-10.435	69.9

Table C.1. FBA results and percent changes - continued

Reaction Name	Reaction	Normal	O_2 unlim.	%	carnitine	%	complex I	%	fasting	%	hmg-coa	%	ischemia	%
TRANS 20	h[e] + pi[e] <=> h[c] + pi[c]	0.2	0.2	0	0.2	0	0.036	81.9	0.2	0	0.2	0	0.2	0
TRANS 21	h2o[e] <=> h2o[c]	-5.516	-11.966	116.9	-5.649	-2.4	-0.74	86.6	-4.444	19.4	-4.441	19.5	-1.754	68.2
TRANS 23	coa[e] <=> coa[c]	-0.002	0	100	-0.003	-91.7	0	92.3	0	100	0	100	-0.003	93.9
TRANS 24	triglyc[e] <=> triglyc[c]	-0.02	0.06	400	-0.02	0	-0.002	92.3	0.022	208.3	0.032	261.6	-0.02	0
TRANS 22	h2o2[e] -> h2o2[c]	0	0	0	0	-	0	0	0	0	0	0	0	0
ATP	[c]: atp + h2o -> adp + pi + h	37.759	96.045	154.4	37.742	0	7.649	79.7	35.501	6	35.47	6.1	12.181	67.7
GLY 01	[c]: atp + glc-D -> adp + g6p	0.56	0.56	0	0.56	0	0.444	20.6	0.093	83.4	0.093	83.4	0.56	0
GLY 02	[c]: g6p <=> f6p	0.76	0.76	0	0.76	0	0.481	36.7	0.293	61.4	0.293	61.4	0.76	0
GLY 03	[c]: atp + f6p -> adp + f26bp	0	0	0	0	557.3	0	0	0	0	0	0	0	0
GLY 04	[c]: f26bp + h2o -> f6p + pi	0	0	0	0	557.3	0	0	0	0	0	0	0	0
GLY 05	[c]: atp + f6p -> adp + fbp	0.76	0.76	0	0.76	0	0.481	36.7	0.293	61.4	0.293	61.4	0.76	0
GLY 06	[c]: fbp <=> dhap + g3p	0.76	0.76	0	0.76	0	0.481	36.7	0.293	61.4	0.293	61.4	0.76	0
GLY 07	[c]: dhap <=> g3p	0.76	0.76	0	0.76	0	0.481	36.7	0.293	61.4	0.293	61.4	0.76	0
GLY 08	[c]: g3p + nad + pi <=> 13dpg + h + nadh	1.52	1.52	0	1.52	0	0.962	36.7	0.586	61.4	0.586	61.4	1.52	0
GLY 09	[c]: 13dpg + adp <=> 3pg + atp	1.52	1.52	0	1.52	0	0.962	36.7	0.586	61.4	0.586	61.4	1.52	0
GLY 10	[c]: 3pg <=> 2pg	1.5	1.58	5.3	1.5	0	0.96	36	0.608	59.5	0.618	58.8	1.5	0
GLY 11	[c]: 2pg <=> pep + h2o	1.5	1.58	5.3	1.5	0	0.96	36	0.608	59.5	0.618	58.8	1.5	0
GLY 12	[c]: adp + pep -> atp + pyr	1.5	1.58	5.3	1.5	0	0.96	36	0.608	59.5	0.618	58.8	1.5	0
PPP 01	[c]: g6p + nadp -> 6pgl + nadph + h	0	0	0	0	327.6	0	0	0	0	0	0	0	0
PPP 02	[c]: 6pgl + h2o -> 6pgc	0	0	0	0	327.6	0	0	0	0	0	0	0	0
PPP 03	[c]: 6pgc + nadp -> ru5p + co2 + nadph + h	0	0	0	0	327.6	0	0	0	0	0	0	0	0
PPP 04	[c]: ru5p <=> x5p	0	0	0	0	327.5	0	0	0	0	0	0	0	0
PPP 05	[c]: ru5p <=> r5p	0	0	0	0	327.1	0	0	0	0	0	0	0	0

Table C.1. FBA results and percent changes - continued

Reaction Name	Reaction	Normal	O_2 unlim.	%	carnitine	%	complex I	%	fasting	%	hmg-coa	%	ischemia	%
PPP 06	[c]: g3p + s7p <=> e4p + f6p	0	0	0	0	330.1	0	0	0	0	0	0	0	0
PPP 07	[c]: r5p + x5p <=> s7p + g3p	0	0	0	0	327.6	0	0	0	0	0	0	0	0
PPP 08	[c]: x5p + e4p <=> g3p + f6p	0	0	0	0	328.3	0	0	0	0	0	0	0	0
OTHERS	[c]: glut-ox + nadph + h -> (2) glut-red + nadp	0	0	0	0	623.9	0	0	0	0	0	0	0	0
OTHERS	[c]: (2) glut-red + h2o2 <=> glut-ox + (2) h2o	0	0	0	0	-	0	0	0	0	0	0	0	0
GLYCGN 01	[c]: g6p <=> g1p	-0.2	-0.2	0	-0.2	0	-0.036	81.9	-0.2	0	-0.2	0	-0.2	0
GLYCGN 02	[c]: g1p + utp -> ppi + udpg	0	0	0	0	563.2	0	0	0	0	0	0	0	0
GLYCGN 03	[c]: udpg -> glycogen + udp	0	0	0	0	563.2	0	0	0	0	0	0	0	0
NUCLEO	[c]: udp + atp <=> utp + adp	0	0	0	0	576.2	0	0	0	0	0	0	0	0
GLYCGN 04	[c]: glycogen + pi + atp -> g1p + adp	0.2	0.2	0	0.2	0	0.036	81.9	0.2	0	0.2	0	0.2	0
PYR	[c]: lac-L + nad <=> pyr + nadh + h	0.258	0.413	60.2	0.338	31	-0.96	472.4	0.066	74.4	0.066	74.4	-0.96	472.4
PYR	pyr[c] + h[c] -> pyr[m] + h[m]	0.178	0.091	48.8	0.176	1.8	0.173	2.5	0.139	21.5	0.134	24.6	0.178	0
PYR	[m]: coa + nad + pyr -> accoa + co2 + nadh	1.758	1.993	13.4	1.838	4.5	0	100	0.674	61.7	0.684	61.1	0.54	69.3
PYR	[m]: mal-L + nad <=> pyr + nadh + co2 + h	1.58	1.846	16.8	1.662	4.9	-0.179	111.4	0.516	67.4	0.53	66.4	0.362	77.1
PYR	[c]: pyr + co2 + atp -> adp + pi + oaa	0	0	0	0	574.4	0	0	0	0	0	0	0	0
PYR	[c]: mal-L + nadp <=> pyr + co2 + nadph + h	-1.58	-1.902	20.4	-1.662	-4.9	0.173	111	-0.534	66.2	-0.55	65.2	-0.362	77.1
PYR	[m]: mal-L + nadp <=> pyr + co2 + nadph + h	0	0.056	-	0	83.7	0.006	-	0.018	-	0.02	-	0	0
BOX 01	[c]: atp + coa + ei-ca <=> amp + ei-coa + ppi	0	0	0	0	120.8	0	0	0	0	0	0	0	0
BOX 02	[c]: crn + ei-coa <=> ei-crn + coa	0	0	0	0	280	0	0	0	0	0	0	0	0
BOX 03	ei-crn[c] -> ei-crn[m]	0	0	0	0	247.3	0	0	0	0	0	0	0	0
BOX 04	[m]: ei-crn + coa <=> crn + ei-coa	0	0	0	0	183.3	0	0	0	0	0	0	0	0

Table C.1. FBA results and percent changes - continued

Reaction Name	Reaction	Normal	O_2 unlim.	%	carnitine	%	complex I	%	fasting	%	hmg-coa	%	ischemia	%
BOX 05	[m]: ei-coa + fad -> t-ei-coa + fadh2	0	0	0	0	191.2	0	0	0	0	0	0	0	0
BOX 06	[m]: t-ei-coa + h2o <=> 3h-ei-coa	0	0	0	0	2550	0	0	0	0	0	0	0	0
BOX 07	[m]: 3h-ei-coa + nad <=> 3o-ei-coa + nadh + h	0	0	0	0	1120	0	0	0	0	0	0	0	0
BOX 08	[m]: 3o-ei-coa + coa <=> od-coa + accoa	0	0	0	0	1917.1	0	0	0	0	0	0	0	0
BOX 09	[c]: atp + coa + od-ca <=> amp + od-coa + ppi	0.009	0.042	366.7	0.017	91.7	0.004	55.6	0.012	36.1	0.014	53.9	0.017	93.9
BOX 10	[c]: crn + od-coa <=> od-crn + coa	0	0.042	-	0	380.5	0.003	-	0.012	-	0.014	-	0	0
BOX 11	od-crn[c] -> od-crn[m]	0	0.042	-	0	133.7	0.003	-	0.012	-	0.014	-	0	0
BOX 12	[m]: od-crn + coa <=> crn + od-coa	0	0.042	-	0	419.6	0.003	-	0.012	-	0.014	-	0	0
BOX 13	[m]: od-coa + fad -> t-od-coa + fadh2	0	0.042	-	0	541.8	0.003	-	0.012	-	0.014	-	0	0
BOX 14	[m]: t-od-coa + h2o <=> 3h-od-coa	0	0.042	-	0	1115	0.003	-	0.012	-	0.014	-	0	0
BOX 15	[m]: 3h-od-coa + nad <=> 3o-od-coa + nadh + h	0	0.042	-	0	108.2	0.003	-	0.012	-	0.014	-	0	0
BOX 16	[m]: 3o-od-coa + coa <=> hd-coa + accoa	0	0.042	-	0	1552.9	0.003	-	0.012	-	0.014	-	0	0
BOX 17	[c]: atp + coa + hd-ca <=> amp + hd-coa + ppi	0.022	0.105	371.2	0.043	91.7	0.009	59.5	0.029	30.7	0.033	48.4	0.043	93.9
BOX 18	[c]: crn + hd-coa <=> hd-crn + coa	0	0.105	-	0	522.6	0.007	-	0.029	-	0.033	-	0	0
BOX 19	hd-crn[c] -> hd-crn[m]	0	0.105	-	0	551.9	0.007	-	0.029	-	0.033	-	0	0
BOX 20	[m]: hd-crn + coa <=> crn + hd-coa	0	0.105	-	0	950	0.007	-	0.029	-	0.033	-	0	0
BOX 21	[m]: hd-coa + fad -> t-hd-coa + fadh2	0	0.147	-	0	387.9	0.011	-	0.041	-	0.047	-	0	0
BOX 22	[m]: t-hd-coa + h2o <=> 3h-hd-coa	0	0.147	-	0	240	0.011	-	0.041	-	0.047	-	0	0
BOX 23	[m]: 3h-hd-coa + nad <=> 3o-hd-coa + nadh + h	0	0.147	-	0	308.3	0.011	-	0.041	-	0.047	-	0	0
BOX 24	[m]: 3o-hd-coa + coa <=> td-coa + accoa	0	0.147	-	0	674.8	0.011	-	0.041	-	0.047	-	0	0
BOX 25	[c]: atp + coa + td-ca <=> amp + td-coa + ppi	0.002	0.008	366.7	0.003	91.7	0.001	44.4	0.002	8.3	0.002	9.4	0.003	93.9

Table C.1. FBA results and percent changes - continued

Reaction Name	Reaction	Normal	O_2 unlim.	%	carnitine	%	complex I	%	fasting	%	hmg-coa	%	ischemia	%
BOX 26	[c]: crn + td-coa <=> td-crn + coa	0	0.008	-	0	-3586.1	0.001	-	0.002	-	0.002	-	0	0
BOX 27	td-crn[c] -> td-crn[m]	0	0.008	-	0	226.6	0.001	-	0.002	-	0.002	-	0	0
BOX 28	[m]: td-crn + coa <=> crn + td-coa	0	0.008	-	0	506	0.001	-	0.002	-	0.002	-	0	0
BOX 29	[m]: td-coa + fad -> t-td-coa + fadh2	0	0.155	-	0	413.9	0.011	-	0.043	-	0.049	-	0	0
BOX 30	[m]: t-td-coa + h2o <=> 3h-td-coa	0	0.155	-	0	176.4	0.011	-	0.043	-	0.049	-	0	0
BOX 31	[m]: 3h-td-coa + nad <=> 3o-td-coa + nadh + h	0	0.155	-	0	347.4	0.011	-	0.043	-	0.049	-	0	0
BOX 32	[m]: 3o-td-coa + coa <=> dd-coa + accoa	0	0.155	-	0	153.6	0.011	-	0.043	-	0.049	-	0	0
BOX 33	[c]: atp + coa + dd-ca <=> amp + dd-coa + ppi	0	0	0	0	109.4	0	0	0	0	0	0	0	0
BOX 34	[c]: crn + dd-coa <=> dd-crn + coa	0	0	0	0	214.3	0	0	0	0	0	0	0	0
BOX 35	dd-crn[c] -> dd-crn[m]	0	0	0	0	405.5	0	0	0	0	0	0	0	0
BOX 36	[m]: dd-crn + coa <=> crn + dd-coa	0	0	0	0	-	0	0	0	0	0	0	0	0
BOX 37	[m]: dd-coa + fad -> t-dd-coa + fadh2	0	0.155	-	0	849.1	0.011	-	0.043	-	0.049	-	0	0
BOX 38	[m]: t-dd-coa + h2o <=> 3h-dd-coa	0.009	0.288	3034.8	0.001	91.7	0.033	263	0.1	985.8	0.108	1076.1	0.001	93.9
BOX 39	[m]: 3h-dd-coa + nad <=> 3o-dd-coa + nadh + h	0.009	0.288	3034.8	0.001	91.7	0.033	263	0.1	985.8	0.108	1076.1	0.001	93.9
BOX 40	[m]: 3o-dd-coa + coa <=> d-coa + accoa	0.009	0.288	3034.8	0.001	91.7	0.033	263	0.1	985.8	0.108	1076.1	0.001	93.9
BOX 41	[c]: atp + coa + d-ca <=> amp + d-coa + ppi	0	0	0	0	103.9	0	0	0	0	0	0	0	0
BOX 42	[c]: crn + d-coa <=> d-crn + coa	0	0	0	0	250	0	0	0	0	0	0	0	0
BOX 43	d-crn[c] -> d-crn[m]	0	0	0	0	422.6	0	0	0	0	0	0	0	0
BOX 44	[m]: d-crn + coa <=> crn + d-coa	0	0	0	0	-436.9	0	0	0	0	0	0	0	0
BOX 45	[m]: d-coa + fad -> t-d-coa + fadh2	0.009	0.288	3034.8	0.001	91.7	0.033	263	0.1	985.8	0.108	1076.1	0.001	93.9
BOX 46	[m]: t-d-coa + h2o <=> 3h-d-coa	0.012	0.371	2888.7	0.003	76.9	0.045	259.1	0.131	956.6	0.141	1039.8	0.003	78.7
BOX 47	[m]: 3h-d-coa + nad <=> 3o-d-coa + nadh + h	0.012	0.371	2888.7	0.003	76.9	0.045	259.1	0.131	956.6	0.141	1039.8	0.003	78.7

Table C.1. FBA results and percent changes - continued

Reaction Name	Reaction	Normal	O_2 unlim.	%	carnitine	%	complex I	%	fasting	%	hmg-coa	%	ischemia	%
BOX 48	[m]: 3o-d-coa + coa <=> o-coa + accoa	0.012	0.371	2888.7	0.003	76.9	0.045	259.1	0.131	956.6	0.141	1039.8	0.003	78.7
BOX 49	[c]: atp + coa + o-ca <=> amp + o-coa + ppi	0	0	0	0	107.7	0	0	0	0	0	0	0	0
BOX 50	[c]: crn + o-coa <=> o-crn + coa	0	0	0	0	404	0	0	0	0	0	0	0	0
BOX 51	o-crn[c] -> o-crn[m]	0	0	0	0	539.9	0	0	0	0	0	0	0	0
BOX 52	[m]: o-crn + coa <=> crn + o-coa	0	0	0	0	-89.9	0	0	0	0	0	0	0	0
BOX 53	[m]: o-coa + fad -> t-o-coa + fadh2	0.012	0.371	2888.7	0.003	76.9	0.045	259.1	0.131	956.6	0.141	1039.8	0.003	78.7
BOX 54	[m]: t-o-coa + h2o <=> 3h-o-coa	0.012	0.371	2888.7	0.003	76.9	0.045	259.1	0.131	956.6	0.141	1039.8	0.003	78.7
BOX 55	[m]: 3h-o-coa + nad <=> 3o-o-coa + nadh + h	0.012	0.371	2888.7	0.003	76.9	0.045	259.1	0.131	956.6	0.141	1039.8	0.003	78.7
BOX 56	[m]: 3o-o-coa + coa <=> h-coa + accoa	0.012	0.371	2888.7	0.003	76.9	0.045	259.1	0.131	956.6	0.141	1039.8	0.003	78.7
BOX 57	[m]: h-coa + fad -> t-h-coa + fadh2	0.012	0.371	2888.7	0.003	76.9	0.045	259.1	0.131	956.6	0.141	1039.8	0.003	78.7
BOX 58	[m]: t-h-coa + h2o <=> 3h-h-coa	0.012	0.371	2888.7	0.003	76.9	0.045	259.1	0.131	956.6	0.141	1039.8	0.003	78.7
BOX 59	[m]: 3h-h-coa + nad <=> 3o-h-coa + nadh + h	0.012	0.371	2888.7	0.003	76.9	0.045	259.1	0.131	956.6	0.141	1039.8	0.003	78.7
BOX 60	[m]: 3o-h-coa + coa <=> but-coa + accoa	0.012	0.371	2888.7	0.003	76.9	0.045	259.1	0.131	956.6	0.141	1039.8	0.003	78.7
BOX 61	[m]: but-coa + fad -> t-but-coa + fadh2	0.012	0.371	2888.7	0.003	76.9	0.045	259.1	0.131	956.6	0.141	1039.8	0.003	78.7
BOX 62	[m]: t-but-coa + h2o <=> 3h-but-coa	0.012	0.371	2888.7	0.003	76.9	0.045	259.1	0.131	956.6	0.141	1039.8	0.003	78.7
BOX 63	[m]: 3h-but-coa + nad <=> acaccoa + nadh + h	0.012	0.371	2888.7	0.003	76.9	0.045	259.1	0.131	956.6	0.141	1039.8	0.003	78.7
BOX 64	[m]: acaccoa + coa <=> (2) accoa	0.012	0.372	2896.8	0.003	76.9	0.046	267.1	0.211	1601.7	0.149	1104.4	0.003	78.7
U-BOX 01	[c]: atp + coa + od9-ca <=> amp + od9-coa + ppi	0.023	0.133	480	0.027	18.3	0.023	0	0.057	147.8	0.059	158.4	0.027	18.8
U-BOX 02	[c]: crn + od9-coa <=> od9-crn + coa	0.009	0.133	1350	0.001	91.7	0.022	138.5	0.057	519.4	0.059	546	0.001	93.9
U-BOX 03	od9-crn[c] -> od9-crn[m]	0.009	0.133	1350	0.001	91.7	0.022	138.5	0.057	519.4	0.059	546	0.001	93.9
U-BOX 04	[m]: od9-crn + coa <=> crn + od9-coa	0.009	0.133	1350	0.001	91.7	0.022	138.5	0.057	519.4	0.059	546	0.001	93.9

Table C.1. FBA results and percent changes - continued

Reaction Name	Reaction	Normal	O_2 unlim.	%	carnitine	%	complex I	%	fasting	%	hmg-coa	%	ischemia	%
U-BOX 05	[m]: od9-coa + fad -> t-od9-coa + fadh2	0.009	0.133	1350	0.001	91.7	0.022	138.5	0.057	519.4	0.059	546	0.001	93.9
U-BOX 06	[m]: t-od9-coa + h2o <=> 3h-od9-coa	0.009	0.133	1350	0.001	91.7	0.022	138.5	0.057	519.4	0.059	546	0.001	93.9
U-BOX 07	[m]: 3h-od9-coa + nad <=> 3o-od9-coa + nadh + h	0.009	0.133	1350	0.001	91.7	0.022	138.5	0.057	519.4	0.059	546	0.001	93.9
U-BOX 08	[m]: 3o-od9-coa + coa <=> hd7-coa + accoa	0.009	0.133	1350	0.001	91.7	0.022	138.5	0.057	519.4	0.059	546	0.001	93.9
U-BOX 09	[m]: hd7-coa + fad -> t-hd7-coa + fadh2	0.009	0.133	1350	0.001	91.7	0.022	138.5	0.057	519.4	0.059	546	0.001	93.9
U-BOX 10	[m]: t-hd7-coa + h2o <=> 3h-hd7-coa	0.009	0.133	1350	0.001	91.7	0.022	138.5	0.057	519.4	0.059	546	0.001	93.9
U-BOX 11	[m]: 3h-hd7-coa + nad <=> 3o-hd7-coa + nadh + h	0.009	0.133	1350	0.001	91.7	0.022	138.5	0.057	519.4	0.059	546	0.001	93.9
U-BOX 12	[m]: 3o-hd7-coa + coa <=> td5-coa + accoa	0.009	0.133	1350	0.001	91.7	0.022	138.5	0.057	519.4	0.059	546	0.001	93.9
U-BOX 13	[m]: td5-coa + fad -> t-td5-coa + fadh2	0.009	0.133	1350	0.001	91.7	0.022	138.5	0.057	519.4	0.059	546	0.001	93.9
U-BOX 14	[m]: t-td5-coa + h2o <=> 3h-td5-coa	0.009	0.133	1350	0.001	91.7	0.022	138.5	0.057	519.4	0.059	546	0.001	93.9
U-BOX 15	[m]: 3h-td5-coa + nad <=> 3o-td5-coa + nadh + h	0.009	0.133	1350	0.001	91.7	0.022	138.5	0.057	519.4	0.059	546	0.001	93.9
U-BOX 16	[m]: 3o-td5-coa + coa <=> cisdd-coa + accoa	0.009	0.133	1350	0.001	91.7	0.022	138.5	0.057	519.4	0.059	546	0.001	93.9
U-BOX 17	[m]: cisdd-coa <=> t-dd-coa	0.009	0.133	1350	0.001	91.7	0.022	138.5	0.057	519.4	0.059	546	0.001	93.9
U-BOX 18	[c]: atp + coa + od9-12-ca <=> amp + od9-12-coa + ppi	0.01	0.056	481.2	0.018	91.7	0.007	27.1	0.018	92.4	0.02	110.1	0.019	93.9
U-BOX 19	[c]: crn + od9-12-coa <=> od9-12-crn + coa	0	0.056	-	0	286.1	0.006	-	0.018	-	0.02	-	0	0
U-BOX 20	od9-12-crn[c] -> od9-12-crn[m]	0	0.056	-	0	441.2	0.006	-	0.018	-	0.02	-	0	0
U-BOX 21	[m]: od9-12-crn + coa <=> crn + od9-12-coa	0	0.056	-	0	556.3	0.006	-	0.018	-	0.02	-	0	0
U-BOX 22	[m]: od9-12-coa + fad -> t-od9-12-coa + fadh2	0	0.056	-	0	332.3	0.006	-	0.018	-	0.02	-	0	0
U-BOX 23	[m]: t-od9-12-coa + h2o <=> 3h-od9-12-coa	0	0.056	-	0	525.6	0.006	-	0.018	-	0.02	-	0	0
U-BOX 24	[m]: 3h-od9-12-coa + nad <=> 3o-od9-12-coa + nadh + h	0	0.056	-	0	162.6	0.006	-	0.018	-	0.02	-	0	0

Table C.1. FBA results and percent changes - continued

Reaction Name	Reaction	Normal	O_2 unlim.	%	carnitine	%	complex I	%	fasting	%	hmg-coa	%	ischemia	%
U-BOX 25	[m]: 3o-od9-12-coa + coa <=> hd-7-10-coa + accoa	0	0.056	-	0	582.8	0.006	-	0.018	-	0.02	-	0	0
U-BOX 26	[m]: hd-7-10-coa + fad -> t-hd-7-10-coa + fadh2	0	0.056	-	0	558.3	0.006	-	0.018	-	0.02	-	0	0
U-BOX 27	[m]: t-hd-7-10-coa + h2o <=> 3h-hd-7-10-coa	0	0.056	-	0	870.8	0.006	-	0.018	-	0.02	-	0	0
U-BOX 28	[m]: 3h-hd-7-10-coa + nad <=> 3o-hd-7-10-coa + nadh + h	0	0.056	-	0	351.6	0.006	-	0.018	-	0.02	-	0	0
U-BOX 29	[m]: 3o-hd-7-10-coa + coa <=> td-5-8-coa + accoa	0	0.056	-	0	266.1	0.006	-	0.018	-	0.02	-	0	0
U-BOX 30	[m]: td-5-8-coa + fad -> t-td-5-8-coa + fadh2	0	0.056	-	0	0.5	0.006	-	0.018	-	0.02	-	0	0
U-BOX 31	[m]: t-td-5-8-coa + h2o <=> 3h-td-5-8-coa	0	0.056	-	0	75.4	0.006	-	0.018	-	0.02	-	0	0
U-BOX 32	[m]: 3h-td-5-8-coa + nad <=> 3o-td-5-8-coa + nadh + h	0	0.056	-	0	456.4	0.006	-	0.018	-	0.02	-	0	0
U-BOX 33	[m]: 3o-td-5-8-coa + coa <=> cis-3-6-dd-coa + accoa	0	0.056	-	0	231.6	0.006	-	0.018	-	0.02	-	0	0
U-BOX 34	[m]: cis-3-6-dd-coa <=> t-2-6-dd-coa	0	0.056	-	0	110.8	0.006	-	0.018	-	0.02	-	0	0
U-BOX 35	[m]: t-2-6-dd-coa + h2o <=> 3h-2-6-dd-coa	0	0.056	-	0	108.9	0.006	-	0.018	-	0.02	-	0	0
U-BOX 36	[m]: 3h-2-6-dd-coa + nad <=> 3o-2-6-dd-coa + nadh + h	0	0.056	-	0	155.8	0.006	-	0.018	-	0.02	-	0	0
U-BOX 37	[m]: 3o-2-6-dd-coa + coa <=> d4-coa + accoa	0	0.056	-	0	248.4	0.006	-	0.018	-	0.02	-	0	0
U-BOX 38	[m]: d4-coa + fad -> d2-4-coa + fadh2	0	0.056	-	0	281.6	0.006	-	0.018	-	0.02	-	0	0
U-BOX 39	[m]: d2-4-coa + nadph + h <=> cis-d-coa + nadp	0	0.056	-	0	-2319.2	0.006	-	0.018	-	0.02	-	0	0
U-BOX 40	[m]: cis-d-coa <=> t-d-coa	0	0.056	-	0	1.5	0.006	-	0.018	-	0.02	-	0	0
U-BOX 41	[c]: atp + coa + hd9-ca <=> amp + hd9-coa + ppi	0.005	0.026	428	0.006	11	0.005	0	0.013	153	0.013	159.4	0.006	11.3
U-BOX 42	[c]: crn + hd9-coa <=> hd9-crn + coa	0.003	0.026	725	0.002	34.4	0.005	51.9	0.013	295.3	0.013	305.3	0.002	35.2
U-BOX 43	hd9-crn[c] -> hd9-crn[m]	0.003	0.026	725	0.002	34.4	0.005	51.9	0.013	295.3	0.013	305.3	0.002	35.2
U-BOX 44	[m]: hd9-crn + coa <=> crn + hd9-coa	0.003	0.026	725	0.002	34.4	0.005	51.9	0.013	295.3	0.013	305.3	0.002	35.2

Table C.1. FBA results and percent changes - continued

Reaction Name	Reaction	Normal	O_2 unlim.	%	carnitine	%	complex I	%	fasting	%	hmg-coa	%	ischemia	%
U-BOX 45	[m]: hd9-coa + fad -> t-hd9-coa + fadh2	0.003	0.026	725	0.002	34.4	0.005	51.9	0.013	295.3	0.013	305.3	0.002	35.2
U-BOX 46	[m]: t-hd9-coa + h2o <=> 3h-hd9-coa	0.003	0.026	725	0.002	34.4	0.005	51.9	0.013	295.3	0.013	305.3	0.002	35.2
U-BOX 47	[m]: 3h-hd9-coa + nad <=> 3o-hd9-coa + nadh + h	0.003	0.026	725	0.002	34.4	0.005	51.9	0.013	295.3	0.013	305.3	0.002	35.2
U-BOX 48	[m]: 3o-hd9-coa + coa <=> td7-coa + accoa	0.003	0.026	725	0.002	34.4	0.005	51.9	0.013	295.3	0.013	305.3	0.002	35.2
U-BOX 49	[m]: td7-coa + fad -> t-td7-coa + fadh2	0.003	0.026	725	0.002	34.4	0.005	51.9	0.013	295.3	0.013	305.3	0.002	35.2
U-BOX 50	[m]: t-td7-coa + h2o <=> 3h-td7-coa	0.003	0.026	725	0.002	34.4	0.005	51.9	0.013	295.3	0.013	305.3	0.002	35.2
U-BOX 51	[m]: 3h-td7-coa + nad <=> 3o-td7-coa + nadh + h	0.003	0.026	725	0.002	34.4	0.005	51.9	0.013	295.3	0.013	305.3	0.002	35.2
U-BOX 52	[m]: 3o-td7-coa + coa <=> dd5-coa + accoa	0.003	0.026	725	0.002	34.4	0.005	51.9	0.013	295.3	0.013	305.3	0.002	35.2
U-BOX 53	[m]: dd5-coa + fad -> t-dd5-coa + fadh2	0.003	0.026	725	0.002	34.4	0.005	51.9	0.013	295.3	0.013	305.3	0.002	35.2
U-BOX 54	[m]: t-dd5-coa + h2o <=> 3h-dd5-coa	0.003	0.026	725	0.002	34.4	0.005	51.9	0.013	295.3	0.013	305.3	0.002	35.2
U-BOX 55	[m]: 3h-dd5-coa + nad <=> 3o-dd5-coa + nadh + h	0.003	0.026	725	0.002	34.4	0.005	51.9	0.013	295.3	0.013	305.3	0.002	35.2
U-BOX 56	[m]: 3o-dd5-coa + coa <=> cisd-coa + accoa	0.003	0.026	725	0.002	34.4	0.005	51.9	0.013	295.3	0.013	305.3	0.002	35.2
U-BOX 57	[m]: cisd-coa <=> t-d-coa	0.003	0.026	725	0.002	34.4	0.005	51.9	0.013	295.3	0.013	305.3	0.002	35.2
PBOX 01	tcs-coa[c] -> tcs-coa[p]	0	0	0	0	821.1	0	0	0	0	0	0	0	0
PBOX 02	[c]: atp + coa + tcs-ca <=> amp + tcs-coa + ppi	0	0	0	0	65.2	0	0	0	0	0	0	0	0
PBOX 03	[p]: tcs-coa + o2 <=> t-tcs-coa + h2o2	0	0	0	0	587.5	0	0	0	0	0	0	0	0
PBOX 04	[p]: t-tcs-coa + h2o <=> 3h-tcs-coa	0	0	0	0	600	0	0	0	0	0	0	0	0
PBOX 05	[p]: 3h-tcs-coa + nad <=> 3o-tcs-coa + nadh + h	0	0	0	0	1600	0	0	0	0	0	0	0	0
PBOX 06	[p]: 3o-tcs-coa + coa <=> dcs-coa + accoa	0	0	0	0	281.8	0	0	0	0	0	0	0	0
PBOX 07	dcs-coa[c] -> dcs-coa[p]	0	0	0	0	751.3	0	0	0	0	0	0	0	0

Table C.1. FBA results and percent changes - continued

Reaction Name	Reaction	Normal	O_2 unlim.	%	carnitine	%	complex I	%	fasting	%	hmg-coa	%	ischemia	%
PBOX 08	[c]: atp + coa + dcs-ca <=> amp + dcs-coa + ppi	0	0	0	0	117.9	0	0	0	0	0	0	0	0
PBOX 09	[p]: dcs-coa + o2 <=> t-dcs-coa + h2o2	0	0	0	0	273.9	0	0	0	0	0	0	0	0
PBOX 10	[p]: t-dcs-coa + h2o <=> 3h-dcs-coa	0	0	0	0	182.6	0	0	0	0	0	0	0	0
PBOX 11	[p]: 3h-dcs-coa + nad <=> 3o-dcs-coa + nadh + h	0	0	0	0	183.3	0	0	0	0	0	0	0	0
PBOX 12	[p]: 3o-dcs-coa + coa <=> ei-coa + accoa	0	0	0	0	236.7	0	0	0	0	0	0	0	0
PBOX 13	ei-coa[p] -> ei-coa[c]	0	0	0	0	359.7	0	0	0	0	0	0	0	0
PBOX 14	[p]: ei-coa + o2 <=> t-ei-coa + h2o2	0	0	0	0	587.5	0	0	0	0	0	0	0	0
PBOX 15	[p]: t-ei-coa + h2o <=> 3h-ei-coa	0	0	0	0	109.1	0	0	0	0	0	0	0	0
PBOX 16	[p]: 3h-ei-coa + nad <=> 3o-ei-coa + nadh + h	0	0	0	0	252.6	0	0	0	0	0	0	0	0
PBOX 17	[p]: 3o-ei-coa + coa <=> od-coa + accoa	0	0	0	0	285.2	0	0	0	0	0	0	0	0
PBOX 18	od-coa[p] -> od-coa[c]	0	0	0	0	198.8	0	0	0	0	0	0	0	0
PBOX 19	[p]: od-coa + o2 <=> t-od-coa + h2o2	0	0	0	0	594.7	0	0	0	0	0	0	0	0
PBOX 20	[p]: t-od-coa + h2o <=> 3h-od-coa	0	0	0	0	95.7	0	0	0	0	0	0	0	0
PBOX 21	[p]: 3h-od-coa + nad <=> 3o-od-coa + nadh + h	0	0	0	0	212.9	0	0	0	0	0	0	0	0
PBOX 22	[p]: 3o-od-coa + coa <=> hd-coa + accoa	0	0	0	0	444.4	0	0	0	0	0	0	0	0
PBOX 23	hd-coa[p] -> hd-coa[c]	0	0	0	0	343	0	0	0	0	0	0	0	0
PBOX 24	[p]: hd-coa + o2 <=> t-hd-coa + h2o2	0	0	0	0	10	0	0	0	0	0	0	0	0
PBOX 25	[p]: t-hd-coa + h2o <=> 3h-hd-coa	0	0	0	0	433.3	0	0	0	0	0	0	0	0
PBOX 26	[p]: 3h-hd-coa + nad <=> 3o-hd-coa + nadh + h	0	0	0	0	240.7	0	0	0	0	0	0	0	0
PBOX 27	[p]: 3o-hd-coa + coa <=> td-coa + accoa	0	0	0	0	315.2	0	0	0	0	0	0	0	0
PBOX 28	td-coa[p] -> td-coa[c]	0	0	0	0	268.8	0	0	0	0	0	0	0	0

Table C.1. FBA results and percent changes - continued

Reaction Name	Reaction	Normal	O_2 unlim.	%	carnitine	%	complex I	%	fasting	%	hmg-coa	%	ischemia	%
PBOX 29	[p]: td-coa + o2 <=> t-td-coa + h2o2	0	0	0	0	300	0	0	0	0	0	0	0	0
PBOX 30	[p]: t-td-coa + h2o <=> 3h-td-coa	0	0	0	0	1340	0	0	0	0	0	0	0	0
PBOX 31	[p]: 3h-td-coa + nad <=> 3o-td-coa + nadh + h	0	0	0	0	595.2	0	0	0	0	0	0	0	0
PBOX 32	[p]: 3o-td-coa + coa <=> dd-coa + accoa	0	0	0	0	157.9	0	0	0	0	0	0	0	0
PBOX 33	dd-coa[p] -> dd-coa[c]	0	0	0	0	343.5	0	0	0	0	0	0	0	0
PBOX 34	[p]: dd-coa + o2 <=> t-dd-coa + h2o2	0	0	0	0	220	0	0	0	0	0	0	0	0
PBOX 35	[p]: t-dd-coa + h2o <=> 3h-dd-coa	0	0	0	0	-6900	0	0	0	0	0	0	0	0
PBOX 36	[p]: 3h-dd-coa + nad <=> 3o-dd-coa + nadh + h	0	0	0	0	763.6	0	0	0	0	0	0	0	0
PBOX 37	[p]: 3o-dd-coa + coa <=> d-coa + accoa	0	0	0	0	120	0	0	0	0	0	0	0	0
PBOX 38	d-coa[p] -> d-coa[c]	0	0	0	0	430.1	0	0	0	0	0	0	0	0
PBOX 39	[p]: d-coa + o2 <=> t-d-coa + h2o2	0	0	0	0	526.7	0	0	0	0	0	0	0	0
PBOX 40	[p]: t-d-coa + h2o <=> 3h-d-coa	0	0	0	0	-300	0	0	0	0	0	0	0	0
PBOX 41	[p]: 3h-d-coa + nad <=> 3o-d-coa + nadh + h	0	0	0	0	371.4	0	0	0	0	0	0	0	0
PBOX 42	[p]: 3o-d-coa + coa <=> o-coa + accoa	0	0	0	0	96.2	0	0	0	0	0	0	0	0
P-BOX 43	o-coa[p] -> o-coa[c]	0	0	0	0	301.2	0	0	0	0	0	0	0	0
P-BOX 44	accoa[p] -> accoa[c]	0	0	0	0	231.5	0	0	0	0	0	0	0	0
P-BOX 45	accoa[c] + crn[c] -> accrn[c] + coa[c]	0	0	0	0	231.5	0	0	0	0	0	0	0	0
P-BOX 46	accrn[c] -> accrn[m]	0	0	0	0	231.5	0	0	0	0	0	0	0	0
P-BOX 47	[m]: accrn + coa -> accoa + crn	0	0	0	0	231.5	0	0	0	0	0	0	0	0
I-TRANS	coa[m] <=> coa[p]	0	0	0	0	424	0	0	0	0	0	0	0	0
I-TRANS	h2o[c] <=> h2o[p]	0	0	0	0	-287.5	0	0	0	0	0	0	0	0
I-TRANS	nad[m] <=> nad[p]	0	0	0	0	413.4	0	0	0	0	0	0	0	0

Table C.1. FBA results and percent changes - continued

Reaction Name	Reaction	Normal	O_2 unlim.	%	carnitine	%	complex I	%	fasting	%	hmg-coa	%	ischemia	%
I-TRANS	nadh[p] <=> nadh[m]	0	0	0	0	423.2	0	0	0	0	0	0	0	0
I-TRANS	h[p] <=> h[m]	0	0	0	0	436.1	0	0	0	0	0	0	0	0
OTHERS	[p]: (2) h2o2 --> (2) h2o + o2	0	0	0	0	365.2	0	0	0	0	0	0	0	0
NUCLEO	[c]: amp + atp <=> (2) adp	0.071	0.371	424.9	0.114	62.1	0.049	30.6	0.131	85.6	0.141	100.2	0.115	63.6
TCA 01	[m]: accoa + h2o + oaa -> cit + coa	1.866	5.183	177.7	1.861	0.3	0.389	79.2	1.968	5.4	1.923	3	0.562	69.9
TCA 02	[m]: cit <=> cacon + h2o	1.866	5.183	177.7	1.861	0.3	0.389	79.2	1.968	5.4	1.923	3	0.562	69.9
TCA 03	[m]: cacon + h2o <=> icit	1.866	5.183	177.7	1.861	0.3	0.389	79.2	1.968	5.4	1.923	3	0.562	69.9
TCA 04	[m]: icit + nad -> akg + co2 + nadh + h	1.866	5.183	177.7	1.861	0.3	0.389	79.2	1.968	5.4	1.923	3	0.562	69.9
TCA 05	[m]: akg + coa + nad -> co2 + nadh + succoa	1.866	5.183	177.7	1.861	0.3	0.389	79.2	1.968	5.4	1.923	3	0.562	69.9
TCA 06	[m]: gdp + pi + succoa <=> gtp + succ + coa	0.658	1.718	161.1	0.708	3.5	0.155	76.5	0.78	18.6	0.675	2.6	0.238	63.7
TCA 07	[m]: adp + pi + succoa <=> atp + succ + coa	1.208	3.465	186.7	1.154	1.8	0.234	80.6	1.188	1.7	1.248	3.2	0.323	73.3
TCA 08	[m]: succ + fad <=> fum + fadh2	1.866	5.183	177.7	1.861	0.3	0.389	79.2	1.968	5.4	1.923	3	0.562	69.9
TCA 09	[m]: fum + h2o <=> mal-L	1.866	5.183	177.7	1.861	0.3	0.389	79.2	1.968	5.4	1.923	3	0.562	69.9
TCA 10	[m]: mal-L + nad -> oaa + nadh + h	2.024	5.334	163.5	2.017	0.1	0.56	72.3	2.129	5.2	2.089	3.2	0.719	64.5
MAL-ASP 01	mal-L[m] + pi[c] <=> mal-L[c] + pi[m]	-1.58	-1.902	20.4	-1.662	-4.9	0.173	111	-0.534	66.2	-0.55	65.2	-0.362	77.1
MAL-ASP 02	[c]: akg + asp-L <=> glu-L + oaa	0.158	0.151	4.2	0.156	2	0.172	8.9	0.161	2.2	0.166	5.5	0.158	0
MAL-ASP 03	[m]: glu-L + oaa <=> akg + asp-L	0.158	0.151	4.2	0.156	2	0.172	8.9	0.161	2.2	0.166	5.5	0.158	0
MAL-ASP 04	[c]: oaa + h + nadh -> mal-L + nad	0.158	0.151	4.2	0.156	2	0.172	8.9	0.161	2.2	0.166	5.5	0.158	0
MAL-ASP 06	mal-L[m] + akg[c] <=> mal-L[c] + akg[m]	-0.158	-0.151	4.2	-0.156	-2	-0.172	8.9	-0.161	2.2	-0.166	5.5	-0.158	0
MAL-ASP 07	asp-L[m] + glu-L[c] -> asp-L[c] + glu-L[m]	0.158	0.151	4.2	0.156	2	0.172	8.9	0.161	2.2	0.166	5.5	0.158	0
ETC 01	nadh[m] + (5) h[m] + ubq[mim] -> nad[m] + (4) h[mis] + qh2[mim]	9.19	22.355	143.2	9.261	0.8	1.501	83.7	8.257	10.2	8.229	10.5	2.764	69.9

Table C.1. FBA results and percent changes - continued

Reaction Name	Reaction	Normal	O_2 unlim.	%	carnitine	%	complex I	%	fasting	%	hmg-coa	%	ischemia	%
ETC 02	fadh2[m] + ubq[mim] <=> fad[m] + qh2[mim]	1.95	7.784	299.2	1.879	3.6	0.698	64.2	2.883	47.9	2.911	49.3	0.578	70.4
ETC 03	qh2[mim] + (2) h[m] + (2) cytc-o[mim] -> ubq[mim] + (2) cytc-r[mim] + (4) h[mis]	11.14	30.139	170.5	11.14	0	2.199	80.3	11.14	0	11.14	0	3.342	70
ETC 04	o2[m] + (8) h[m] + (4) cytc-r[mim] -> (2) h2o[m] + (4) h[mis] + (4) cytc-o[mim]	5.57	15.07	170.5	5.57	0	1.1	80.3	5.57	0	5.57	0	1.671	70
NUCLEO	adp[m] + pi[m] + (3) h[mis] -> atp[m] + (3) h[m] + h2o[m]	34.534	90.085	160.9	34.627	0.3	6.399	81.5	33.29	3.6	33.252	3.7	10.369	70
NUCLEO	atp[m] + adp[c] -> atp[c] + adp[m]	36.4	95.266	161.7	36.489	0.2	6.787	81.4	35.177	3.4	35.167	3.4	10.931	70
I-TRANS	acac[c] -> acac[m]	0	0.001	-	0	795.9	0.001	-	0.08	-	0.008	-	0	0
KETONE 01	[m]: acac + coa + atp -> acaccoa + adp + pi	0	0.001	-	0	795.9	0.001	-	0.08	-	0.008	-	0	0
OTHERS	[c]: ppi + h2o -> (2) pi + h	0.071	0.371	424.9	0.114	62.1	0.049	30.6	0.131	85.6	0.141	100.2	0.115	63.6
NUCLEO	[m]: atp + gdp <=> adp + gtp	-0.658	-1.718	161.1	-0.708	-3.5	-0.155	76.5	-0.78	18.6	-0.675	2.6	-0.238	63.7
I-TRANS	crn[m] <=> crn[c]	0.012	0.371	2888.7	0.003	76.9	0.045	259.1	0.131	956.6	0.141	1039.8	0.003	78.7
I-TRANS	h[c] <=> h[m]	-34.534	-90.084	160.9	-34.627	-0.3	-6.398	81.5	-33.21	3.8	-33.244	3.7	-10.369	70
I-TRANS	co2[c] <=> co2[m]	-7.07	-14.26	101.7	-7.222	-2.1	-0.605	91.4	-5.144	27.3	-5.08	28.2	-2.026	71.3
I-TRANS	coa[c] <=> coa[m]	0	0	0	0	2482.6	0	0	0	0	0	0	0	0
I-TRANS	glu-L[c] + h[c] <=> glu-L[m] + h[m]	0	0	0	0	100	0	0	0	0	0	0	0	0
I-TRANS	h2o[c] <=> h2o[m]	-41.845	-107.041	155.8	-42.024	-0.4	-7.479	82.1	-39.491	5.6	-39.466	5.7	-12.569	70
I-TRANS	o2[c] <=> o2[m]	5.57	15.07	170.5	5.57	0	1.1	80.3	5.57	0	5.57	0	1.671	70
I-TRANS	o2[c] <=> o2[p]	0	0	0	0	230.2	0	0	0	0	0	0	0	0
I-TRANS	h[c] + pi[c] <=> h[m] + pi[m]	37.98	97.168	155.8	38.151	0.4	6.614	82.6	35.712	6	35.717	6	11.293	70.3
TRIGLY 00	[c]: dhap + nadh <=> glyc3p + nad	0	0	0	0	-	0	0	0	0	0	0	0	0
TRIGLY 01	[c]: 3pg + adp <=> atp + glycrt	0.02	-0.06	400	0.02	0	0.002	92.3	-0.022	208.3	-0.032	261.6	0.02	0

Table C.1. FBA results and percent changes - continued

Reaction Name	Reaction	Normal	O_2 unlim.	%	carnitine	%	complex I	%	fasting	%	hmg-coa	%	ischemia	%
TRIGLY 02	[c]: glycrt + nadh + h <=> glyc-ald + nad + h2o	0.02	-0.06	400	0.02	0	0.002	92.3	-0.022	208.3	-0.032	261.6	0.02	0
TRIGLY 03	[c]: glyc-ald + nadph + h <=> glyc + nadp	-1.58	-1.902	20.4	-1.662	-4.9	0.173	111	-0.534	66.2	-0.55	65.2	-0.362	77.1
TRIGLY 04	[c]: glyc-ald + nadh + h <=> glyc + nad	1.6	1.842	15.1	1.682	4.8	-0.172	110.7	0.513	68	0.518	67.6	0.382	76.1
TRIGLY 05	[c]: glyc + atp -> glyc-3p + adp	0.02	0	100	0.038	91.7	0.002	92.3	0	100	0	100	0.039	93.9
TRIGLY 06	[c]: glyc-3p + fa-coa -> lpa + coa	0.02	0	100	0.038	91.7	0.002	92.3	0	100	0	100	0.039	93.9
TRIGLY 07	[c]: lpa + fa-coa -> pda + coa	0.02	0	100	0.038	91.7	0.002	92.3	0	100	0	100	0.039	93.9
TRIGLY 08	[c]: pda + h2o -> 12glyc + pi	0.02	0	100	0.038	91.7	0.002	92.3	0	100	0	100	0.039	93.9
TRIGLY 09	[c]: 12glyc + fa-coa -> triglyc + coa	0.02	0	100	0.038	91.7	0.002	92.3	0	100	0	100	0.039	93.9
TRIGLY 10	[c]: triglyc -> glyc + fa	0	0	0	0.018	2.929E +10	0	0	0.022	-	0.032	-	0.019	-
TRIGLY 11	[c]: triglyc + h2o -> 12glyc + fa	0	0.06	-	0	473.2	0	0	0	0	0	0	0	0
TRIGLY 12	[c]: 12glyc + atp -> pda + adp	0	0	0	0	517.7	0	0	0	0	0	0	0	0
TRIGLY 13	[c]: 12glyc + h2o -> aglyc + fa	0	0.06	-	0	477.7	0	0	0	0	0	0	0	0
TRIGLY 14	[c]: aglyc + h2o -> glyc + fa	0	0.06	-	0	597.8	0	0	0	0	0	0	0	0
TRIGLY 15	[c]: atp + aglyc -> adp + lpa	0	0	0	0	433.4	0	0	0	0	0	0	0	0
TRIGLY 16	[c]: (0.03) td-coa + (0.37) hd-coa + (0.03) hd9-coa + (0.23) od9-coa + (0.16) od9-12-coa + (0.15) od-coa <=> fa-coa	0.06	0	100	0.115	91.7	0.005	92.3	0	100	0	100	0.116	93.9
TRIGLY 17	[c]: fa -> (0.03) td-ca + (0.37) hd-ca + (0.03) hd9-ca + (0.23) od9-ca + (0.16) od9-12-ca + (0.15) od-ca	0	0.18	-	0.018	1.556E +10	0	0	0.022	-	0.032	-	0.019	-

APPENDIX D

Table D.1. Reaction that have never been used

Reaction Name	Reaction	Max value	Min value
TRANS 04	ei-ca[e] -> ei-ca[c]	0.000	0.000
TRANS 08	dd-ca[e] -> dd-ca[c]	0.000	0.000
TRANS 09	d-ca[e] -> d-ca[c]	0.000	0.000
TRANS 10	o-ca[e] -> o-ca[c]	0.000	0.000
TRANS 15	tcs-ca[e] -> tcs-ca[c]	0.000	0.000
TRANS 16	dcs-ca[e] -> dcs-ca[c]	0.000	0.000
TRANS 22	h2o2[e] -> h2o2[c]	0.000	0.000
OTHERS	[c]: glut-ox + nadph + h -> (2) glut-red + nadp	0.000	0.000
OTHERS	[c]: (2) glut-red + h2o2 ⇔ glut-ox + (2) h2o	0.000	0.000
BOX 01	[c]: atp + coa + ei-ca ⇔ amp + ei-coa + ppi	0.000	0.000
BOX 02	[c]: crn + ei-coa ⇔ ei-crn + coa	0.000	0.000
BOX 03	ei-crn[c] -> ei-crn[m]	0.000	0.000
BOX 04	[m]: ei-crn + coa ⇔ crn + ei-coa	0.000	0.000
BOX 05	[m]: ei-coa + fad -> t-ei-coa + fadh2	0.000	0.000
BOX 06	[m]: t-ei-coa + h2o ⇔ 3h-ei-coa	0.000	0.000
BOX 07	[m]: 3h-ei-coa + nad ⇔ 3o-ei-coa + nadh + h	0.000	0.000
BOX 08	[m]: 3o-ei-coa + coa ⇔ od-coa + accoa	0.000	0.000
BOX 33	[c]: atp + coa + dd-ca ⇔ amp + dd-coa + ppi	0.000	0.000
BOX 34	[c]: crn + dd-coa ⇔ dd-crn + coa	0.000	0.000
BOX 35	dd-crn[c] -> dd-crn[m]	0.000	0.000
BOX 36	[m]: dd-crn + coa ⇔ crn + dd-coa	0.000	0.000
BOX 41	[c]: atp + coa + d-ca ⇔ amp + d-coa + ppi	0.000	0.000
BOX 42	[c]: crn + d-coa ⇔ d-crn + coa	0.000	0.000
BOX 43	d-crn[c] -> d-crn[m]	0.000	0.000
BOX 44	[m]: d-crn + coa ⇔ crn + d-coa	0.000	0.000
BOX 49	[c]: atp + coa + o-ca ⇔ amp + o-coa + ppi	0.000	0.000
BOX 50	[c]: crn + o-coa ⇔ o-crn + coa	0.000	0.000
BOX 51	o-crn[c] -> o-crn[m]	0.000	0.000
BOX 52	[m]: o-crn + coa ⇔ crn + o-coa	0.000	0.000
PBOX 01	tcs-coa[c] -> tcs-coa[p]	0.000	0.000
PBOX 02	[c]: atp + coa + tcs-ca ⇔ amp + tcs-coa + ppi	0.000	0.000
PBOX 03	[p]: tcs-coa + o2 ⇔ t-tcs-coa + h2o2	0.000	0.000
PBOX 04	[p]: t-tcs-coa + h2o ⇔ 3h-tcs-coa	0.000	0.000
PBOX 05	[p]: 3h-tcs-coa + nad ⇔ 3o-tcs-coa + nadh + h	0.000	0.000
PBOX 06	[p]: 3o-tcs-coa + coa ⇔ dcs-coa + accoa	0.000	0.000
PBOX 07	dcs-coa[c] -> dcs-coa[p]	0.000	0.000
PBOX 08	[c]: atp + coa + dcs-ca ⇔ amp + dcs-coa + ppi	0.000	0.000
PBOX 09	[p]: dcs-coa + o2 ⇔ t-dcs-coa + h2o2	0.000	0.000
PBOX 10	[p]: t-dcs-coa + h2o ⇔ 3h-dcs-coa	0.000	0.000
PBOX 11	[p]: 3h-dcs-coa + nad ⇔ 3o-dcs-coa + nadh + h	0.000	0.000
PBOX 12	[p]: 3o-dcs-coa + coa ⇔ ei-coa + accoa	0.000	0.000
PBOX 13	ei-coa[p] -> ei-coa[c]	0.000	0.000
PBOX 14	[p]: ei-coa + o2 <=> t-ei-coa + h2o2	0.000	0.000
PBOX 15	[p]: t-ei-coa + h2o <=> 3h-ei-coa	0.000	0.000
PBOX 16	[p]: 3h-ei-coa + nad <=> 3o-ei-coa + nadh + h	0.000	0.000
PBOX 17	[p]: 3o-ei-coa + coa <=> od-coa + accoa	0.000	0.000
PBOX 18	od-coa[p] -> od-coa[c]	0.000	0.000
PBOX 19	[p]: od-coa + o2 <=> t-od-coa + h2o2	0.000	0.000
PBOX 20	[p]: t-od-coa + h2o <=> 3h-od-coa	0.000	0.000

Table D.1. Reaction that have never been used - continued

Reaction Name	Reaction	Max value	Min value
PBOX 21	[p]: 3h-od-coa + nad <=> 3o-od-coa + nadh + h	0.000	0.000
PBOX 22	[p]: 3o-od-coa + coa <=> hd-coa + accoa	0.000	0.000
PBOX 23	hd-coa[p] -> hd-coa[c]	0.000	0.000
PBOX 24	[p]: hd-coa + o2 <=> t-hd-coa + h2o2	0.000	0.000
PBOX 25	[p]: t-hd-coa + h2o <=> 3h-hd-coa	0.000	0.000
PBOX 26	[p]: 3h-hd-coa + nad <=> 3o-hd-coa + nadh + h	0.000	0.000
PBOX 27	[p]: 3o-hd-coa + coa <=> td-coa + accoa	0.000	0.000
PBOX 28	td-coa[p] -> td-coa[c]	0.000	0.000
PBOX 29	[p]: td-coa + o2 <=> t-td-coa + h2o2	0.000	0.000
PBOX 30	[p]: t-td-coa + h2o <=> 3h-td-coa	0.000	0.000
PBOX 31	[p]: 3h-td-coa + nad <=> 3o-td-coa + nadh + h	0.000	0.000
PBOX 32	[p]: 3o-td-coa + coa <=> dd-coa + accoa	0.000	0.000
PBOX 33	dd-coa[p] -> dd-coa[c]	0.000	0.000
PBOX 34	[p]: dd-coa + o2 <=> t-dd-coa + h2o2	0.000	0.000
PBOX 35	[p]: t-dd-coa + h2o <=> 3h-dd-coa	0.000	0.000
PBOX 36	[p]: 3h-dd-coa + nad <=> 3o-dd-coa + nadh + h	0.000	0.000
PBOX 37	[p]: 3o-dd-coa + coa <=> d-coa + accoa	0.000	0.000
PBOX 38	d-coa[p] -> d-coa[c]	0.000	0.000
PBOX 39	[p]: d-coa + o2 <=> t-d-coa + h2o2	0.000	0.000
PBOX 40	[p]: t-d-coa + h2o <=> 3h-d-coa	0.000	0.000
PBOX 41	[p]: 3h-d-coa + nad <=> 3o-d-coa + nadh + h	0.000	0.000
PBOX 42	[p]: 3o-d-coa + coa <=> o-coa + accoa	0.000	0.000
P-BOX 43	o-coa[p] -> o-coa[c]	0.000	0.000
P-BOX 44	accoa[p] -> accoa[c]	0.000	0.000
P-BOX 45	accoa[c] + crn[c] -> accrn[c] + coa[c]	0.000	0.000
P-BOX 46	accrn[c] -> accrn[m]	0.000	0.000
P-BOX 47	[m]: accrn + coa -> accoa + crn	0.000	0.000
I-TRANS	coa[m] <=> coa[p]	0.000	0.000
I-TRANS	h2o[c] <=> h2o[p]	0.000	0.000
I-TRANS	nad[m] <=> nad[p]	0.000	0.000
I-TRANS	nadh[p] <=> nadh[m]	0.000	0.000
I-TRANS	h[p] <=> h[m]	0.000	0.000
OTHERS	[p]: (2) h2o2 --> (2) h2o + o2	0.000	0.000
I-TRANS	coa[c] <=> coa[m]	0.000	0.000
I-TRANS	glu-L[c] + h[c] <=> glu-L[m] + h[m]	0.000	0.000
I-TRANS	o2[c] <=> o2[p]	0.000	0.000
TRIGLY 00	[c]: dhap + nadh <=> glyc3p + nad	0.000	0.000

Table D.2. Flux Variability Data

Reaction Name	Reaction	Max value	Min value	Δ	Fract.
BOX 09	[c]: atp + coa + od-ca <=> amp + od-coa + ppi	0.616	0.004	0.612	1.0
BOX 10	[c]: crn + od-coa <=> od-crn + coa	0.041	0.000	0.041	1.0
BOX 11	od-crn[c] -> od-crn[m]	0.041	0.000	0.041	1.0
BOX 12	[m]: od-crn + coa <=> crn + od-coa	0.041	0.000	0.041	1.0
BOX 13	[m]: od-coa + fad -> t-od-coa + fadh2	0.041	0.000	0.041	1.0
BOX 14	[m]: t-od-coa + h2o <=> 3h-od-coa	0.041	0.000	0.041	1.0
BOX 15	[m]: 3h-od-coa + nad <=> 3o-od-coa + nadh + h	0.041	0.000	0.041	1.0
BOX 16	[m]: 3o-od-coa + coa <=> hd-coa + accoa	0.041	0.000	0.041	1.0
BOX 17	[c]: atp + coa + hd-ca <=> amp + hd-coa + ppi	1.521	0.009	1.512	1.0
BOX 18	[c]: crn + hd-coa <=> hd-crn + coa	0.096	0.000	0.096	1.0
BOX 19	hd-crn[c] -> hd-crn[m]	0.096	0.000	0.096	1.0
BOX 20	[m]: hd-crn + coa <=> crn + hd-coa	0.096	0.000	0.096	1.0
BOX 21	[m]: hd-coa + fad -> t-hd-coa + fadh2	0.128	0.000	0.128	1.0
BOX 22	[m]: t-hd-coa + h2o <=> 3h-hd-coa	0.128	0.000	0.128	1.0
BOX 23	[m]: 3h-hd-coa + nad <=> 3o-hd-coa + nadh + h	0.128	0.000	0.128	1.0
BOX 24	[m]: 3o-hd-coa + coa <=> td-coa + accoa	0.128	0.000	0.128	1.0
BOX 25	[c]: atp + coa + td-ca <=> amp + td-coa + ppi	0.123	0.001	0.122	1.0
BOX 26	[c]: crn + td-coa <=> td-crn + coa	0.008	0.000	0.008	1.0
BOX 27	td-crn[c] -> td-crn[m]	0.008	0.000	0.008	1.0
BOX 28	[m]: td-crn + coa <=> crn + td-coa	0.008	0.000	0.008	1.0
BOX 29	[m]: td-coa + fad -> t-td-coa + fadh2	0.134	0.000	0.134	1.0
BOX 30	[m]: t-td-coa + h2o <=> 3h-td-coa	0.134	0.000	0.134	1.0
BOX 31	[m]: 3h-td-coa + nad <=> 3o-td-coa + nadh + h	0.134	0.000	0.134	1.0
BOX 32	[m]: 3o-td-coa + coa <=> dd-coa + accoa	0.134	0.000	0.134	1.0
BOX 37	[m]: dd-coa + fad -> t-dd-coa + fadh2	0.134	0.000	0.134	1.0
BOX 38	[m]: t-dd-coa + h2o <=> 3h-dd-coa	0.201	0.000	0.201	1.0
BOX 39	[m]: 3h-dd-coa + nad <=> 3o-dd-coa + nadh + h	0.201	0.000	0.201	1.0
BOX 40	[m]: 3o-dd-coa + coa <=> d-coa + accoa	0.201	0.000	0.201	1.0
BOX 45	[m]: d-coa + fad -> t-d-coa + fadh2	0.201	0.000	0.201	1.0
BOX 46	[m]: t-d-coa + h2o <=> 3h-d-coa	0.231	0.002	0.229	1.0
BOX 47	[m]: 3h-d-coa + nad <=> 3o-d-coa + nadh + h	0.231	0.002	0.229	1.0
BOX 48	[m]: 3o-d-coa + coa <=> o-coa + accoa	0.231	0.002	0.229	1.0
BOX 53	[m]: o-coa + fad -> t-o-coa + fadh2	0.231	0.002	0.229	1.0
BOX 54	[m]: t-o-coa + h2o <=> 3h-o-coa	0.231	0.002	0.229	1.0
BOX 55	[m]: 3h-o-coa + nad <=> 3o-o-coa + nadh + h	0.231	0.002	0.229	1.0
BOX 56	[m]: 3o-o-coa + coa <=> h-coa + accoa	0.231	0.002	0.229	1.0
BOX 57	[m]: h-coa + fad -> t-h-coa + fadh2	0.231	0.002	0.229	1.0
BOX 58	[m]: t-h-coa + h2o <=> 3h-h-coa	0.231	0.002	0.229	1.0
BOX 59	[m]: 3h-h-coa + nad <=> 3o-h-coa + nadh + h	0.231	0.002	0.229	1.0
BOX 60	[m]: 3o-h-coa + coa <=> but-coa + accoa	0.231	0.002	0.229	1.0
BOX 61	[m]: but-coa + fad -> t-but-coa + fadh2	0.231	0.002	0.229	1.0
BOX 62	[m]: t-but-coa + h2o <=> 3h-but-coa	0.231	0.002	0.229	1.0
BOX 63	[m]: 3h-but-coa + nad <=> acaccoa + nadh + h	0.231	0.002	0.229	1.0

Table D.2. Flux Variability Data - continued

Reaction Name	Reaction	Max value	Min value	Δ	Fract.
BOX 64	[m]: acaccoa + coa <=> (2) accoa	0.232	0.002	0.230	1.0
ETC 01	nadh[m] + (5) h[m] + ubq[mim] -> nad[m] + (4) h[mis] + qh2[mim]	9.304	6.497	2.807	0.3
ETC 02	fadh2[m] + ubq[mim] <=> fad[m] + qh2[mim]	3.569	1.444	2.125	0.6
ETC 03	qh2[mim] + (2) h[m] + (2) cytc-o[mim] -> ubq[mim] + (2) cytc-r[mim] + (4) h[mis]	11.140	8.773	2.367	0.2
ETC 04	o2[m] + (8) h[m] + (4) cytc-r[mim] -> (2) h2o[m] + (4) h[mis] + (4) cytc-o[mim]	5.570	4.386	1.184	0.2
GLY 01	[c]: atp + glc-D -> adp + g6p	0.560	0.430	0.130	0.2
GLY 02	[c]: g6p <=> f6p	0.760	0.120	0.640	0.8
GLY 03	[c]: atp + f6p -> adp + f26bp	7.759	0.000	7.759	1.0
GLY 04	[c]: f26bp + h2o -> f6p + pi	7.759	0.000	7.759	1.0
GLY 05	[c]: atp + f6p -> adp + fbp	0.760	0.193	0.567	0.7
GLY 06	[c]: fbp <=> dhap + g3p	0.760	0.193	0.567	0.7
GLY 07	[c]: dhap <=> g3p	0.760	0.193	0.567	0.7
GLY 08	[c]: g3p + nad + pi <=> 13dpg + h + nadh	1.520	0.423	1.097	0.7
GLY 09	[c]: 13dpg + adp <=> 3pg + atp	1.520	0.423	1.097	0.7
GLY 10	[c]: 3pg <=> 2pg	1.580	0.403	1.177	0.7
GLY 11	[c]: 2pg <=> pep + h2o	1.580	0.403	1.177	0.7
GLY 12	[c]: adp + pep -> atp + pyr	1.580	0.403	1.177	0.7
GLYCGN 01	[c]: g6p <=> g1p	0.200	-0.200	0.400	2.0
GLYCGN 02	[c]: g1p + utp -> ppi + udpg	3.879	0.000	3.879	1.0
GLYCGN 03	[c]: udpg -> glycogen + udp	3.879	0.000	3.879	1.0
GLYCGN 04	[c]: glycogen + pi + atp -> g1p + adp	4.079	0.000	4.079	1.0
I-TRANS	co2[c] <=> co2[m]	-3.160	-7.399	4.239	1.3
I-TRANS	acac[c] -> acac[m]	0.001	0.000	0.001	1.0
I-TRANS	crn[m] <=> crn[c]	0.231	0.002	0.229	1.0
I-TRANS	h2o[c] <=> h2o[m]	-32.176	-42.162	9.986	0.3
I-TRANS	h[c] <=> h[m]	-27.077	-34.685	7.608	0.3
I-TRANS	h[c] + pi[c] <=> h[m] + pi[m]	38.340	29.068	9.272	0.2
I-TRANS	o2[c] <=> o2[m]	5.570	4.386	1.184	0.2
KETONE 01	[m]: acac + coa + atp -> acaccoa + adp + pi	0.001	0.000	0.001	1.0
MAL-ASP 01	mal-L[m] + pi[c] <=> mal-L[c] + pi[m]	0.201	-1.842	2.042	10.2
MAL-ASP 02	[c]: akg + asp-L <=> glu-L + oaa	0.200	0.000	0.200	1.0
MAL-ASP 03	[m]: glu-L + oaa <=> akg + asp-L	0.200	0.000	0.200	1.0
MAL-ASP 04	[c]: oaa + h + nadh -> mal-L + nad	7.959	0.000	7.959	1.0
MAL-ASP 06	mal-L[m] + akg[c] <=> mal-L[c] + akg[m]	0.000	-0.200	0.200	-
MAL-ASP 07	asp-L[m] + glu-L[c] -> asp-L[c] + glu-L[m]	0.200	0.000	0.200	1.0
NUCLEOTIDE	[c]: udp + atp <=> utp + adp	3.879	0.000	3.879	1.0
NUCLEOTIDE	[c]: amp + atp <=> (2) adp	3.988	0.049	3.939	1.0
NUCLEOTIDE	adp[m] + pi[m] + (3) h[mis] -> atp[m] + (3) h[m] + h2o[m]	34.685	27.078	7.607	0.2
NUCLEOTIDE	atp[m] + adp[c] -> atp[c] + adp[m]	36.509	28.578	7.931	0.2
OTHERS	[c]: ppi + h2o -> (2) pi + h	3.988	0.049	3.939	1.0
PPP 01	[c]: g6p + nadp -> 6pgl + nadph + h	0.110	0.000	0.110	1.0
PPP 02	[c]: 6pgl + h2o -> 6pgc	0.110	0.000	0.110	1.0
PPP 03	[c]: 6pgc + nadp -> ru5p + co2 + nadph + h	0.110	0.000	0.110	1.0

Table D.2. Flux Variability Data - continued

Reaction Name	Reaction	Max value	Min value	Δ	Fract.
PPP 04	[c]: ru5p <=> x5p	0.073	0.000	0.073	1.0
PPP 05	[c]: ru5p <=> r5p	0.037	0.000	0.037	1.0
PPP 06	[c]: g3p + s7p <=> e4p + f6p	0.037	0.000	0.037	1.0
PPP 07	[c]: r5p + x5p <=> s7p + g3p	0.037	0.000	0.037	1.0
PPP 08	[c]: x5p + e4p <=> g3p + f6p	0.037	0.000	0.037	1.0
PYR 01	[c]: lac-L + nad <=> pyr + nadh + h	0.413	-0.960	1.373	3.3
PYR 02	pyr[c] + h[c] -> pyr[m] + h[m]	0.220	0.000	0.220	1.0
PYR 03	[m]: coa + nad + pyr -> accoa + co2 + nadh	1.845	0.000	1.845	1.0
PYR 04	[m]: mal-L + nad <=> pyr + nadh + co2 + h	1.842	-0.227	2.069	1.1
PYR 05	[c]: pyr + co2 + atp -> adp + pi + oaa	7.759	0.000	7.759	1.0
PYR 06	[c]: mal-L + nadp <=> pyr + co2 + nadph + h	6.253	-1.842	8.095	1.3
PYR 07	[m]: mal-L + nadp <=> pyr + co2 + nadph + h	0.053	0.000	0.053	1.0
TCA 01	[m]: accoa + h2o + oaa -> cit + coa	1.963	1.432	0.531	0.3
TCA 02	[m]: cit <=> cacon + h2o	1.963	1.432	0.531	0.3
TCA 03	[m]: cacon + h2o <=> icit	1.963	1.432	0.531	0.3
TCA 04	[m]: icit + nad -> akg + co2 + nadh + h	1.963	1.432	0.531	0.3
TCA 05	[m]: akg + coa + nad -> co2 + nadh + succoa	1.963	1.432	0.531	0.3
TCA 08	[m]: succ + fad <=> fum + fadh2	1.963	1.432	0.531	0.3
TCA 09	[m]: fum + h2o <=> mal-L	1.963	1.432	0.531	0.3
TCA 10	[m]: mal-L + nad -> oaa + nadh + h	2.163	1.464	0.699	0.3
TRANS 01	glc-D[e] -> glc-D[c]	0.560	0.430	0.130	0.2
TRANS 02	glycogen[c] <=> glycogen[e]	0.200	-0.200	0.400	2.0
TRANS 03	lac-L[e] + h[e] <=> lac-L[c] + h[c]	0.413	-0.960	1.373	3.3
TRANS 05	hd-ca[e] -> hd-ca[c]	0.038	0.009	0.029	0.8
TRANS 06	od-ca[e] -> od-ca[c]	0.015	0.004	0.011	0.7
TRANS 07	td-ca[e] -> td-ca[c]	0.003	0.001	0.002	0.7
TRANS 12	od9-ca[e] -> od9-ca[c]	0.092	0.023	0.069	0.7
TRANS 13	od9-12-ca[e] -> od9-12-ca[c]	0.027	0.007	0.020	0.7
TRANS 14	hd9-ca[e] -> hd9-ca[c]	0.021	0.005	0.016	0.8
TRANS 16	acac[e] -> acac[c]	0.001	0.000	0.001	1.0
TRANS 17	co2[e] <=> co2[c]	-3.336	-5.567	2.231	0.7
TRANS 18	o2[e] <=> o2[c]	5.570	4.386	1.184	0.2
TRANS 19	h[e] <=> h[c]	-26.831	-34.746	7.915	0.3
TRANS 20	h[e] + pi[e] <=> h[c] + pi[c]	4.079	0.000	4.079	1.0
TRANS 21	h2o[e] <=> h2o[c]	-3.110	-13.402	10.291	3.3
TRANS 23	coa[e] <=> coa[c]	0.000	-0.123	0.123	-
TRANS 24	triglyc[e] <=> triglyc[c]	0.060	-0.020	0.080	1.3
TRIGLY 01	[c]: 3pg + adp <=> atp + glycrt	0.020	-0.060	0.080	4.0
TRIGLY 02	[c]: glycrt + nadh + h <=> glyc-ald + nad + h2o	0.020	-0.060	0.080	4.0
TRIGLY 03	[c]: glyc-ald + nadph + h <=> glyc + nadp	6.264	-1.842	8.106	1.3
TRIGLY 04	[c]: glyc-ald + nadh + h <=> glyc + nad	1.845	-6.256	8.101	4.4
TRIGLY 05	[c]: glyc + atp -> glyc-3p + adp	1.626	0.000	1.626	1.0
TRIGLY 06	[c]: glyc-3p + fa-coa -> lpa + coa	1.626	0.000	1.626	1.0

Table D.2. Flux Variability Data - continued

Reaction Name	Reaction	Max value	Min value	Δ	Fract.
TRIGLY 07	[c]: lpa + fa-coa -> pda + coa	2.673	0.000	2.673	1.0
TRIGLY 08	[c]: pda + h2o -> 12glyc + pi	7.780	0.000	7.780	1.0
TRIGLY 09	[c]: 12glyc + fa-coa -> triglyc + coa	4.030	0.000	4.030	1.0
TRIGLY 10	[c]: triglyc -> glyc + fa	0.140	0.000	0.140	1.0
TRIGLY 11	[c]: triglyc + h2o -> 12glyc + fa	3.999	0.000	3.999	1.0
TRIGLY 12	[c]: 12glyc + atp -> pda + adp	7.759	0.000	7.759	1.0
TRIGLY 13	[c]: 12glyc + h2o -> aglyc + fa	2.639	0.000	2.639	1.0
TRIGLY 14	[c]: aglyc + h2o -> glyc + fa	1.590	0.000	1.590	1.0
TRIGLY 15	[c]: atp + aglyc -> adp + lpa	2.639	0.000	2.639	1.0
TRIGLY 16	[c]: (0.03) td-coa + (0.37) hd-coa + (0.03) hd9-coa + (0.23) od9-coa + (0.16) od9-12-coa + (0.15) od-coa <=> fa-coa	4.110	0.000	4.110	1.0
TRIGLY 17	[c]: fa -> (0.03) td-ca + (0.37) hd-ca + (0.03) hd9-ca + (0.23) od9-ca + (0.16) od9-12-ca + (0.15) od-ca	4.010	0.000	4.010	1.0
U-BOX 01	[c]: atp + coa + od9-ca <=> amp + od9-coa + ppi	0.945	0.023	0.922	1.0
U-BOX 02	[c]: crn + od9-coa <=> od9-crn + coa	0.117	0.000	0.117	1.0
U-BOX 03	od9-crn[c] -> od9-crn[m]	0.117	0.000	0.117	1.0
U-BOX 04	[m]: od9-crn + coa <=> crn + od9-coa	0.117	0.000	0.117	1.0
U-BOX 05	[m]: od9-coa + fad -> t-od9-coa + fadh2	0.117	0.000	0.117	1.0
U-BOX 06	[m]: t-od9-coa + h2o <=> 3h-od9-coa	0.117	0.000	0.117	1.0
U-BOX 07	[m]: 3h-od9-coa + nad <=> 3o-od9-coa + nadh + h	0.117	0.000	0.117	1.0
U-BOX 08	[m]: 3o-od9-coa + coa <=> hd7-coa + accoa	0.117	0.000	0.117	1.0
U-BOX 09	[m]: hd7-coa + fad -> t-hd7-coa + fadh2	0.117	0.000	0.117	1.0
U-BOX 10	[m]: t-hd7-coa + h2o <=> 3h-hd7-coa	0.117	0.000	0.117	1.0
U-BOX 11	[m]: 3h-hd7-coa + nad <=> 3o-hd7-coa + nadh + h	0.117	0.000	0.117	1.0
U-BOX 12	[m]: 3o-hd7-coa + coa <=> td5-coa + accoa	0.117	0.000	0.117	1.0
U-BOX 13	[m]: td5-coa + fad -> t-td5-coa + fadh2	0.117	0.000	0.117	1.0
U-BOX 14	[m]: t-td5-coa + h2o <=> 3h-td5-coa	0.117	0.000	0.117	1.0
U-BOX 15	[m]: 3h-td5-coa + nad <=> 3o-td5-coa + nadh + h	0.117	0.000	0.117	1.0
U-BOX 16	[m]: 3o-td5-coa + coa <=> cisdd-coa + accoa	0.117	0.000	0.117	1.0
U-BOX 17	[m]: cisdd-coa <=> t-dd-coa	0.117	0.000	0.117	1.0
U-BOX 18	[c]: atp + coa + od9-12-ca <=> amp + od9-12-coa + ppi	0.658	0.007	0.651	1.0
U-BOX 19	[c]: crn + od9-12-coa <=> od9-12-crn + coa	0.053	0.000	0.053	1.0
U-BOX 20	od9-12-crn[c] -> od9-12-crn[m]	0.053	0.000	0.053	1.0
U-BOX 21	[m]: od9-12-crn + coa <=> crn + od9-12-coa	0.053	0.000	0.053	1.0
U-BOX 22	[m]: od9-12-coa + fad -> t-od9-12-coa + fadh2	0.053	0.000	0.053	1.0
U-BOX 23	[m]: t-od9-12-coa + h2o <=> 3h-od9-12-coa	0.053	0.000	0.053	1.0
U-BOX 24	[m]: 3h-od9-12-coa + nad <=> 3o-od9-12-coa + nadh + h	0.053	0.000	0.053	1.0
U-BOX 25	[m]: 3o-od9-12-coa + coa <=> hd-7-10-coa + accoa	0.053	0.000	0.053	1.0
U-BOX 26	[m]: hd-7-10-coa + fad -> t-hd-7-10-coa + fadh2	0.053	0.000	0.053	1.0
U-BOX 27	[m]: t-hd-7-10-coa + h2o <=> 3h-hd-7-10-coa	0.053	0.000	0.053	1.0
U-BOX 28	[m]: 3h-hd-7-10-coa + nad <=> 3o-hd-7-10-coa + nadh + h	0.053	0.000	0.053	1.0
U-BOX 29	[m]: 3o-hd-7-10-coa + coa <=> td-5-8-coa + accoa	0.053	0.000	0.053	1.0
U-BOX 30	[m]: td-5-8-coa + fad -> t-td-5-8-coa + fadh2	0.053	0.000	0.053	1.0
U-BOX 31	[m]: t-td-5-8-coa + h2o <=> 3h-td-5-8-coa	0.053	0.000	0.053	1.0
U-BOX 32	[m]: 3h-td-5-8-coa + nad <=> 3o-td-5-8-coa + nadh + h	0.053	0.000	0.053	1.0

Table D.2. Flux Variability Data - continued

Reaction Name	Reaction	Max value	Min value	Δ	Fract.
U-BOX 33	[m]: 3o-td-5-8-coa + coa <=> cis-3-6-dd-coa + accoa	0.053	0.000	0.053	1.0
U-BOX 34	[m]: cis-3-6-dd-coa <=> t-2-6-dd-coa	0.053	0.000	0.053	1.0
U-BOX 35	[m]: t-2-6-dd-coa + h2o <=> 3h-2-6-dd-coa	0.053	0.000	0.053	1.0
U-BOX 36	[m]: 3h-2-6-dd-coa + nad <=> 3o-2-6-dd-coa + nadh + h	0.053	0.000	0.053	1.0
U-BOX 37	[m]: 3o-2-6-dd-coa + coa <=> d4-coa + accoa	0.053	0.000	0.053	1.0
U-BOX 38	[m]: d4-coa + fad -> d2-4-coa + fadh2	0.053	0.000	0.053	1.0
U-BOX 39	[m]: d2-4-coa + nadph + h <=> cis-d-coa + nadp	0.053	0.000	0.053	1.0
U-BOX 40	[m]: cis-d-coa <=> t-d-coa	0.053	0.000	0.053	1.0
U-BOX 41	[c]: atp + coa + hd9-ca <=> amp + hd9-coa + ppi	0.139	0.005	0.134	1.0
U-BOX 42	[c]: crn + hd9-coa <=> hd9-crn + coa	0.026	0.002	0.024	0.9
U-BOX 43	hd9-crn[c] -> hd9-crn[m]	0.026	0.002	0.024	0.9
U-BOX 44	[m]: hd9-crn + coa <=> crn + hd9-coa	0.026	0.002	0.024	0.9
U-BOX 45	[m]: hd9-coa + fad -> t-hd9-coa + fadh2	0.026	0.002	0.024	0.9
U-BOX 46	[m]: t-hd9-coa + h2o <=> 3h-hd9-coa	0.026	0.002	0.024	0.9
U-BOX 47	[m]: 3h-hd9-coa + nad <=> 3o-hd9-coa + nadh + h	0.026	0.002	0.024	0.9
U-BOX 48	[m]: 3o-hd9-coa + coa <=> td7-coa + accoa	0.026	0.002	0.024	0.9
U-BOX 49	[m]: td7-coa + fad -> t-td7-coa + fadh2	0.026	0.002	0.024	0.9
U-BOX 50	[m]: t-td7-coa + h2o <=> 3h-td7-coa	0.026	0.002	0.024	0.9
U-BOX 51	[m]: 3h-td7-coa + nad <=> 3o-td7-coa + nadh + h	0.026	0.002	0.024	0.9
U-BOX 52	[m]: 3o-td7-coa + coa <=> dd5-coa + accoa	0.026	0.002	0.024	0.9
U-BOX 53	[m]: dd5-coa + fad -> t-dd5-coa + fadh2	0.026	0.002	0.024	0.9
U-BOX 54	[m]: t-dd5-coa + h2o <=> 3h-dd5-coa	0.026	0.002	0.024	0.9
U-BOX 55	[m]: 3h-dd5-coa + nad <=> 3o-dd5-coa + nadh + h	0.026	0.002	0.024	0.9
U-BOX 56	[m]: 3o-dd5-coa + coa <=> cisd-coa + accoa	0.026	0.002	0.024	0.9
U-BOX 57	[m]: cisd-coa <=> t-d-coa	0.026	0.002	0.024	0.9

APPENDIX E

Table E.1. Reactions and their corresponding clusters

Reaction Name	Reaction	Cluster #
TRANS 05	hd-ca[e] -> hd-ca[c]	0
TRANS 13	od9-12-ca[e] -> od9-12-ca[c]	0
BOX 09	[c]: atp + coa + od-ca <=> amp + od-coa + ppi	0
U-BOX 18	[c]: atp + coa + od9-12-ca <=> amp + od9-12-coa + ppi	0
TRANS 16	acac[e] -> acac[c]	1
I-TRANS	acac[c] -> acac[m]	1
KETONE 01	[m]: acac + coa + atp -> acaccoa + adp + pi	1
TRANS 20	h[e] + pi[e] <=> h[c] + pi[c]	3
GLYCGN 04	[c]: glycogen + pi + atp -> g1p + adp	3
PYR 02	pyr[c] + h[c] -> pyr[m] + h[m]	3
MAL-ASP 02	[c]: akg + asp-L <=> glu-L + oaa	3
MAL-ASP 03	[m]: glu-L + oaa <=> akg + asp-L	3
MAL-ASP 04	[c]: oaa + h + nadh -> mal-L + nad	3
MAL-ASP 07	asp-L[m] + glu-L[c] -> asp-L[c] + glu-L[m]	3
TRANS 01	glc-D[e] -> glc-D[c]	4
GLY 01	[c]: atp + glc-D -> adp + g6p	4
GLY 02	[c]: g6p <=> f6p	4
GLY 05	[c]: atp + f6p -> adp + fbp	4
GLY 06	[c]: fbp <=> dhap + g3p	4
GLY 07	[c]: dhap <=> g3p	4
GLY 08	[c]: g3p + nad + pi <=> 13dpg + h + nadh	6
GLY 09	[c]: 13dpg + adp <=> 3pg + atp	6
GLY 10	[c]: 3pg <=> 2pg	6
GLY 11	[c]: 2pg <=> pep + h2o	6
GLY 12	[c]: adp + pep -> atp + pyr	6
BOX 10	[c]: crn + od-coa <=> od-crn + coa	7
BOX 11	od-crn[c] -> od-crn[m]	7
BOX 12	[m]: od-crn + coa <=> crn + od-coa	7
BOX 13	[m]: od-coa + fad -> t-od-coa + fadh2	7
BOX 14	[m]: t-od-coa + h2o <=> 3h-od-coa	7
BOX 15	[m]: 3h-od-coa + nad <=> 3o-od-coa + nadh + h	7
BOX 16	[m]: 3o-od-coa + coa <=> hd-coa + accoa	7
TRIGLY 11	[c]: triglyc + h2o -> 12glyc + fa	7
TRIGLY 13	[c]: 12glyc + h2o -> aglyc + fa	7
TRIGLY 14	[c]: aglyc + h2o -> glyc + fa	7
TRANS 24	triglyc[e] <=> triglyc[c]	8
PYR 07	[m]: mal-L + nadp <=> pyr + co2 + nadph + h	8
U-BOX 19	[c]: crn + od9-12-coa <=> od9-12-crn + coa	8
U-BOX 20	od9-12-crn[c] -> od9-12-crn[m]	8

Table E.1. Reactions and their corresponding clusters - continued

Reaction Name	Reaction	Cluster #
U-BOX 21	[m]: od9-12-crn + coa <=> crn + od9-12-coa	8
U-BOX 22	[m]: od9-12-coa + fad -> t-od9-12-coa + fadh2	8
U-BOX 23	[m]: t-od9-12-coa + h2o <=> 3h-od9-12-coa	8
U-BOX 24	[m]: 3h-od9-12-coa + nad <=> 3o-od9-12-coa + nadh + h	8
U-BOX 25	[m]: 3o-od9-12-coa + coa <=> hd-7-10-coa + accoa	8
U-BOX 26	[m]: hd-7-10-coa + fad -> t-hd-7-10-coa + fadh2	8
U-BOX 27	[m]: t-hd-7-10-coa + h2o <=> 3h-hd-7-10-coa	8
U-BOX 28	[m]: 3h-hd-7-10-coa + nad <=> 3o-hd-7-10-coa + nadh + h	8
U-BOX 29	[m]: 3o-hd-7-10-coa + coa <=> td-5-8-coa + accoa	8
U-BOX 30	[m]: td-5-8-coa + fad -> t-td-5-8-coa + fadh2	8
U-BOX 31	[m]: t-td-5-8-coa + h2o <=> 3h-td-5-8-coa	8
U-BOX 32	[m]: 3h-td-5-8-coa + nad <=> 3o-td-5-8-coa + nadh + h	8
U-BOX 33	[m]: 3o-td-5-8-coa + coa <=> cis-3-6-dd-coa + accoa	8
U-BOX 34	[m]: cis-3-6-dd-coa <=> t-2-6-dd-coa	8
U-BOX 35	[m]: t-2-6-dd-coa + h2o <=> 3h-2-6-dd-coa	8
U-BOX 36	[m]: 3h-2-6-dd-coa + nad <=> 3o-2-6-dd-coa + nadh + h	8
U-BOX 37	[m]: 3o-2-6-dd-coa + coa <=> d4-coa + accoa	8
U-BOX 38	[m]: d4-coa + fad -> d2-4-coa + fadh2	8
U-BOX 39	[m]: d2-4-coa + nadph + h <=> cis-d-coa + nadp	8
U-BOX 40	[m]: cis-d-coa <=> t-d-coa	8
BOX 46	[m]: t-d-coa + h2o <=> 3h-d-coa	10
BOX 47	[m]: 3h-d-coa + nad <=> 3o-d-coa + nadh + h	10
BOX 48	[m]: 3o-d-coa + coa <=> o-coa + accoa	10
BOX 53	[m]: o-coa + fad -> t-o-coa + fadh2	10
BOX 54	[m]: t-o-coa + h2o <=> 3h-o-coa	10
BOX 55	[m]: 3h-o-coa + nad <=> 3o-o-coa + nadh + h	10
BOX 56	[m]: 3o-o-coa + coa <=> h-coa + accoa	10
BOX 57	[m]: h-coa + fad -> t-h-coa + fadh2	10
BOX 58	[m]: t-h-coa + h2o <=> 3h-h-coa	10
BOX 59	[m]: 3h-h-coa + nad <=> 3o-h-coa + nadh + h	10
BOX 60	[m]: 3o-h-coa + coa <=> but-coa + accoa	10
BOX 61	[m]: but-coa + fad -> t-but-coa + fadh2	10
BOX 62	[m]: t-but-coa + h2o <=> 3h-but-coa	10
BOX 63	[m]: 3h-but-coa + nad <=> acaccoa + nadh + h	10
BOX 64	[m]: acaccoa + coa <=> (2) accoa	10
NUCLEO	[c]: amp + atp <=> (2) adp	10
OTHERS	[c]: ppi + h2o -> (2) pi + h	10
I-TRANS	crn[m] <=> crn[c]	10
PYR 03	[m]: coa + nad + pyr -> accoa + co2 + nadh	12
PYR 04	[m]: mal-L + nad <=> pyr + nadh + co2 + h	12
TRIGLY 04	[c]: glyc-ald + nadh + h <=> glyc + nad	12
TCA 07	[m]: adp + pi + succoa <=> atp + succ + coa	13
TRANS 06	od-ca[e] -> od-ca[c]	14

Table E.1. Reactions and their corresponding clusters - continued

Reaction Name	Reaction	Cluster #
TRANS 14	hd9-ca[e] -> hd9-ca[c]	14
U-BOX 41	[c]: atp + coa + hd9-ca <=> amp + hd9-coa + ppi	14
U-BOX 42	[c]: crn + hd9-coa <=> hd9-crn + coa	14
U-BOX 43	hd9-crn[c] -> hd9-crn[m]	14
U-BOX 44	[m]: hd9-crn + coa <=> crn + hd9-coa	14
U-BOX 45	[m]: hd9-coa + fad -> t-hd9-coa + fadh2	14
U-BOX 46	[m]: t-hd9-coa + h2o <=> 3h-hd9-coa	14
U-BOX 47	[m]: 3h-hd9-coa + nad <=> 3o-hd9-coa + nadh + h	14
U-BOX 48	[m]: 3o-hd9-coa + coa <=> td7-coa + accoa	14
U-BOX 49	[m]: td7-coa + fad -> t-td7-coa + fadh2	14
U-BOX 50	[m]: t-td7-coa + h2o <=> 3h-td7-coa	14
U-BOX 51	[m]: 3h-td7-coa + nad <=> 3o-td7-coa + nadh + h	14
U-BOX 52	[m]: 3o-td7-coa + coa <=> dd5-coa + accoa	14
U-BOX 53	[m]: dd5-coa + fad -> t-dd5-coa + fadh2	14
U-BOX 54	[m]: t-dd5-coa + h2o <=> 3h-dd5-coa	14
U-BOX 55	[m]: 3h-dd5-coa + nad <=> 3o-dd5-coa + nadh + h	14
U-BOX 56	[m]: 3o-dd5-coa + coa <=> cisd-coa + accoa	14
U-BOX 57	[m]: cisd-coa <=> t-d-coa	14
TRIGLY 10	[c]: triglyc -> glyc + fa	14
TRANS 12	od9-ca[e] -> od9-ca[c]	15
BOX 17	[c]: atp + coa + hd-ca <=> amp + hd-coa + ppi	15
BOX 18	[c]: crn + hd-coa <=> hd-crn + coa	15
BOX 19	hd-crn[c] -> hd-crn[m]	15
BOX 20	[m]: hd-crn + coa <=> crn + hd-coa	15
BOX 21	[m]: hd-coa + fad -> t-hd-coa + fadh2	16
BOX 22	[m]: t-hd-coa + h2o <=> 3h-hd-coa	16
BOX 23	[m]: 3h-hd-coa + nad <=> 3o-hd-coa + nadh + h	16
BOX 24	[m]: 3o-hd-coa + coa <=> td-coa + accoa	16
BOX 29	[m]: td-coa + fad -> t-td-coa + fadh2	16
BOX 30	[m]: t-td-coa + h2o <=> 3h-td-coa	16
BOX 31	[m]: 3h-td-coa + nad <=> 3o-td-coa + nadh + h	16
BOX 32	[m]: 3o-td-coa + coa <=> dd-coa + accoa	16
BOX 37	[m]: dd-coa + fad -> t-dd-coa + fadh2	16
U-BOX 01	[c]: atp + coa + od9-ca <=> amp + od9-coa + ppi	16
U-BOX 02	[c]: crn + od9-coa <=> od9-crn + coa	16
U-BOX 03	od9-crn[c] -> od9-crn[m]	16
U-BOX 04	[m]: od9-crn + coa <=> crn + od9-coa	16
U-BOX 05	[m]: od9-coa + fad -> t-od9-coa + fadh2	16
U-BOX 06	[m]: t-od9-coa + h2o <=> 3h-od9-coa	16
U-BOX 07	[m]: 3h-od9-coa + nad <=> 3o-od9-coa + nadh + h	16
U-BOX 08	[m]: 3o-od9-coa + coa <=> hd7-coa + accoa	16
U-BOX 09	[m]: hd7-coa + fad -> t-hd7-coa + fadh2	16
U-BOX 10	[m]: t-hd7-coa + h2o <=> 3h-hd7-coa	16

Table E.1. Reactions and their corresponding clusters - continued

Reaction Name	Reaction	Cluster #
U-BOX 11	[m]: 3h-hd7-coa + nad <=> 3o-hd7-coa + nadh + h	16
U-BOX 12	[m]: 3o-hd7-coa + coa <=> td5-coa + accoa	16
U-BOX 13	[m]: td5-coa + fad -> t-td5-coa + fadh2	16
U-BOX 14	[m]: t-td5-coa + h2o <=> 3h-td5-coa	16
U-BOX 15	[m]: 3h-td5-coa + nad <=> 3o-td5-coa + nadh + h	16
U-BOX 16	[m]: 3o-td5-coa + coa <=> cisdd-coa + accoa	16
U-BOX 17	[m]: cisdd-coa <=> t-dd-coa	16
TRIGLY 17	[c]: fa -> (0.03) td-ca + (0.37) hd-ca + (0.03) hd9-ca + (0.23) od9-ca + (0.16) od9-12-ca + (0.15) od-ca	16
BOX 38	[m]: t-dd-coa + h2o <=> 3h-dd-coa	17
BOX 39	[m]: 3h-dd-coa + nad <=> 3o-dd-coa + nadh + h	17
BOX 40	[m]: 3o-dd-coa + coa <=> d-coa + accoa	17
BOX 45	[m]: d-coa + fad -> t-d-coa + fadh2	17
TCA 01	[m]: accoa + h2o + oaa -> cit + coa	20
TCA 02	[m]: cit <=> cacon + h2o	20
TCA 03	[m]: cacon + h2o <=> icit	20
TCA 04	[m]: icit + nad -> akg + co2 + nadh + h	20
TCA 05	[m]: akg + coa + nad -> co2 + nadh + succoa	20
TCA 08	[m]: succ + fad <=> fum + fadh2	20
TCA 09	[m]: fum + h2o <=> mal-L	20
TCA 10	[m]: mal-L + nad -> oaa + nadh + h	20
TRANS 04	ei-ca[e] -> ei-ca[c]	21
TRANS 07	td-ca[e] -> td-ca[c]	21
TRANS 08	dd-ca[e] -> dd-ca[c]	21
TRANS 09	d-ca[e] -> d-ca[c]	21
TRANS 10	o-ca[e] -> o-ca[c]	21
TRANS 15	tcs-ca[e] -> tcs-ca[c]	21
TRANS 16	dcs-ca[e] -> dcs-ca[c]	21
TRANS 22	h2o2[e] -> h2o2[c]	21
GLY 03	[c]: atp + f6p -> adp + f26bp	21
GLY 04	[c]: f26bp + h2o -> f6p + pi	21
PPP 01	[c]: g6p + nadp -> 6pgl + nadph + h	21
PPP 02	[c]: 6pgl + h2o -> 6pgc	21
PPP 03	[c]: 6pgc + nadp -> ru5p + co2 + nadph + h	21
PPP 04	[c]: ru5p <=> x5p	21
PPP 05	[c]: ru5p <=> r5p	21
PPP 06	[c]: g3p + s7p <=> e4p + f6p	21
PPP 07	[c]: r5p + x5p <=> s7p + g3p	21
PPP 08	[c]: x5p + e4p <=> g3p + f6p	21
OTHERS	[c]: glut-ox + nadph + h -> (2) glut-red + nadp	21
OTHERS	[c]: (2) glut-red + h2o2 <=> glut-ox + (2) h2o	21
GLYCGN 02	[c]: g1p + utp -> ppi + udpg	21
GLYCGN 03	[c]: udpg -> glycogen + udp	21
NUCLEO	[c]: udp + atp <=> utp + adp	21

Table E.1. Reactions and their corresponding clusters - continued

Reaction Name	Reaction	Cluster #
PYR 05	[c]: pyr + co2 + atp -> adp + pi + oaa	21
BOX 01	[c]: atp + coa + ei-ca <=> amp + ei-coa + ppi	21
BOX 02	[c]: crn + ei-coa <=> ei-crn + coa	21
BOX 03	ei-crn[c] -> ei-crn[m]	21
BOX 04	[m]: ei-crn + coa <=> crn + ei-coa	21
BOX 05	[m]: ei-coa + fad -> t-ei-coa + fadh2	21
BOX 06	[m]: t-ei-coa + h2o <=> 3h-ei-coa	21
BOX 07	[m]: 3h-ei-coa + nad <=> 3o-ei-coa + nadh + h	21
BOX 08	[m]: 3o-ei-coa + coa <=> od-coa + accoa	21
BOX 25	[c]: atp + coa + td-ca <=> amp + td-coa + ppi	21
BOX 26	[c]: crn + td-coa <=> td-crn + coa	21
BOX 27	td-crn[c] -> td-crn[m]	21
BOX 28	[m]: td-crn + coa <=> crn + td-coa	21
BOX 33	[c]: atp + coa + dd-ca <=> amp + dd-coa + ppi	21
BOX 34	[c]: crn + dd-coa <=> dd-crn + coa	21
BOX 35	dd-crn[c] -> dd-crn[m]	21
BOX 36	[m]: dd-crn + coa <=> crn + dd-coa	21
BOX 41	[c]: atp + coa + d-ca <=> amp + d-coa + ppi	21
BOX 42	[c]: crn + d-coa <=> d-crn + coa	21
BOX 43	d-crn[c] -> d-crn[m]	21
BOX 44	[m]: d-crn + coa <=> crn + d-coa	21
BOX 49	[c]: atp + coa + o-ca <=> amp + o-coa + ppi	21
BOX 50	[c]: crn + o-coa <=> o-crn + coa	21
BOX 51	o-crn[c] -> o-crn[m]	21
BOX 52	[m]: o-crn + coa <=> crn + o-coa	21
PBOX 01	tcs-coa[c] -> tcs-coa[p]	21
PBOX 02	[c]: atp + coa + tcs-ca <=> amp + tcs-coa + ppi	21
PBOX 03	[p]: tcs-coa + o2 <=> t-tcs-coa + h2o2	21
PBOX 04	[p]: t-tcs-coa + h2o <=> 3h-tcs-coa	21
PBOX 05	[p]: 3h-tcs-coa + nad <=> 3o-tcs-coa + nadh + h	21
PBOX 06	[p]: 3o-tcs-coa + coa <=> dcs-coa + accoa	21
PBOX 07	dcs-coa[c] -> dcs-coa[p]	21
PBOX 08	[c]: atp + coa + dcs-ca <=> amp + dcs-coa + ppi	21
PBOX 09	[p]: dcs-coa + o2 <=> t-dcs-coa + h2o2	21
PBOX 10	[p]: t-dcs-coa + h2o <=> 3h-dcs-coa	21
PBOX 11	[p]: 3h-dcs-coa + nad <=> 3o-dcs-coa + nadh + h	21
PBOX 12	[p]: 3o-dcs-coa + coa <=> ei-coa + accoa	21
PBOX 13	ei-coa[p] -> ei-coa[c]	21
PBOX 14	[p]: ei-coa + o2 <=> t-ei-coa + h2o2	21
PBOX 15	[p]: t-ei-coa + h2o <=> 3h-ei-coa	21
PBOX 16	[p]: 3h-ei-coa + nad <=> 3o-ei-coa + nadh + h	21
PBOX 17	[p]: 3o-ei-coa + coa <=> od-coa + accoa	21
PBOX 18	od-coa[p] -> od-coa[c]	21

Table E.1. Reactions and their corresponding clusters - continued

Reaction Name	Reaction	Cluster #
PBOX 19	[p]: od-coa + o2 <=> t-od-coa + h2o2	21
PBOX 20	[p]: t-od-coa + h2o <=> 3h-od-coa	21
PBOX 21	[p]: 3h-od-coa + nad <=> 3o-od-coa + nadh + h	21
PBOX 22	[p]: 3o-od-coa + coa <=> hd-coa + accoa	21
PBOX 23	hd-coa[p] -> hd-coa[c]	21
PBOX 24	[p]: hd-coa + o2 <=> t-hd-coa + h2o2	21
PBOX 25	[p]: t-hd-coa + h2o <=> 3h-hd-coa	21
PBOX 26	[p]: 3h-hd-coa + nad <=> 3o-hd-coa + nadh + h	21
PBOX 27	[p]: 3o-hd-coa + coa <=> td-coa + accoa	21
PBOX 28	td-coa[p] -> td-coa[c]	21
PBOX 29	[p]: td-coa + o2 <=> t-td-coa + h2o2	21
PBOX 30	[p]: t-td-coa + h2o <=> 3h-td-coa	21
PBOX 31	[p]: 3h-td-coa + nad <=> 3o-td-coa + nadh + h	21
PBOX 32	[p]: 3o-td-coa + coa <=> dd-coa + accoa	21
PBOX 33	dd-coa[p] -> dd-coa[c]	21
PBOX 34	[p]: dd-coa + o2 <=> t-dd-coa + h2o2	21
PBOX 35	[p]: t-dd-coa + h2o <=> 3h-dd-coa	21
PBOX 36	[p]: 3h-dd-coa + nad <=> 3o-dd-coa + nadh + h	21
PBOX 37	[p]: 3o-dd-coa + coa <=> d-coa + accoa	21
PBOX 38	d-coa[p] -> d-coa[c]	21
PBOX 39	[p]: d-coa + o2 <=> t-d-coa + h2o2	21
PBOX 40	[p]: t-d-coa + h2o <=> 3h-d-coa	21
PBOX 41	[p]: 3h-d-coa + nad <=> 3o-d-coa + nadh + h	21
PBOX 42	[p]: 3o-d-coa + coa <=> o-coa + accoa	21
P-BOX 43	o-coa[p] -> o-coa[c]	21
P-BOX 44	accoa[p] -> accoa[c]	21
P-BOX 45	accoa[c] + crn[c] -> accrn[c] + coa[c]	21
P-BOX 46	accrn[c] -> accrn[m]	21
P-BOX 47	[m]: accrn + coa -> accoa + crn	21
I-TRANS	coa[m] <=> coa[p]	21
I-TRANS	h2o[c] <=> h2o[p]	21
I-TRANS	nad[m] <=> nad[p]	21
I-TRANS	nadh[p] <=> nadh[m]	21
I-TRANS	h[p] <=> h[m]	21
OTHERS	[p]: (2) h2o2 --> (2) h2o + o2	21
I-TRANS	coa[c] <=> coa[m]	21
I-TRANS	glu-L[c] + h[c] <=> glu-L[m] + h[m]	21
I-TRANS	o2[c] <=> o2[p]	21
TRIGLY 00	[c]: dhap + nadh <=> glyc3p + nad	21
TRIGLY 12	[c]: 12glyc + atp -> pda + adp	21
TRIGLY 15	[c]: atp + aglyc -> adp + lpa	21
TRANS 23	coa[e] <=> coa[c]	22
TRANS 02	glycogen[c] <=> glycogen[e]	23

Table E.1. Reactions and their corresponding clusters - continued

Reaction Name	Reaction	Cluster #
GLYCGN 01	[c]: g6p <=> g1p	23
MAL-ASP 06	mal-L[m] + akg[c] <=> mal-L[c] + akg[m]	23
TRANS 03	lac-L[e] + h[e] <=> lac-L[c] + h[c]	24
PYR 01	[c]: lac-L + nad <=> pyr + nadh + h	24
TCA 06	[m]: gdp + pi + succoa <=> gtp + succ + coa	25
ETC 02	fadh2[m] + ubq[mim] <=> fad[m] + qh2[mim]	26
TRIGLY 01	[c]: 3pg + adp <=> atp + glycrt	28
TRIGLY 02	[c]: glycrt + nadh + h <=> glyc-ald + nad + h2o	28
TRIGLY 05	[c]: glyc + atp -> glyc-3p + adp	28
TRIGLY 06	[c]: glyc-3p + fa-coa -> lpa + coa	28
TRIGLY 07	[c]: lpa + fa-coa -> pda + coa	28
TRIGLY 08	[c]: pda + h2o -> 12glyc + pi	28
TRIGLY 09	[c]: 12glyc + fa-coa -> triglyc + coa	28
TRIGLY 16	[c]: (0.03) td-coa + (0.37) hd-coa + (0.03) hd9-coa + (0.23) od9-coa + (0.16) od9-12-coa + (0.15) od-coa <=> fa-coa	28
PYR 06	[c]: mal-L + nadp <=> pyr + co2 + nadph + h	30
MAL-ASP 01	mal-L[m] + pi[c] <=> mal-L[c] + pi[m]	30
NUCLEO	[m]: atp + gdp <=> adp + gtp	30
TRIGLY 03	[c]: glyc-ald + nadph + h <=> glyc + nadp	30
ETC 01	nadh[m] + (5) h[m] + ubq[mim] -> nad[m] + (4) h[mis] + qh2[mim]	34
ETC 03	qh2[mim] + (2) h[m] + (2) cytc-o[mim] -> ubq[mim] + (2) cytc-r[mim] + (4) h[mis]	34
TRANS 17	co2[e] <=> co2[c]	36
TRANS 21	h2o[e] <=> h2o[c]	36
I-TRANS	co2[c] <=> co2[m]	36
TRANS 19	h[e] <=> h[c]	42
I-TRANS	h[c] <=> h[m]	42
I-TRANS	h2o[c] <=> h2o[m]	42
TRANS 18	o2[e] <=> o2[c]	46
ETC 04	o2[m] + (8) h[m] + (4) cytc-r[mim] -> (2) h2o[m] + (4) h[mis] + (4) cytc-o[mim]	46
I-TRANS	o2[c] <=> o2[m]	46
ATP	[c]: atp + h2o -> adp + pi + h	48
NUCLEO	adp[m] + pi[m] + (3) h[mis] -> atp[m] + (3) h[m] + h2o[m]	48
NUCLEO	atp[m] + adp[c] -> atp[c] + adp[m]	48
I-TRANS	h[c] + pi[c] <=> h[m] + pi[m]	48

REFERENCES

Bassingthwaighte, J. B. and K. C. Vinnakota, 2004, "The Computational Integrated Myocyte", *Ann. N.Y. Acad. Sci*., Vol. 1015, pp. 391-404.

Belke D. D., T. S. Larsen, E. M. Gibbs and D. L. Severson, 2000, "Altered metabolism causes cardiac dysfunction in perfused hearts from diabetic (db/db) mice*", Am. J. Physiol. Endocrinol. Metab*., Vol. 279, pp. 1104-1113.

Bergmann, S. R., C. J. Weinheimer, J. Markham and P. Herrero, 1996, "Quantitation of Myocardial Fatty Acid Metabolism Using PET", *J. Nucl. Med*., Vol. 37, pp. 1723-1730.

Bittl, J. A., M. L. Weisfeldt and W. E. Jacobus, 1985, "Creatine Kinase of Heart Mitochondria", *The Journal Of Biological Chemistry,* Vol. 260-1, pp. 208-214.

Bosetti, F., G. Yu, R. Zucchi, S. Ronca-Testoni and G. Solaini, 2000, "Myocardial ischemic preconditioning and mitochondrial F_1F_0-ATPase activity", *Molecular and Cellular Biochemistry,* Vol. 215, pp. 31–38.

Burgard, A. P., E. V. Nikolaev, C. H. Schilling and C. D. Maranas, 2004, "Flux Coupling Analysis of Genome-Scale Metabolic Network Reconstructions", *Genome Research,* Vol. 14, pp. 301-312.

Bouchard, L., M. Robert, D. Vinarov, C. A. Stanley, G. N. Thompson, A. Morris, J. V. Leonard, P. Quant, B.Y.L. Hsu, A. Boneh, Y. Boukaftane, L. Ashmarina, S. Wang, H. Miziorko and G. A. Mitchell, 2001, "Mitochondrial 3-Hydroxy-3-Methylglutaryl-CoA Synthase Deficiency: Clinical Course and Description of Causal Mutations in Two Patients", *Pediatric Research,* Volume 49-3, pp. 326-331.

Calvani, M., E. Reda and E. Arrigoni-Martelli, 2000, "Regulation by carnitine of myocardial fatty acid and carbohydrate metabolism under normal and pathological conditions", *Basic Res. Cardiol,* Vol. 95, pp. 75-83.

Carjaval, K. and R. Moreno-Sanchez, 2002, "Heart Metabolic Disturbances in Cardiovascular Diseases", *Archives of Medical Research,* Vol. 34, pp. 88-99.

Clarke, J. T. R., 2007, "Narrative Review: Fabry Disease", *Ann. Intern. Med*., Vol. 146, pp. 425-433.

Cortassa, S., M. A. Aon, E. Marban, R. L. Winslow and B. O'Rourke, 2003, "An Integrated Model of Cardiac Mitochondrial Energy Metabolism and Calcium Dynamics*", Biophysical Journal*, Vol. 84, pp. 2734–2755.

Depre, C., M. R. Rider and L. Hue, 1998, "Mechanism of control of heart glycolysis*", Eur. J. Biochem*., Vol. 258, pp. 277-290.

Depre, C., J. J. Vanoverschelde and H. Taegtmeyer, 1999, "Glucose for the Heart", *Circulation*, Vol. 99, pp. 578-588.

Depre, C., and H. Taegtmeyer, 2000, "Metabolic aspects of programmed cell survival and cell death in the heart", *Cardiovascular Research,* Vol. 45, pp. 538–548.

Eaton, S., K. Bartlett and M. Pourfarzam, 1996, "Mammalian mitochondrial β-oxidation", *Biochem. J.*, Vol. 320, pp. 345-357.

Elzinga, G. and W. J. van der Laarse, 1990, "MVO_{2max} of the heart cannot be determined from uncoupled myocytes", *Basic Res. Cardiol*., Vol. 85, pp. 315-317.

Ferrans, V. J. and D. S. Fredrickson, 1975, "The Pathology of Tangier Disease", *Am. J. Pathol.*, Vol. 78, pp. 101-158.

Giordano, F. J., 2005, “Oxygen, oxidative stress, hypoxia, and heart failure”, *The Journal of Clinical Investigation*, Vol. 115-3, pp. 500-508.

Gleeson, M., 2005, "Basic metabolism I : fat", *Surgery*, Vol. 23:3, pp. 83-88.

Goodwin, G. W., F. Ahmad, T. Doenst and H. Taegtmeyer, 1998, “Energy provision from glycogen, glucose, and fatty acids on adrenergic stimulation of isolated working rat hearts”, *Am. J. Physiol. Heart Circ. Physiol.*, Vol. 274, pp. 1239-1247.

Goodwin, G. W., and H. Taegtmeyer, 2000, “Improved energy homeostasis of the heart in the metabolic state of exercise”, *Am J Physiol Heart Circ Physiol*, Vol. 279, pp. H1490–H1501.

Hall, J. L., G. D. Lopaschuk, A. Barr, J. Bringas, R. D. Pizzurro, W. C. Stanley, 1996, “Increased cardiac fatty acid uptake with dobutamine infusion in swine is accompanied by a decrease in malonyl-CoA levels”, *Cardiovascular Research*, Vol. 32, pp. 879-885.

Hegart, F. G, 1999, “Mitochondrial 3-hydroxy-3-methylglutaryl-CoA synthase: a control enzyme in ketogenesis”, *Biochem. J,* Vol. 338, pp. 569-582.

Huss, J. M., and D. P. Kelly, 2005, “Mitochondrial energy metabolism in heart failure: a question of balance”, *The Journal of Clinical Investigation*, Vol. 115- 3, pp. 547-555.

Janssen, R. J. R. J., L. G. Nijtmans, L. P. van den Heuvel and J. A. M. Smeitink, 2006, “Mitochondrial complex I: Structure, function and pathology”, *J. Inherit. Metab. Dis.,* Vol. 29, pp. 499–515.

Kaijser, L., B. W. Lassers, M. L. Wahlqvist, L. A. Carlson, 1962, “Myocardial lipid and carbohydrate metabolism in fasting men during prolonged exercise”, *Journal of Applied Physiology*, Vol. 32-6, pp. 847-858.

Kantor, P. F., A. Lucien, R. Kozak and G. D. Lopaschuk, 2000, "The Antianginal Drug Trimetazidine Shifts Cardiac Energy Metabolism From Fatty Acid Oxidation to Glucose Oxidation by Inhibiting Mitochondrial Long-Chain 3-Ketoacyl Coenzyme A Thiolase", *Circ. Res.*, Vol.86, pp. 580-588.

Kemppainen, J., T. Fujimoto, K. K. Kalliokoski, T. Viljanen, P. Nuutila and J. Knuuti, 2000, "Myocardial and skeletal muscle glucose uptake during exercise in humans", *Journal of Physiology*, Vol. 542.2, pp. 403–412.

Kim, J., G. M. Saidel and M. E. Cabrera, 2007, "Multi-Scale Computational Model of Fuel Homeostasis During Exercise:Effect of Hormonal Control", *Annals of Biomedical Engineering*, Vol. 35-1, pp. 69–90.

King, L.M. and L. H. Opie, 1998, "Glucose and glycogen utilisation in myocardial ischemia – Changes in metabolism and consequences for the myocyte", *Molecular and Cellular Biochemistry*, Vol. 180, pp. 3–26.

Kodde, I. F., J. Van der Stok, R. T. Smolenski and J. W. de Jong, 2007, "Metabolic and genetic regulation of cardiac energy substrate preference", *Comparative Biochemistry and Physiology*, Vol. 146, pp. 26-39.

Kofoed, K. F., S. Carstensen, J. D. Hove, J. Freiberg, R. Bangsgaard, S. Holm, A. Rabøl, B. Hesse, H. Arendrup, H. Kelbæk, 2002, "Low whole-body insulin sensitivity in patients with ischaemic heart disease is associated with impaired myocardial glucose uptake predictive of poor outcome after revascularization", *Eur. J. Nucl. Med.*, Vol. 29, pp. 991–998.

Koga, Y., I. Nonaka, M. Kobayashi, M. Tojyo and K. Nihei, 1988, "Findings in Muscle in Complex I (NADH Coenzyme Q Reductase) Deficiency", Vol. 24, pp. 747-756.

Lesnefsky, E. D., S. Moghaddas, B. Tandler, J. Kerner and C. L. Hoppel, 2001, "Mitochondrial Dysfunction in Cardiac Disease: Ischemia-Reperfusion, Aging and Heart failure", *J. Mol. Cell. Cardiol*., Vol. 33, pp.1065–1089.

Loeffen, J. L. C. M., J. A. M. Smeitink, J. M. F. Trijbels, A. J. M. Janssen, R. H. Triepels, R. C. A. Sengers and L.P. van den Heuvel, 2006, "Isolated Complex I Deficiency in Children: Clinical, Biochemical and Genetic Aspects", *Human Mutation,* Vol. 15, pp. 123-134.

Longnus, S. L., R. B. Wambolt, R. L. Barr, G. D. Lopaschuk and M. F. Allard, 2001," Regulation of myocardial fatty acid oxidation by substrate supply", Am. *J. Physiol. Heart Circ. Physiol.*, Vol. 281, pp. H1561–H1567.

Luo, R., S. Liao, G. Tao, Y. Li, S. Zeng, Y. Li and Q. Luo, 2006, "Dynamic analysis of optimality in myocardial energy metabolism under normal and ischemic conditions", *Molecular Systems Biology,* Vol.2, pp. 1-6.

Mahadevan, R. and C. H. Schilling, 2003, "The effects of alternate optimal solutions in constraint-based genome-scale metabolic models", *Metabolic Engineering*, Vol. 5, pp. 264–276.

Marin-Garcia, J. and M. J. Goldenthal, 2002, "Fatty acid metabolism in cardiac failure: biochemical, genetic and cellular analysis", *Cardiovascular Research*, Vol. 54, pp. 516-527.

Maughan, R., 2005, "Basic metabolism II : carbobohydrate", *Surgery*, Vol. 23:5, pp. 154-158.

Meyer, C. and M. Schwaiger, 1997, "Myocardial Blood Flow and Glucose Metabolism in Diabetes Mellitus", *Am. J. Cardiol.*, Vol. 80(3A), pp. 94A–101A.

Nakao, S., H. Nakao, T. Takenaka, M. Maeda, C. Kodama, A. Tanaka, M. Tahara, A. Yoshida, M. Kuriyama, H. Hayashibe, H. Sakuraba and H. Tanaka, 1995, "An Atypical Variant Of Fabry's Disease In Men With Left Ventricular Hypertrophy**",** *N. Eng.l J. Med.*, Vol. 333, pp. 288-293.

O'Donnell, J. M., N. M. Alpert, L. T. White and E. D. Lewandowski, 2002, "Coupling of Mitochondrial Fatty Acid Uptake to Oxidative Flux in the Intact Heart", *Biophysical Journal*, Vol. 82, pp.11–18.

Opie, L. H. and P. G. Carnici, 1992, "Myocardial Blood Flow, Deoxyglucose Uptake, and Myocyte Viability in lschemia", *The Journal of Nuclear Medicine*, Vol.33-7, pp. 1353-1356.

Opie, L. H., 1999, *Heart Physiology: From Cell to Circulation*, Lippincott Williams & Wilkins, New York.

Paulson, D. J., 1998, "Carnitine deficiency-induced cardiomyopathy", *Molecular and Cellular Biochemistry*, Vol. 180, pp. 33–41.

Quin, D. W. and D. Pagano, 2004, "Applied Physiology of the Heart", *Surgery*, Vol. 22(6), pp. 144a-e.

Salem, J. E., G. M. Saidel, W. C. Stanley and M. E. Cabrera, 2002, "Mechanistic Model of Myocardial Energy Metabolism Under Normal and Ischemic Conditions", *Annals of Biomedical Engineering*, Vol. 30, pp. 202–216.

Shaap, F. G., G. J. van der Vusse and J. F. C. Glatz, 1998, "Fatty acid-binding proteins in the heart", *Molecular and Cellular Biochemistry*, Vol. 180, pp. 43-51.

Smeitink, J. A. M., L. W. P.J. van den Heuvel, 1994, "Human Mitochondrial Complex I in Health and Disease", *Am. J. Hum. Genet.*, Vol. 64, pp. 1505–1510.

Smeitink, J. A. M., L. W. P.J. van den Heuvel, W. J. H. Koopman, L. G. J. Nijtmans, C. Ugalde and P. H. G. M Willems, 2004, "Cell Biological Consequences of Mitochondrial NADH: Ubiquinone Oxidoreductase Deficiency", *Current Neurovascular Research*, Vol. 1, pp. 29-40.

Stanley, W. C., G. D. Lopaschuk, J. L. Hall and J. G. McCormack, 1997, "Regulation of myocardial carbohydrate metabolism under normal and ischaemic conditions Potential for pharmacological interventions", *Cardiovascular Research*, Vol. 33, pp. 243–257.

Stanley, W. C., and M. P. Chandler, 2002, "Energy Metabolism in the Normal and Failing Heart: Potential for Therapeutic Interventions", *Heart Failure Reviews*, Vol. 7, pp. 115–130.

Stanley, W. C., F. A. Recchia, G. D. Lopaschuk, 2005, "Myocardial Substrate Metabolism in the Normal and Failing Heart", *Physiol. Rev.*, Vol. 85c, pp. 1093-1129.

Tamayo, P., D. Slonim, J. Mesirov, Q. Zhu, S. Kitareewan, E. Dmitrovsky, E. S. Lander and T. R. Golub, 1999, "Interpreting patterns of gene expression with self-organizing maps: Methods and application to hematopoietic differentiation", *Proc. Natl. Acad. Sci.*, Vol. 96, pp. 2907–2912.

Thompson, G. N., B. Y. L. Hsu, J. J. Pitt, E. Treacy and C. H. Stanley, 1997, "Fasting Hypoketotic Coma In A Child With Deficiency Of Mitochondrial 3-Hydroxy-3-Methylglutaryl-Coa Synthase", *The New England Journal of Medicine*, Vol. 337-17, pp. 1203-1207.

van der Vusse, G. J., M. van Bilsen and J. F. C. Glatz, 2000, "Cardiac fatty acid uptake and transport in health and disease", *Cardiovascular Research*, Vol. 45, pp. 279-293.

van der Vusse, G. J., M. van Bilsen, J. F. C. Glatz, D. M. Hasselbaink and J. J. F. P. Luiken, 2002, "Critical steps in cellular fatty acid uptake and utilization", *Molecular and Cellular Biochemistry*, Vol. 239, pp. 9–15.

Vance, D. E. and J. Vance (editors), 1991, *Biochemistry of Lipids, Lipoproteims and Membranes*, Elsevier, Amsterdam.

Ventura-Clapier, R., A.Garnier and V. Veksler, 2003, "Energy Metabolism in Heart Failure*", J. Physiol*., Vol. 555-1, pp. 1-13.

Voet, D., J. G. Voet and C. W. Pratt, 2006, *Fundamentals of Biochemistry:Life at Molecular Level,* Wiley, New York.

Ward, J., 2006, "Oxygen Delivery and Demand", *Surgery*, Vol. 24:10, pp. 354-360.